universität wien

DISSERTATION

Titel der Dissertation

“ Analysis of plasmid isoforms and supercoiled topoisomers by liquid chromatography “

Verfasser

Mag. Marek Mahut

angestrebter akademischer Grad

Doktor der Naturwissenschaften (Dr. rer.nat.)

Wien, 2010

Studienkennzahl lt. Studienblatt	**A 091 419**
Dissertationsgebiet lt. Studienblatt	**Chemie**
Betreuer:	**Univ.-Prof. Dr. Michael Lämmerhofer**

Table of contents

1 Abstracts

1.1 Abstract (English)

In this thesis a separation of different forms of plasmid DNA by means of chromatographic methods is presented. The work was split into two general objectives, the first dealing with separation of plasmid isoforms, such as the supercoiled, open-circular and linear plasmid DNA. The second general topic deals with the separation of topologically different forms of supercoiled plasmids, such with a different degree of supercoiling. New silica-based materials were developed and tested in this study, to determine structure-separation relationships between the chromatographic ligand and the analyte. In doing so, we focused on the development of new molecular recognition principles in order to obtain a defined and robust separation behaviour.

Within the first general objective of the isoform separation, various ligands and chromatographic supports were tested, during the course of which an optimal interplay of both in combination with specific mobile phase conditions lead to desired results. A silica gel surface containing acidic silanol groups in combination with a short spacer between the support and the chromatographic ligand showed complete recoveries of all analyte forms to be quantified, outperforming the commercial material that is currently employed for this purpose. It was also shown, that separation based on molecular recognition gives a defined elution behaviour being unaffected by chromatographic conditions.

In the presented work an analytically useful chromatographic separation of different topoisomers of native supercoiled plasmid DNA is presented for the first time. Up to now a topology analysis was only possible with gel electrophoresis with the restriction that not native plasmid DNA but only molecules with a small degree of supercoiling could be analyzed. The key element of the presented method is a chromatographic ligand, which recognizes differently supercoiled plasmid DNA because of high rigidity and a defined geometric arrangement of hydrogen bonding donor and acceptors. We have determined the number of superhelical turns by means of agarose gel electrophoresis. Since chromatography in general allows easier up-scaling compared to electrophoretic methods, new possibilities of producing topological standards arise, both for analytical and biological purposes.

1.2 Abstract (Deutsch)

Im Rahmen meiner Dissertation wurden verschiedene Formen von Plasmid-DNA mit chromatographischen Methoden getrennt. Die Arbeit wurde in zwei Bereiche geteilt, wobei sich der erste mit der Trennung von Isoformen befasste, wie superspiralisierte, offen-zirkuläre und lineare Plasmid-DNA. Der zweite Teil behandelt die Trennung und Identifizierung von topologisch unterschiedlichen Formen von superspiralisierten Plasmiden, solchen mit unterschiedlichem Grad an Superspiralisierung. Dazu wurden in erster Linie neue Trennmaterialien auf Basis von Kieselgelen entwickelt und getestet, um Struktur-Trennbeziehungen zwischen Ligand und Analyt zu bestimmen. Dabei stand die Entwicklung von neuen molekularen Erkennungsprinzipien im Vordergrund, um definiertes und robustes Trennverhalten zu erzielen.

Im ersten Bereich der Trennung von Isoformen wurden diverse Liganden sowie chromatographische Träger getestet, wobei sich erst eine optimale Kombination aus beiden als zielführend erwies. So zeigte eine Kieselgeloberfläche mit sauren Silanolgruppen in Kombination mit einem kurzen Spacer zwischen Träger und Ligand eine vollständige Wiederfindung von allen zu quantifizierenden Analytformen, welche dem heutzutage standardmäßig eingesetzten kommerziellen Material überlegen ist. Ebenso konnte gezeigt werden, dass Trennungen auf Basis von molekularer Erkennung ein definiertes Elutionsverhalten zeigen, welches von den chromatographischen Bedingungen unbeeinflusst ist.

In der vorliegenden Arbeit wird erstmals eine analytisch nützliche chromatographische Trennung von unterschiedlichen Topoisomeren der nativen superspiralisierten Form gezeigt. Bis zu diesem Zeitpunkt war eine topologische Analyse von Plasmid-DNA nur mit der Gelelektrophorese möglich, und dies mit der Einschränkung, dass nicht native Plasmide sondern nur Moleküle mit geringer Superspiralisierung analysiert werden konnten. Hierfür wurde ein chromatographischer Ligand gefunden, der aufgrund der definierten räumlichen Anordnung von Wasserstoffbrücken-Donoren und -Akzeptoren und hoher Rigidität verschieden superspiralisierte DNA erkennt. Mit Hilfe von Agarosegel-Elektrophorese wurde die Zahl der superhelikalen Windungen bestimmt. Da die Chromatographie im Gegensatz zu elektrophoretischen Techniken leichter

skalierbar ist, öffnen sich hiermit Möglichkeiten zur Herstellung von definierten topologischen Standards für analytische und biologische Zwecke.

2 Preface

The work on this thesis emerged from my diploma thesis written in 2006/2007 under the supervision of professors Wolfgang Lindner and Michael Lämmerhofer. The topic as well as the need for a better chromatographic separation of plasmids has been raised up by Boehringer-Ingelheim RCV.

During the work on my diploma thesis, new strategies to approach certain problems have been set up and some potentially useful and interesting concepts have been generated. It was mostly HPLC methodology that has been employed in that study. Briefly, a good separation of the therapeutically most active form, so called ccc-form, from other isoforms has been achieved.

After reporting our first results at Boehringer-Ingelheim RCV, interest was raised during discussions and a cooperation was established. During the first months of my PhD work, the potency of the HPLC columns from the work on the diploma thesis has been evaluated. A very surprising phenomenon has been revealed, when the ccc-form was split into a pattern of discrete narrow peaks. It was so striking, that our work has been split into two parts after that observation. Indeed, when the cooperation was officially launched, two different general objectives were defined, one of them dealing solely with the ccc-form.

Somewhere in the middle of the work we realized that though we are dealing with molecules ("extremely minute particle", i.e. actually bio-nanoparticles), these are in fact so big that we actually could see them by some microscopic techniques. After hypothesizing that, during one of our many sessions behind the round table in one of our professor's office, we decided to look up, who could actually "see" our big molecules for us. We invited professor Hinterdorfer from Linz to join us in our project, because he has long-term experience in atomic force microscopy in, among other things, nucleic acids. Things began to move quite slowly in the beginning, but evolved quickly afterwards into a very friendly cooperation mostly between the young PhD students in Vienna and Linz. At the end of this project, the DNA images are looking fantastic and it is quite impressive to "see" the molecules after they have been hunted through our chromatographic columns. We are still awaiting what will follow next.

In the end, both general topics lead us to many new observations, phenomena, and facts – some expected, but even more of them were unexpected. Although not

all problems have been solved and no ground breaking material has been developed, that could perform well for all purposes under all conditions, we still learned very much from the project. A good example is, that though the result from the first general topic was not as satisfying as that of the second, researchers' *input* and the information *output* from this first general topic is *greater* in my opinion.

There is one more challenging task to deal with, and that is the future of these results. It depends on the interests of all people that are and were involved in this work, and how the interests can be matched. For sure is, many interdisciplinary topics have been briefly touched – such as biochromatography, microscopy, biotechnological process control, preparative material use and biological implication. It would be of great interest to go into details within these fields with the knowledge presented in this work.

3 Introduction

3.1 Plasmid DNA

The presented work deals with a very narrow analyte spectrum, namely plasmidic DNA. A plasmid is, compared to genomic DNA, a small and non-genomic genetic element consisting of double stranded DNA. Though in some cases linear, in most organisms circular plasmids can be found. Plasmids are present in virtually all bacterial species but also in some eukaryotes.

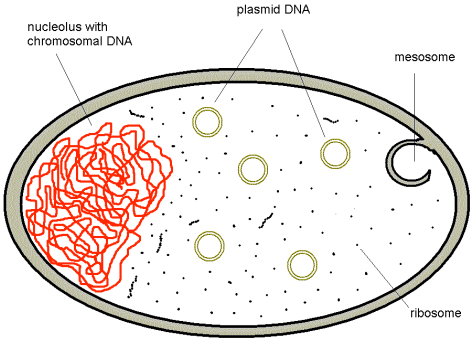

Figure 1: Bacterial cell

Their replication is not bound to the replication of the chromosome, i.e. they are autonomously replicating elements. They have their own origin of replication (*ori*) which contains information about the starting point of replication and the plasmid copy number in the bacterium. The usual size varies between 1 to 200 kb, where 1 kb equals 1,000 base pairs. The function of plasmids in bacteria depends on their type, but generally they do not code any essential growth function while the bacterial cell is without stress. However, if a stressful situation arises, i.e. an antibiotic or a heavy metal is present, plasmids may code for certain gene products that make survival possible. The best known example is antibiotic resistance encoded on plasmids.

In eukaryotes, the *ori* cannot be “read” as there are no DNA-binding proteins for such an element. Very rarely though a similar system for plasmid replication can be found, for example in yeast – the so called “2µ circle” or “2-micrometre-ring”. This element has indeed an autonomous replication site ARS, which is a replication start just like the *ori* but operates differently.

However, eukaryotes always regulate the expression of each genetic product (RNA or protein) separately via a promoter. A promoter is a region located usually near the genes they regulate, on the same strand and upstream. Promoter regions are sequences where the DNA-dependent RNA polymerase attach to the DNA double strand in order to transcribe the genome containing the desired genetic product as mRNA.

Plasmids are used in molecular biology and genetic engineering as vectors to transfer DNA into an organism. Although other vectors such as viruses, cosmids or phages are preferred in some cases, plasmids still remain most important vectors for transforming cells with desired DNA sequences. Plasmids for genetic engineering contain three main constituents:

1. origin of replication (*ori*)
2. cloning site
3. selection marker

The origin of replication is specific for every species, because of specific recognition enzymes, thus the *ori* must match the species that has to be transformed (e.g. a certain *E.coli* strain). The copy number encoded in the *ori* sequence should be relatively high to allow generating of sufficient quantities.

3.2 Plasmid structures

A brief overview about different isoforms of a single plasmid molecule is given. Although the nucleotide sequence of the DNA is identical, the plasmid can be present in many topological forms as can be seen in Figure 2. In the picture, five main forms are shown, the first three being monomers. A dimer can be formed from any of these monomers, so theoretically ccc dimers and linear dimers (not shown) have to be considered as well.

The majority of plasmid molecules are present in the covalently closed circular (ccc) form. These plasmids are supercoiled having a compact structure and the double-helix is wound around itself. Both DNA strands are intact, thus the name “covalently closed”. This form is believed to be most active concerning the potency for genetic vaccination and therapy, as will be discussed later. The majority of ccc plasmids is negatively supercoiled, which means the DNA is

underwound relative to the other forms. The so caused torsional tension drives the temporary partial separation of the DNA strands energetically which is necessary for DNA-controlled processes such as replication or transcription.

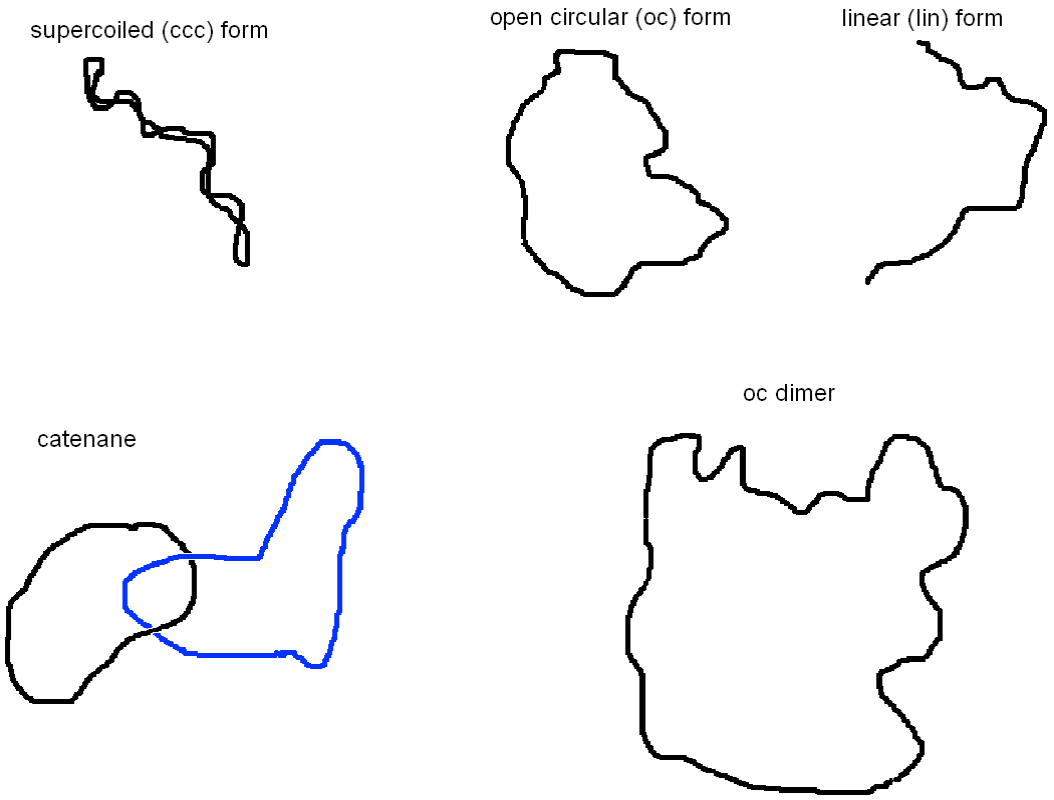

Figure 2: Structure of pDNA forms

By introducing a nick (breakage of one phosphodiester bond) into one DNA strand an open circular (oc) form results while the supercoiling is lost. Oc plasmids are totally relaxed and less compact; they may be produced from ccc plasmids by nucleases, mechanical stress or UV irradiation. If both DNA strands are nicked at the same position, e.g. by an endonuclease, a linear plasmid is produced. Linear plasmids can also be found in nature in some bacterial species.

In addition to these monomeric forms, also dimeric forms may arise during plasmid preparations, two types of which are shown in Fig. 2. If the monomers are present as equal dimers, they are called concatemers, such as the sketched oc dimer. They are formed mainly by homologous recombination, the amount of it being plasmid-specific. Another type of a dimer or multimer species is a catenane, formed by circular monomers which are not chemically bound to each eather, but interlocked mechanically. The simplest catenane is sketched in Fig. 2. Catenation is a crucial process in the mode of action of topoisomerases and during cell replication but the study of these structures is very complex [1].

3.3 DNA supercoiling

The supercoiling of plasmids and its degree are processes controlled by DNA topoisomerases I and ATP-dependent topoisomerases II (so called DNA gyrases). The precise tuned level of supercoiling is kept by an interplay between those two enzymes and is further dependent on cultivation temperature, but in general one negative supercoil is introduced every 200 base pairs [2]. Because plasmid supercoling became an essential part of this thesis after the discovery of chromatographic topoisomer separation, an overview on this topic is given here.

Supercoiling can only occur in DNA where the ends of the molecule or of a segment within that molecule is restrained from free rotation. This is possible either in covalently closed circles or in linear molecules by attaching the ends to a membrane or protein entities. We will only consider covalently closed circles here.

3.3.1 Linking number

The fundamental topological parameter of ccc plasmid DNA is the linking number (*Lk*), which is explained in the figure below. The picture on the left shows a covalently closed circle made of a double helix, one strand in red, the other one in black. The helix axis is the grey circle. Now if we assume that the red DNA strand is the edge of an imaginary surface and count the number of times that the black strand crosses this surface, we get the linking number. It is important to note also the sign of every intersection.

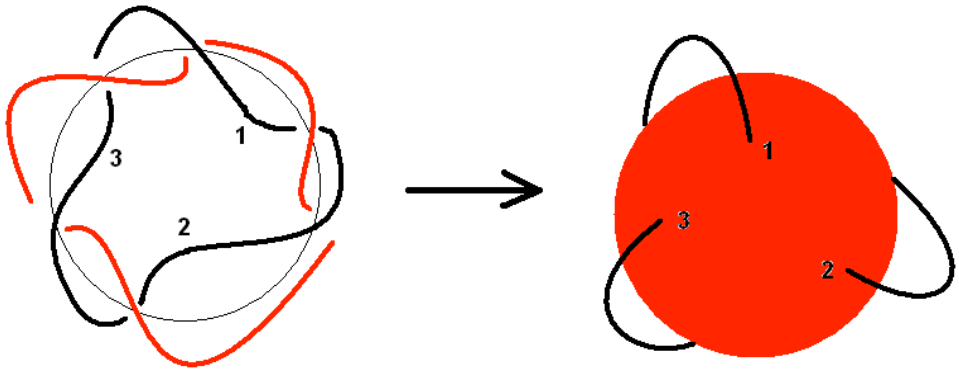

Figure 3: Model for determination of the linking number. The *Lk* here is +3.

Two important features are evident from figure 3. First, the linking number is always an integer. Secondly, *Lk* cannot be changed by deformation of the strands, it is topologically invariant. The only way to change *Lk* is to break at least one

strand and rotate it relative to the other and seal the break again. This is realized in practice by topoisomerases, formerly called the nicking-closing enzyme [3].

A real plasmid molecule has a very large number of such crossings, which arises from the nature of the well-known double helix published by Watson, Crick and Wilkins in 1953. The actual linking number of a certain molecule is dependent on the number of base pairs per turn of the double helix, *h* (in some literature, γ is used instead). This value changes with different conditions, such as ionic strength, temperature or pH, but under standard conditions (0.2M NaCl, pH 7, 37°C [4]) often the value 10.5 bp/turn is taken, denoted as h^0. The linking number is thus obtained by dividing the number of base pairs, *N*, by *h*. When bringing the ends of the DNA in close vicinity in order to close a circle without twisting them against each other, probably the ends will not precisely match each other. Thus, a slight twisting will be required to join the ends together, which is negligible over the whole molecule. This small angular displacement is denoted as ω ($-0{,}5 \leq \omega \leq 0{,}5$). The so obtained closed circle has a linking number which can be described by the following equation (also called the “standard linking number”) [5]:

$$Lk_m \approx \frac{N}{h} \approx \frac{N}{10.5} \tag{1}$$

The linking number of the two strands in right-handed DNA is positive by convention. For example in a 4892 bp plasmid the standard linking number Lk_m is 4892 / 10.5 = 465,9 ≈ + 466.

Anyway, when speaking strictly, most of the covalently closed circles are already supercoiled by ω, the difference between Lk_m and N/h. The quotient N/h is also referred to as Lk^0. However, Lk^0 is not a linking number, as it is not an integer. It serves as a reference point between the actual level of supercoiling and the relaxed, i.e. not supercoiled, state. The actual supercoiling can be expressed by one of the following equations:

$$\Delta Lk = Lk - Lk^0 = Lk - \frac{N}{h} \tag{2}$$

$$\sigma = \frac{Lk - Lk^0}{Lk^0} = \frac{\Delta Lk}{Lk^0} \tag{3}$$

Equation (2) introduces the quantity ΔLk, the so called linking number difference. It gives an absolute measure of supercoiling, or more roughly speaking the "number of supercoils". In Equation (3) the relative measure of supercoiling σ is expressed, also referred to as the specific linking difference or superhelical density (which however may be confusing with other terms). This value nearly always turns out to be in the range between -0.03 and -0.09, but typically near the middle of this range, when isolating bacterial plasmid populations [6].

3.3.2 Twist and Writhe

If we want to change the linking number, one possibility how to do this can be easily concluded from the previous section. We may cut the double helix, then introduce a full turn on one end while keeping the other fixed ("twisting one end against the other"), and finally reseal both strands. By this twisting procedure, we alter the number of base pairs per turn, *h*. The difference between the new linking number and Lk_m will be exactly 1. This type of supercoiling is called twist and is abbreviated *Tw*. Because we changed the superhelicity by 1 twist, we can express this as $\Delta Tw = 1$. Now, look at figure 4.

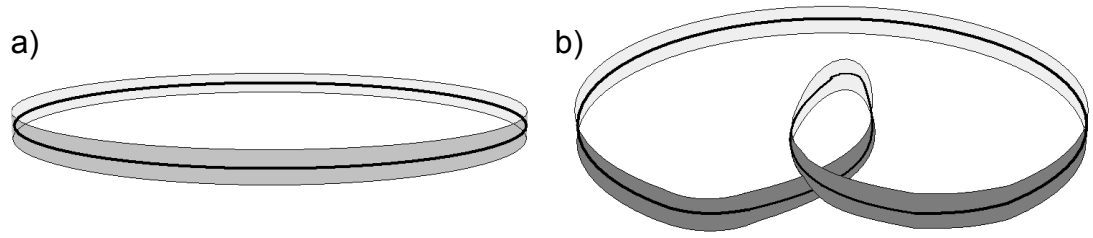

Lk = 0, *Tw* = 0, *Wr* = 0 *Lk* = +1, *Tw* ~ 0, *Wr* ~ +1

Figure 4: Illustration of the Writhe quantity

Both ribbons lie on a plane surface, the edges of the ribbons indicating a DNA strand. In the picture on the left, the imaginary DNA strands do not cross each other ('s plane), therefore the twist must equal zero. In fact, figure 4 a shows a topoisomer with the linking number Lk_m, and thus no supercoiling (strictly speaking: with least supercoiling possible).

Now in figure 4 b we can see another topoisomer, however it is somehow evident, that a structure of higher order is present. Although there is nearly no twist of the helix, the linking number of this model is +1. The difference between figure 4a and 4b is called writhe, *Wr*. The writhing number ("number of superhelical turns) depends exclusively on the curve of the axis of the ribbon.

Twist and writhe, both are forms of supercoiling which can occur in ccc DNA. Although first derived purely mathematically, these findings were applied some 40 years ago to DNA [7]. Both, twist and writhe, can be changed within a molecule without changing the topology, i.e. the supercoiling. This is maybe more obvious if we think of a telephone wire. Imagine we take the telephone earpiece into our hands and do not rotate it – this means we keep the linking number constant. If we pull the earpiece far away from the telephone apparatus, the wire will be outstretched and almost straight - this situation is sketched in figure 5a. One can feel that the wire is very twisted, but the coiling of the axis, the writhe, is low. In Fig. 5b, the earpiece was moved closer to the apparatus. The twist has been substantially lowered, but the writhe has simultaneously increased. Note that we did not rotate the earpiece nor the apparatus, i.e. the overall topology of the telephone wire has not been altered. In the last figure (5c), the earpiece is very close to the apparatus. The twist has been lowered further, and as a result of this, the writhe must been raised again. Therefore the already curved axis curves again upon itself to form a supercoil of a higher order.

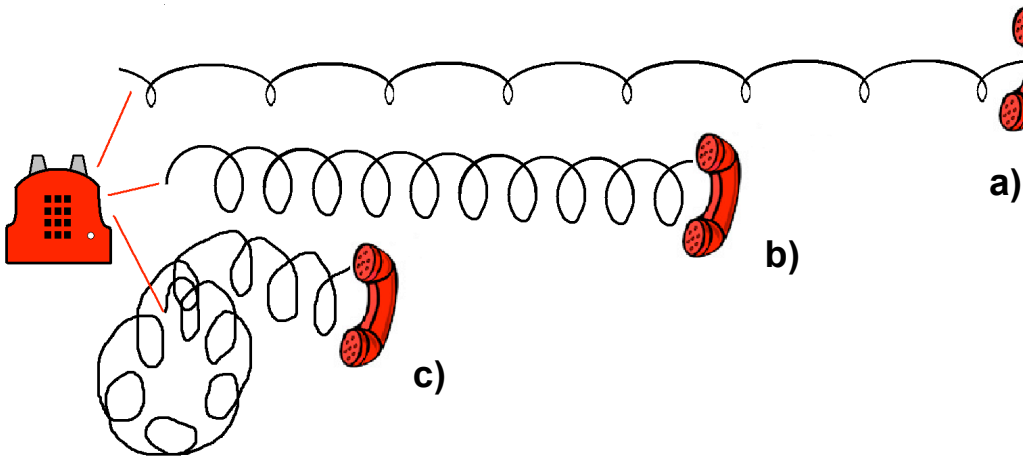

Figure 5: Interconversion of twist and writhe exemplified on a telephone wire

An important deduction of Fig. 5 is that twist and writhe are interconvertible, which also leads to the following important equation.

$$\Delta Lk = \Delta Tw + \Delta Wr \quad (4)$$

The ratio between twist and writhe can be changed and controlled by changing solution parameters, such as ionic strength, temperature and addition of additives which change either the twist or the writhe of DNA specifically. A nice computer simulation of the salt dependence on the shape of closed minicircles can be found in Ref. [8].

Various measurements of plasmids in electron and atomic force microscopy have revealed that the overall supercoiling is spread into about 25% twist and 75% writhe under normal conditions when the σ value is not too high or low. Thus under normal conditions both types of supercoiling are present. However, the value *we* usually connect with supercoiling *ad hoc*, is writhe. Though not absolutely correct, it is an allowed approximation when the twist-to-writhe ratio does not change (i.e. solution conditions shall not change significantly).

It is a very useful approach since the writhe can be calculated or estimated from microscopic images. Also, the overall size of the molecule is much more dependent on the writhe than on twist, which is a major issue in analyses where the size is important. One such analysis is gel electrophoresis, where the size of the plasmid molecule determines its mobility. In fact, topoisomers with the smallest possible *Lk* difference can be separated with this method because of the difference in writhe.

3.4 Intercalators and change of DNA conformation

There are basically two binding sites where molecules can interact with DNA. These two sites also give the name to each group of DNA binders: groove binders and intercalators. The first group is usually split into minor-groove binders (such as the dye SYBR Gold used in agarose gel electrophoresis) and major-groove binders (such as triple-helix forming oligonucleotides, [9]), both of which deform the DNA only minimally. However, a very prominent opposite example exists in the molecule of netropsine, which is used for creating positively supercoiled topoisomer standards (see section 2.6.4).

On the other hand intercalators are mostly aromatic and planar molecules which bind to DNA by inserting themselves between the nucleobases. By doing so, they change the twist of the DNA because they dynamically open up a space between adjacent base pairs.

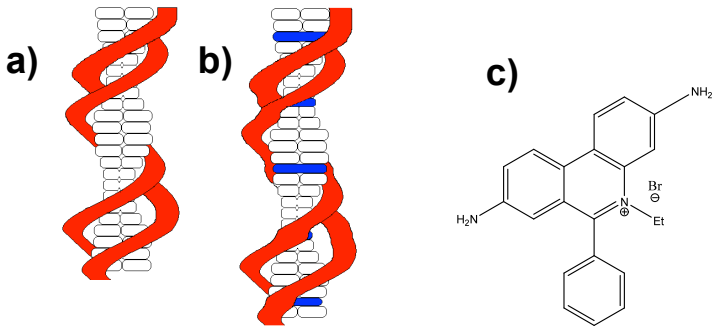

Figure 6: A sketch of double stranded DNA without (a) and with (b) an intercalator (shown in blue). Note the deforming of the backbone (shown in red) which changes the twist of the double helix. In fig. (c) the structure of ethidium bromide, a well-known intercalator, is shown.

For example ethidium bromide (EtBr), which is used for visualizing DNA, unwinds the double helix by 26° per intercalating molecule as a result of increasing distance between adjacent base pairs [10]. By intercalation of the ethidium cation, shown in Fig. 6 c, the twist of the double helix is increased. Because of the interconvertibility of twist and writhe, the writhe must be decreased upon ethidium intercalation, because the topology has not changed (i.e. no topoisomerase is present). Decreasing writhe means that the size of the molecule increases until a point is reached, where all writhe is converted into twist. This is called the relaxed state of a plasmid, because the conformation (and the electrophoretic mobility) is similar to the open circular form. In this special case, equation (5) applies:

$$\Delta Lk = \Delta Tw \tag{5}$$

When ethidium is further added to the solution, the twist should change further, because the theoretical saturation point of DNA and the intercalator is not reached (i.e. an intercalator molecule between every adjacent base pair). However, the twist cannot be changed anymore without changing the topology. Instead a positive writhing occurs and the DNA axis starts to form positive supercoils.

The sign of the writhing in the example reflects the usual situation where the natural occurring plasmid is negatively supercoiled. With increasing concentration of the intercalator, the DNA becomes totally relaxed and at last positively supercoiled. Intercalation does not only increase the adjacent base pair distance but induces also local conformation changes in the backbone. So does the sugar conformation change from C2‘-endo (B-type DNA) to C3’-endo which is typical for A-type DNA [11].

The intercalation of ethidium bromide into DNA was detected to be a two-step process with four kinetic constants (two for the forward reaction, two for the reverse reaction). The results to date indicate that the (slow) intercalation is preceded by a fast preintercalation, although its molecular background is still a matter of debate [12]. Possibly the insertion of the planar ring system between the base pairs is followed by the slow rearrangement of the sugars.

3.5 Topoisomer distribution

We mentioned earlier, that the plasmid DNA in bacteria is negatively supercoiled, and that one supercoil is introduced about every 200 base pairs by topoisomerases. One could deduce, that a plasmid with 4000 bp, or 4 kbp (kilo base pairs), should consist of a single topoisomer with a ΔLk of 20 – having 15 supercoil-loops (75% writhe). Indeed, when analyzing a ccc plasmid sample with electrophoresis or chromatography, a single broad band can be seen (ccc), usually accompanied by a second small peak, which is the oc form.

However, it was found that by changing conditions (see section 2.6.3), the ccc peak can be split into more peaks showing a typical Boltzmann distribution as can be seen in Fig. 7.

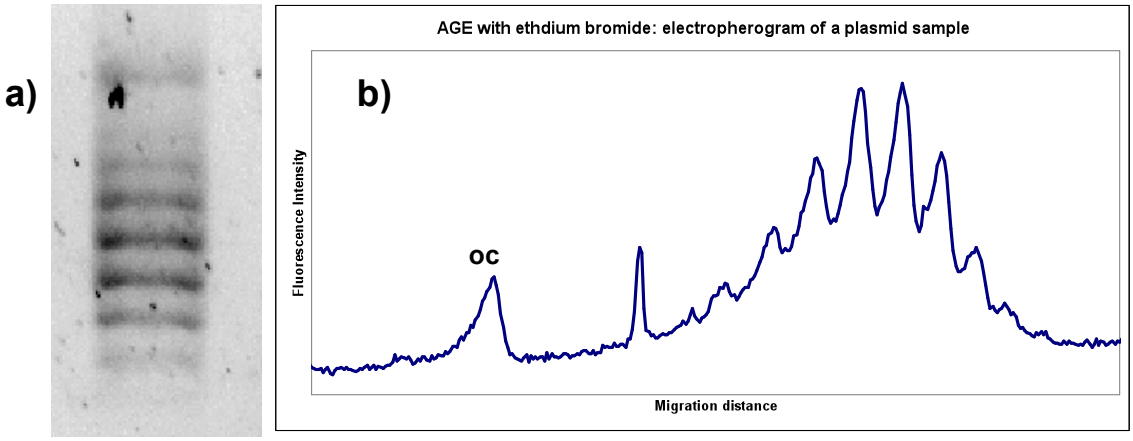

Figure 7: Deconvolution of a ccc plasmid into its topoisomers in EtBr-containing AGE (a). Densitometric quantitation of the lane is shown in (b)

The distribution arises from the way how the topoisomers are produced. Supercoiling is introduced by topoisomerases, which do not "produce" a single topoisomer but rather catalyze a topoisomer equilibrium at given conditions (temperature, salt concentration or specific additives). The energy difference between adjacent topoisomers around Lk^0 is smaller than the fluctuations of the thermal energy (kT per molecule; RT per mole) which explains why a mixture of topoisomers is present. The distribution is Gaussian (Normal) with a center at Lk^0, as follows from the equation of the Boltzmann distribution:

$$P(\Delta Lk) = A \cdot e^{\left(-\frac{(\Delta Lk)^2}{2\langle(\Delta Lk)^2\rangle}\right)} \tag{6}$$

From the concentration of each topoisomer in a mixture the free energy difference between topoisomers can be calculated:

$$\Delta G(Lk_{x-m}) = -RT \cdot ln\frac{[Lk_x]}{[Lk_m]} \tag{7}$$

Equation (7) can be rearranged by using Hooke's law and the parameter ω, defined in section 2.3.1 to yield equation (8):

$$\frac{1}{\Delta Lk} ln\frac{[Lk_x]}{[Lk_m]} = -\frac{K}{RT}\Delta Lk - \frac{2K\omega}{RT} \tag{8}$$

The constant K used here is the proportionality constant from Hooke's law. It is at first an assumption that the free energy associated with supercoiling (e.g. "twisting the DNA ends against each other") is proportional to the square of the amount of supercoiling:

$$G(Lk_x) = K(\Delta Lk + \omega)^2 \quad \text{(Hooke's law applied to topoisomers)} \qquad (9)$$

Equation (8) can be used for plotting the topoisomer distribution data with

$$y = \frac{1}{\Delta Lk} ln \frac{[Lk_x]}{[Lk_m]} \qquad \text{and} \qquad x = \Delta Lk .$$

A straight line is obtained in such plot proving that Hooke's law is valid indeed (supercoiling of DNA is an elastic process). Further, Hooke's constant and ω can be calculated from the slope and intercept, respectively [13].

3.6 Analysis of plasmid isoforms

Today's methods for the analysis of the distribution of plasmid structures in a sample were developed mainly after plasmids were considered to be used in gene therapy or DNA vaccination. There are two important criteria of purity for a plasmid sample. Firstly, it is the purity of the plasmid related to other impurities, such as genomic DNA, RNA, proteins or endotoxins. All these impurities come from bacteria where plasmids have been produced in, mainly *Escherichia coli*. Secondly, it is the purity of the therapeutically active topological form, the ccc form, related to all other topological forms. This criterion is also called homogeneity, and according to recommendations of regulatory bodies, like the Food & Drug Administration (FDA) in the US, plasmid therapeutics must have homogeneities of at least 90% ccc form.

Although this guideline came into effect many years ago, there is still a lack of techniques that would determine homogeneities reliably and accurately. In fact, there is a big need for a method that could selectively separate plasmid isoforms which is independent on the plasmid size as well as its nucleotide sequence, additionally being sensitive and especially robust. The pros and cons of the most

important methods that are in use for quality control nowadays will be discussed briefly. Also a short introduction to each method will be given.

3.6.1 Agarose gel electrophoresis

The most common method to evaluate the plasmid isoform distribution is agarose gel electrophoresis (AGE) which is also the general robust method for separating large DNA molecules. In AGE, an electric field is applied across a migration distance built of an agarose gel and a running buffer, usually TAE (Tris-Acetate-EDTA) or TBE (Tris-Borate-EDTA). The samples are loaded into compartments close to the cathode. When electric field is applied, the DNA molecules, which are negatively charged due to the phosphates in the backbone, migrate towards the anode as separated bands. The migration velocity is dependent on the amount of hindering of the molecule by the agarose network. Thus, very compact molecules migrate faster. However, in the case of pDNA the assignment of the bands is not easy, because the migration velocity and the migration sequence differ very much when operating conditions change (buffer and ionic strength, electric field, gel concentration, temperature and dye concentration). In order to identify the bands correctly, topological standards (linearized and nicked) of the investigated DNA have to be prepared and run in parallel [14].

Also, staining and thus visualizing of the DNA is done *after* the electrophoretic run, while under normal conditions, an intercalating dye is already included in the running buffer. This is because the dye alters the migration velocity and sequence. In general, the plasmid isoforms migrate in the sequence ccc, oc and linear, while the monomers migrate faster than dimers. However this is not true for all plasmids and operating conditions, as the linear form may migrate before, with or after the ccc form. The quantification of the bands can only be done densitometrically, measuring the fluorescence intensity of the DNA•dye complex @ 366 nm. To do so, different amounts of the plasmid are loaded onto the gel, the band intensities are measured after development of the gel and a calibration function can be established. With the observed linear curve the unknown concentration of a plasmid form in a sample can be calculated. However, this method suffers from low reproducibility because of the gel staining, and a small linear range (generally only 1 to 1.5 order of magnitude).

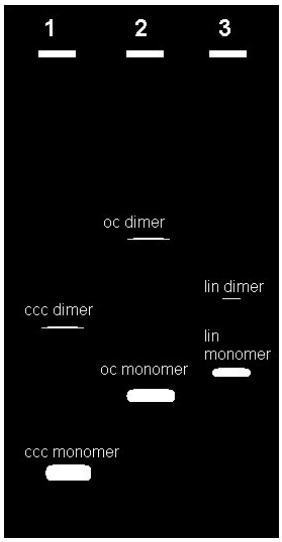

Figure 8: Example of plasmid migration sequence in AGE
Lane 1: a typical untreated plasmid sample showing two bands belonging to the ccc form. Lane 2: an UV irradiated sample creating the nicked forms. Lane 3: an incomplete enzymatic digest showing two linear forms (a complete digest does not contain the linear dimer form)

3.6.2 Capillary gel electrophoresis

A newer technique based on the same theoretical concept as AGE is an electrophoretic separation in capillary format. Just as with AGE, all DNA molecules bear a net negative charge (this is true in water above pH 4) and the mass-to-charge ratio is nearly constant so the separation must be promoted by the sieving effect of the gel, thus the technique is named capillary gel electrophoresis (CGE). The separation efficiency is mainly dependent on the sieving medium and the capillary, the walls of which are deactivated. Buffer choice is of minor importance and usually a Tris-Borate-EDTA (TBE) or phosphate-borate buffer at pH 8 – 9 is used. DNA is detected by absorbance measurement at 260 nm, although labelling with a fluorescing agent or the addition of a DNA-binding dye gives substantial improvement reaching subattomole detection limits [15]. In numbers, the sensitivity of laser-induced fluorescence (LIF) detection is superior to UV absorbance measurement by 5 orders of magnitude [16].

For small DNA fragments, usually polyacrylamide is used, for larger fragments agarose or linear polyacrylamide may be used as sieving media. Another sieving medium can be created when derivatized cellulose is dissolved in the background electrolyte, such as methylcellulose (MC) or hydroxypropyl-methylcellulose (HPMC). Today, a HPMC-containing electrolyte is the buffer of choice if separating plasmids with CGE. The resolution of large DNA molecules in

dilute polymer solutions increases with increasing chain length of the polymer and decreasing concentration. [17]

In general, CGE offers the highest resolution from all methods employed. With typical-sized plasmids, baseline resolution between all six forms (in one injected mixture) can be achieved, while no problems occur with their detection, especially if LIF is measured (see Fig. 9). A general rule for the elution order of plasmids is the following: ccc monomer, ccc dimer, linear monomer, linear dimer, oc monomer and oc dimer. However, it is advised to proof this rule for every plasmid as in many cases the forms may elute differently. For large plasmids the resolution gets much lower, but nevertheless it is still superior to all other quality control methods.

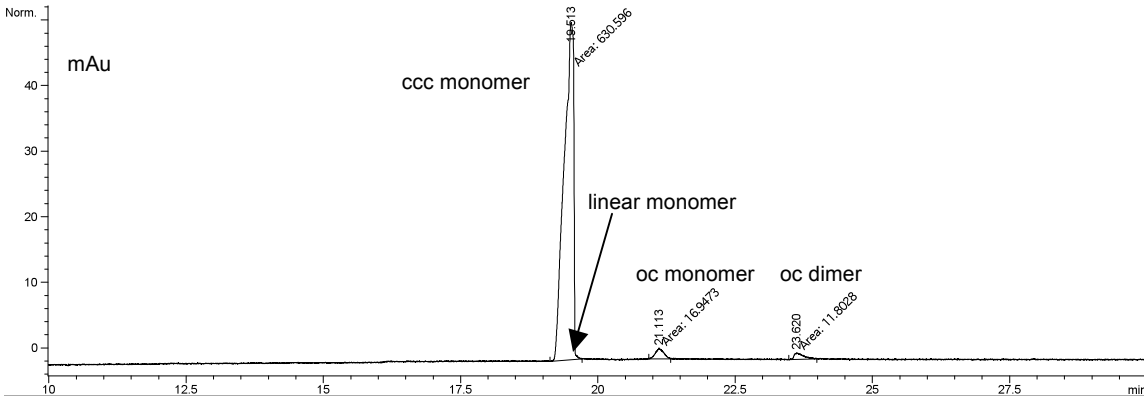

Figure 9: CGE electropherogram of a plasmid

Conditions: 89 mM TBE buffer + 0.1% HPMC pH 9.0, GC-capillary 100 µm I.D., coating thickness 0.1µm, 24 cm eff. length, injection by pressure, - 3.3 kV, 30 min run time, detection UV absorbance @ 260 nm, 25°C

For quantification of plasmid isoforms a calibration curve must be constructed, injecting different amounts of the plasmid and evaluating the peak area. Afterwards, the peak area must be corrected for the migration time, because the slower migrating molecules spend a longer time in the detection window than the faster ones. Between this corrected peak area and the concentration of each plasmid structure a linear correlation can be found. [18] The linear range is much larger than with AGE, thus reproducible results can be obtained with different plasmid concentrations applied. This makes the method also suitable for in-process-control (IPC) in a plasmid preparation process where the concentration of the plasmid is quite low.

Although CGE seems to be very promising in routine pDNA analysis, there are still some concerns about the robustness of the method. From my personal experience the migration times tend to shift, as the capillary gets older, though flushing the capillary with water and buffer after each measuring day and reequilibrating thoroughly before next day's measurement. For example, the retention time of the ccc form may vary between 15 and 20 minutes using the same capillary. On the other hand, the electropherogram pattern remains always the same, causing no problems with pDNA-form identification. Another difficulty can be seen in Fig. 9 which is an electropherogram obtained during my master thesis, where the linear and the ccc form are very close to each other with no baseline resolution or even completely overlap. Also, CE in general requires a lot of expertise and is very time-consuming.

3.6.3 Gel electrophoresis with topoisomer separation

With electrophoresis, either in conventional or capillary format, topoisomers are usually not separated. The principle of separation are the differences in mobility of the analytes, depending on the charge and hydrodynamic radius *r*. In case of topoisomers the charge of the molecules is equal, thus an electrophoretic separation is only possible exploiting differences in *r*.

Different topoisomers have the same writhe-to-twist ratio under identical conditions, when averaged over time (the fluctuations are of much faster time scale than electrophoretic separation). This is valid for such analytes during the same electrophoresis run with a single running buffer. In 1975 it was found by Depew and Wang, that the electrophoretic mobility of supercoiled plasmids is determined by the writhe value (ref. [13]). Topoisomers differing by discrete linking numbers differ also by discrete values of writhe and will hence form separate bands. However, we do see only a single ccc band in conventional electrophoresis.

Plasmids in natural occurring samples show a supercoiling of about σ = -0,06. For a 4892 bp plasmid it follows, that the mean linking number difference is -28. If writhe is, for example, 75% of supercoiling, we should observe 21 superhelical turns. A superhelical turn in this context means a writhing value of 1 (one full circle of the DNA axis). Because ccc plasmids are always present as a mixture of topoisomers (see section 2.5), species with different superhelical turns

between ~ 18 and ~ 24 should be present. However their differences in the hydrodynamic radius are so small, that the electrophoresis separation power is not sufficient to distinguish between them. This is illustrated in Fig. 10b.

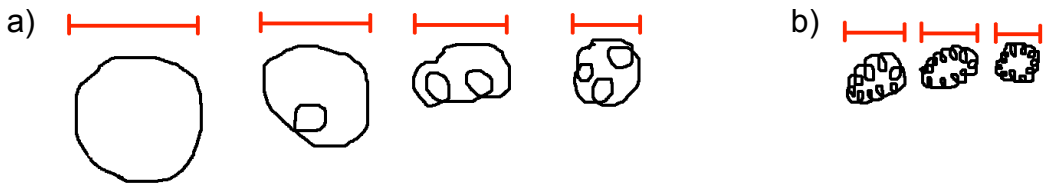

Figure 10: Illustration of the size-dependency on the writhing number. In (a), four plasmids are shown with low numbers of superhelical turns from 0 to 3. In (b), plasmids are shown with a high writhing number. The change in overall size is mostly pronounced when low writhing is present.

On the other hand, plasmids with low writhing number have sufficiently big differences in their hydrodynamic radius in order to be separated in conventional gel electrophoresis [19]. The key to the separation of highly supercoiled plasmids lies in the conversion of the writhe into twist, which can be easily done by adding an intercalator (see section 2.4) to the running buffer. Depending on the concentration of the intercalator, the primary negative writhe is lowered, i.e. superhelical turns are removed at the expense of increasing twist, until a sufficiently low writhing number is gained in order to achieve separation.

Topoisomers of same absolute writhing values but with opposite sign, e.g. Wr = +1 and Wr = -1, migrate in electrophoresis as a single band. A molecule with no writhing (Wr ~ 0) is thus the slowest migrating band in a series of topoisomers, because both adjacent topoisomers with one positive and negative supercoil, respectively, will have a smaller hydrodynamical radius and migrate faster. A plasmid with no writhing is very similar to the open circular form, thus they often comigrate. However when raising the intercalator concentration, the open circular form migrates slower and well separated from the ccc molecule with no writhing (unfortunately, both forms are often called “relaxed plasmid” in the literature).

In practice the intercalator concentration needed to reduce the writhe has to be determined for each sample, because it depends on the plasmid size and superhelicity. In general, a big-sized plasmid will need a higher intercalator concentration than a small one. Ethidium bromide (EtBr) and chloroquine (ClQ) are used almost exclusively for separation of negatively supercoiled species. Ethidium bromide has the advantage of being more popular, well characterized,

binding strongly to DNA. Chloroquine on the other hand is non toxic and thus more easy to handle.

3.6.4 Determination of superhelical turns by intercalator-containing electrophoresis

The procedure for writhe determination in natural occurring ccc DNA samples is theoretically based on the method published by W. Keller [20]. Following this method, the separation of topoisomers in a sample is carried out by means of electrophoresis containing various amounts of ethidium bromide as described in the previous section. The number of superhelical turns of a certain topoisomer within the sample in such an analysis is then referenced to a topological standard with known superhelicity by comparing the migration distances (see Fig. 11 (a)). In most cases, however, no topological standards will be available before analysis and have to be produced yet.

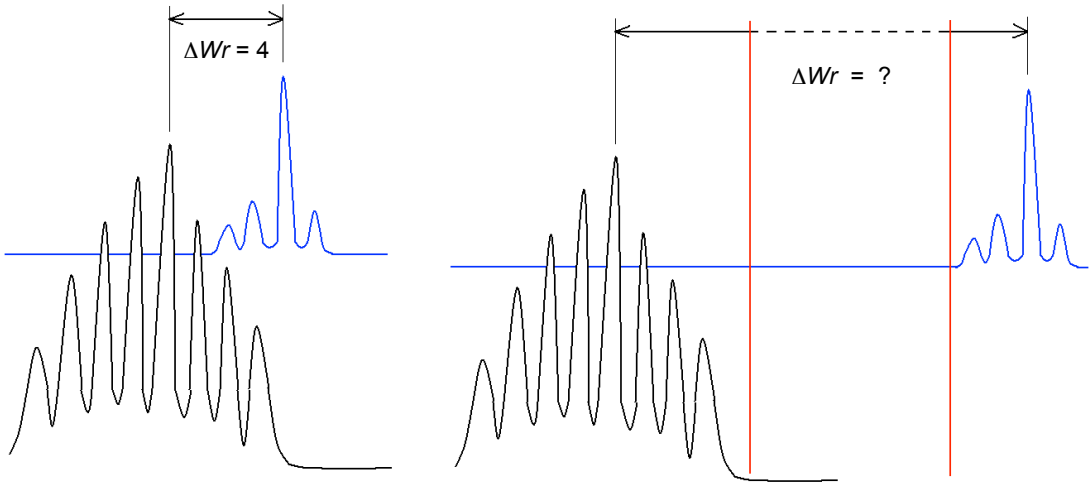

Figure 11: Writhe determination by referencing the electrophoretic migration to a defined species. If the topoisomer distributions in the sample and the reference are overlapping, the superhelical numbers can be determined directly (a). When no common species are present, a gap is produced (b).

The only reference with a defined topology, which can be prepared easily, is a 'relaxed' topoisomer with no superhelical turns (*Wr* ~ 0). Such species can be produced from any negatively supercoiled plasmid by reaction with the enzyme topoisomerase I ("Topo I"). However, positive supercoiling can be relaxed only with the eukaryotic variant. For the sake of completeness it should be mentioned, that DNA supercoiling is introduced by topoisomerase II enzymes, but unlike Topo I these enzyme require ATP. As with Topo I, the prokaryotic variant can only

introduce negative supercoiling, whereas the eukaryotic variant may introduce both, negative and positive supercoiling.

A topoisomerase I-mediated relaxation of supercoiled DNA will produce a topoisomer distribution centred around Lk^0 (see section 2.5) with flanked regions of positively and negatively supercoiled species which are visible to about +/- 5 superhelical turns (depending on the detection sensitivity). In some samples the supercoiling of the analyte DNA will be so low that its writhe can be directly determined by counting the number of topoisomers between the reference and the analyte. This is especially the case when dealing with small plasmids (< 2 kb).

However, larger sized plasmids of “normal” superhelicity have a much higher number of superhelical turns, so that their distribution does not overlap with the one produced by topoisomerase I. In this case a gap is produced when overlapping the densitometric traces of the electrophoretic lanes (see Fig. 11 (b)). This gap can be closed by producing a “topological ladder”, which leads from the analyte topoisomers to the relaxed reference standard. With this ladder, produced for every plasmid separately, the writhe is determined by counting the number of discrete bands from Lk^0 to the analyzed topoisomer distribution. This procedure is shown in Fig. 12 for a single topoisomer of a 5kb plasmid.

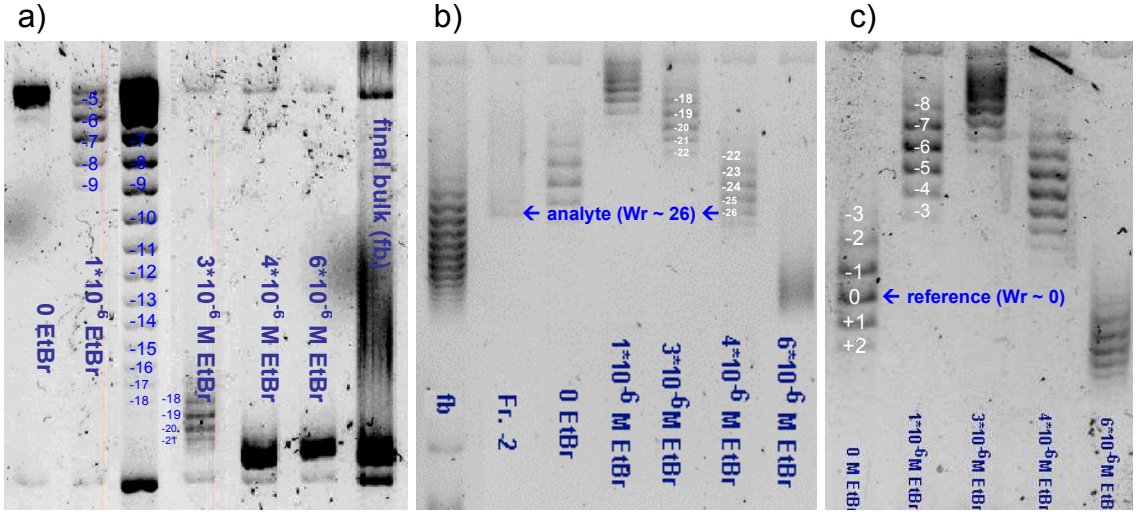

Figure 12: Agarose gel electrophoresis of topological standards with increasing writhe. Gel (a) contains no EtBr. Gels b and c contained the following EtBr concentration in the gel and in the running buffer: 5 µg/L (b) and 10 µg/L (c); The sample “Fr. -2” on gel (b) was the analyte.

Note that it is not enough to run a single gel. In general, the bigger the plasmid, the more gels have to be run in order to resolve all topological standards of the ladder into single bands. For example, the gel in Fig. 12a only resolved

standard $1*10^{-6}$ M EtBr and $3*10^{-6}$ M EtBr (for standard denotation *vide infra*). The standard with least writhe (0 EtBr) as well as samples with higher writhe ($4*10^{-6}$ M EtBr, $6*10^{-6}$ M EtBr and final bulk (f.b.)) could not be separated into single topoisomers. Thus a series of gels with different intercalator concentration (in the gel *and* the running buffer) is needed for a complete analysis. While for a 5 kb plasmid three gels were sufficient, for a 10 kb plasmid 5 to 6 gels with a different intercalator concentration each, are needed.

As can be seen in Figure 12, the topological ladder is not a single standard but a series of standards with different topoisomer distributions differing by the distribution average. Each standard contains about 6 – 8 resolvable and detectable bands. For a complete ladder these standards must overlap through the whole range between the (*Wr*~0)-reference and the analyte.

The standards are produced by relaxation of the plasmid, whose writhe has to be determined, by topoisomerase I in the presence of an intercalator. Again, ethidium bromide is used for this purpose as it is well characterized. Let us think of a 4892 kb plasmid with a Lk^0 of 466 relaxed by topoisomerase I. We obtain the following values: *Tw* ~ 466, *Wr* ~ 0. When adding ethidium bromide, the twist is decreased by, for example 10 turns. Because the topology does not change, the plasmid must adopt a positive writhe: *Tw* ~ 456 and *Wr* ~ +10. The topoisomerase relaxes this positive writhing immediately by changing the topology to *Tw* ~ 456 and *Wr* ~ 0. Subsequent removal of ethidium bromide causes an increase in twist by 10 turns and thus appearance of negative writhe under original conditions: Tw ~ 466, Wr ~ – 10. In this way a topoisomer distribution is produced with a distribution average around ΔWr ~ 10. For explanation see also Fig. 13.

With this procedure any topological standard with a negative writhe can be produced by changing the ethidium bromide concentration during the topoisomerase reaction. The lanes in Fig. 12 are denoted according to the ethidium bromide concentration during the enzymatic reaction, e.g. $3 \cdot 10^{-6}$ mol/L. If desired, positively writhed topological standards can be produced by adding netropsine to the enzymatic reaction. Netropsine is a minor groove binder which *increases* the twist upon binding to DNA.

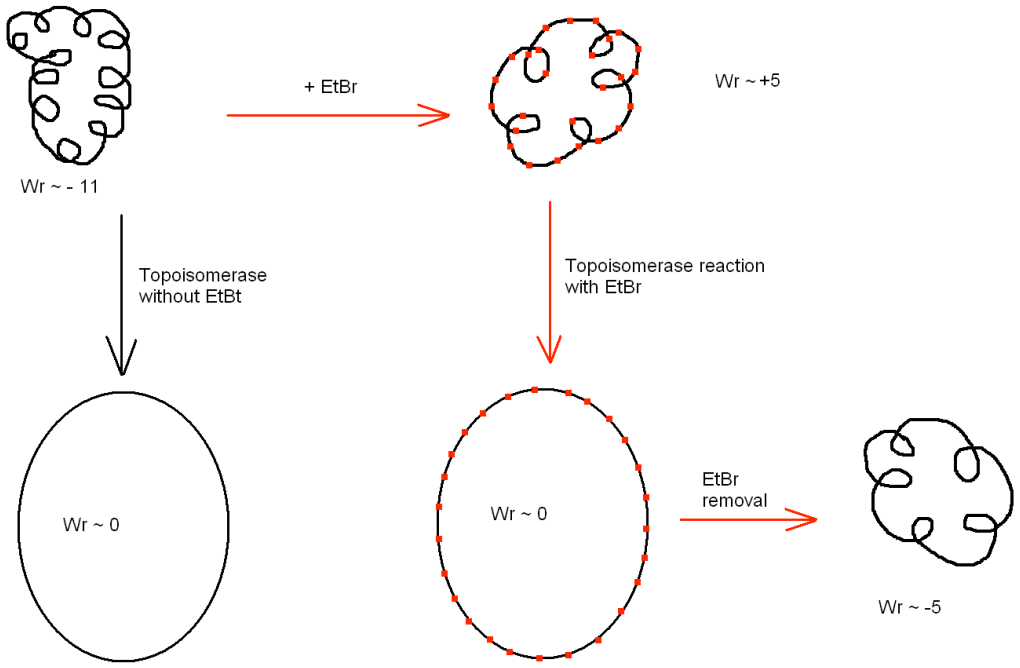

Figure 13: Relaxation of negatively writhed ccc plasmid with topoisomerase I without intercalator (black arrow) and in the presence of EtBr (red arrows). Red squares indicate EtBr molecules.

3.6.5 High-performance liquid chromatography

The last method to be described here is liquid chromatography. The status quo of LC in plasmid form separation is that it offers the least information of all other methods. [21] Practically all chromatographic methods are nowadays based on the anion exchange principle. Such a chromatogram is shown in Fig. 13. The differences mainly arise from the different supports (porous or non-porous silica beads, porous or non-porous methacrylate particles, silica or organic monoliths, superporous agarose beads) which have a huge influence on the peak shape and thus the resolution. It was also shown, that hydrophobic interaction chromatography (HIC) can be used to separate plasmid isoforms. [22] In both cases, a separation only between supercoiled and relaxed form can be achieved, the dimers here being not considered. These methods, however, are well suited for quantification of total plasmid DNA in respect to other molecules like genomic DNA, RNA or proteins [23, 24]. In contrast, a satisfactory pDNA topoisomer separation cannot be achieved.

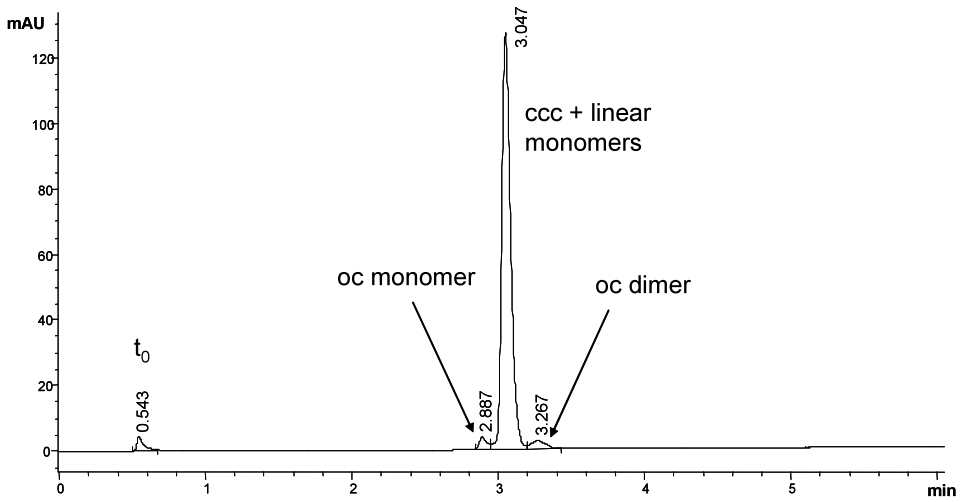

Figure 14: Chromatogram of a plasmid

Ion exchange chromatography (ligand: DEAE), DNA-NPR column (from TOSOH Bioscience), buffer A: 20mM TrisHCl, pH 9.0, buffer B: A + 1 M NaCl, 50 – 75% B in 5 min, 25°C, 3 µl inj.vol.

Separation methods based on chromatography are of great interest because of the robustness and the unlimited possibilities for implying molecular selectivity. In CE the selectivity is determined by the differences in electrophoretic mobilities and the hindrance by the gel network, both of which are physical properties, but not specific chemical criteria. On the other hand, LC is based on different analyte adsorption or distribution between a mobile and a stationary phase. Now if the stationary phase could bear functional groups able to recognize pDNA isoforms differently, a very powerful and robust method could be developed. Furthermore, a chromatographic method can be scaled up to preparative dimensions, which is impossible with CE techniques beyond certain dimensions.

3.7 Plasmids as therapeutic agents

The advent of gene therapy and polynucleotide-based vaccines has resulted in the use of plasmid DNA as a drug substance. Plasmids can be used both as gene carriers in gene therapy or as vectors carrying the code for antigen expression in genetic vaccination. In the following text I will mainly refer to the use of plasmids as genetic vaccines.

In the classical type of human vaccination, the antigen which should evolve an immune response, is introduced directly into the body, e.g. by a subcutaneous injection. The antigens can be proteins which may be parts of a bacterial or viral surface, against whom the immune response is directed. In genetic vaccination,

not the proteins, but their construction manual is introduced into the body. This has two major advantages: Firstly, the antigens are produced *in situ* with correct posttranslational modifications and three-dimensional structure, thus a correct epitope is produced, being potent for B cell (humoral immune response) stimulation. Secondly, exceptional stimulation of the cellular immune response is also achieved with pDNA vaccination. Here, peptides produced by immune-processing pathways from (pDNA encoded) protein antigens efficiently stimulate T cells. Both features are difficult to achieve with recombinant antigens that are produced in non-human, often bacterial, expression systems. Such an immune reaction and highly protective antibodies can only be produced with vaccines based on attenuated live vectors.

Plasmids used as therapeutic agents are constructs with two main parts: one for its expression, i.e. a bacterial backbone because they are produced in *E.coli*, and the second is the human transcription unit for the gene of interest. A simple plasmid with one gene to be delivered is sketched in Fig. 10. The bacterial backbone contains the origin of replication and an antibiotic resistance. The transcription unit contains typical eukaryotic gene constructs starting with a promoter (also enhancer sequences may be added), the gene itself encoding the antigen and the polyadenylation signal for terminating the transcription. However, also plasmids with different genes can be constructed to deliver two antigens or an antigen and a cytokine/chemokine at the same time.

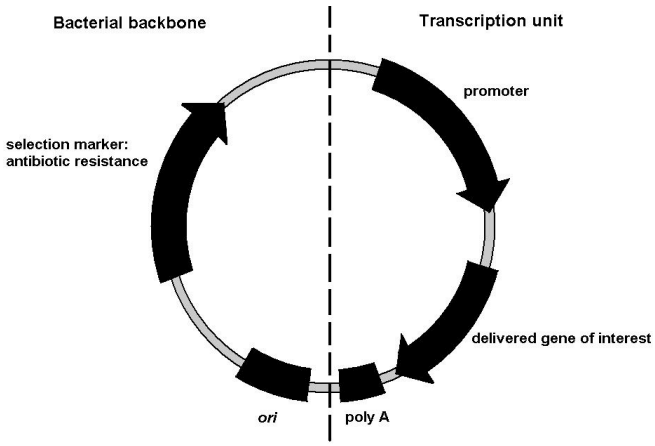

Figure 15: Construct of a therapeutical plasmid
(picture from: Schleef, "Plasmids for Therapy and Vaccination", 2001, Wiley-VCH)

Supercoiled (ccc) plasmids seem to ensure the most efficient transient transfection *in vivo* into immunologically relevant cells. These constructs cannot

replicate in eukaryotic cells and the chances for their integration into the host cell genome are minimized.

There are currently three ways for delivering plasmid DNA into an organism. The DNA may be injected non-packed, i.e. “naked”, requiring the highest amount of DNA, namely 50-100 µg per mouse. Another way is to package the DNA into cellular transport vesicles, such as liposomes, polymers or viral containers. Here the doses are lower than 50 µg down to 1 µg per mouse. Plasmids may also be coated onto gold particles that are shot with the gene gun into the skin delivering between 0.1 – 1 µg nucleic acid. There are different *routes* for delivering these formulations into the organism, but none of them is clearly outstanding. Much improvement is necessary to deliver pDNA with high transfection efficiency and in a way that ensures access of the gene product to antigen-presenting cells which primes the immune response. In this sense, viral vectors are more effective than DNA-based vectors. [25] It is estimated that only 1‰ of all plasmid molecules reaches the nucleus and is expressed. [26] Therefore, before going to market, large-scale manufacturing processes must be developed.

This arises the question what makes plasmid DNA vaccination so interesting? On one hand, it is the generation of the correct epitope *in vivo*, which can only be generated using attenuated live vectors. Here another advantage can be seen, that the DNA vaccination is certainly more cost effective and easy to store compared to live vectors. Another big advantage is that under different delivering conditions, it is possible to regulate the desired T cell response thought to play an important role in the treatment of allergic diseases. T cells are generally classified into two groups, those bearing a CD4 receptor and the other ones with a CD8 (T killer cell, cytotoxic T lymphocyte – CTL). The T helper cells with a CD4 receptor can further be divided into Th1 and Th2 subtypes, producing Th1-type and Th2-type cytokines, respectively. Th1 type cytokines such as interferon gamma (IFN-γ) tend to produce the proinflammatory responses responsible for killing intracellular parasites and for perpetuating autoimmune responses. The Th2-type cytokines include interleukins 4, 5, and 13, which are associated with the promotion of IgE and atopy, and also interleukin-10, which has more of an anti-inflammatory response. [27] But not only a Th1/Th2 bias can be controlled, the immune response can also be primed towards T killer cells partly independent of

the T helper cell level. This is especially interesting for immunocompromized patients with acquired or genetic defects.

DNA vaccines were also shown to be able to override non-responder status being more potent than recombinant vaccinia virus in preclinical animal models. [28] Further they can be directed towards internal viral antigens, i.e. those who do *not* change their structure. Usual vaccines are directed against outer (envelope) proteins of a viral capsid that changes with time, as is well known from the human immunodeficiency virus. For example in the case of influenza virus, DNA vaccination leads to better protection. In the treatment of complex infections, where a priming injection is followed by boosting injections, DNA vaccination may also lead to better results. It has been shown that different vaccine formulations stimulate T cell responses more effective than usual protocols with the same formulation. [29]

DNA vaccines are tested in many areas for medical use, but these are the four main fields of interest in human and veterinary medicine: [30]

- control of infectious disease
- immune therapy of cancer
- specific treatment of autoimmune disease
- immunomodulation of allergic disease

DNA immunization is certainly an exciting new field in medical treatment, but more data and experiments are needed to critical evaluating the data. One should not forget about the potential risks of bringing foreign DNA into an organism.

3.8 Preparative purification of Plasmid DNA

My project was started as a cooperation with the pharmaceutical company Boehringer-Ingelheim RCV producing, among other products, plasmids. The field of interest lied, and still lies, in improvements of the downstream processing of plasmids produced in bacteria. Large-scale plasmid purification for human use is the bottleneck in plasmid production, because under laboratory conditions, it is not a big deal to obtain low amounts of plasmids very quickly. However, plasmid purification kits available on the market do not meet specifications for industrial production. Some methods deliver only low purity plasmids, some are not up-scalable and others do not meet product requirements intended for human use.

Generally three specifications must be fulfilled for an industrial process producing clinical-grade pDNA: [31]

- the product must be a plasmid bulk with the highest possible quality grade of pDNA, free from contaminating bacterial components
- the process must produce a cost-effective yield per volume of culture broth and biomass equivalent
- there must be compliance with regulatory guidelines

Process development is divided into three main sections. Firstly it is the construction and selection of appropriate expression vectors and production microorganisms (upstream processing), followed by the selection and optimization of fermentation conditions (fermentation) and finally the isolation and purification steps (downstream processing). These three sections should not be approached individually, but rather one has to bear in mind, that especially downstream processing is greatly dependent on the conditions for upstream processing and fermentation. [32] For example, plasmid DNA is produced almost exclusively by the cultivation of *Escherichia coli*, thus the knowledge about the genetic background can influence the yield and quality of harvested pDNA. In particular, mutations of genes encoding enzymes involved in nucleic acid–related processes can dramatically improve the final pDNA quality. [33] However, there is nothing like a “guide” or an “overview” for suggesting the optimum bacterial strain for a particular plasmid in literature; rather the most suitable host-strain combination has to be evaluated on a case-by-case basis.

After a suitable fermentation procedure was found, the plasmids need to be isolated from the culture medium. Because no hydrodynamic shear forces can be used in order to protect the supercoiled form, a technique for releasing plasmids from bacterial cells known as alkaline cell lysis has been developed. During this procedure, the releasing effect is achieved by a combination of sodium dodecyl sulfate (SDS) and alkaline pH typically around 12. On the industrial scale special mixing equipment is needed. After lysis, plasmid DNA needs to be isolated from the crude lysate by different steps summarized as downstream processing.

After recovering the lysate one or usually more purification steps take place. A good overview of different published techniques for capture, purification and polishing of pDNA can be found in [34]. The following techniques may be used,

either alone or in combination with another: extraction, HIC (hydrophobic interaction chromatography), AIEX (anion exchange chromatography), RPC (reversed phase chromatography), SEC (size exclusion chromatography), PEG/alcohol/$(NH_4)_2SO_4$/ CTAB precipitation, IMAC (immobilized metal affinity chromatography), anion-exchange membrane separation or ultradiafiltration. However, most of the processes are time-consuming and not scalable, or during their application substances are used that do not meet the appropriate guidelines of the regulatory authorities (enzymes of avian or bovine origin; use of toxic reagents such as phenol or caesium chloride). Those techniques that are in use for pharmaceutical pDNA production include only methods based on chromatography and precipitation with a non-toxic reagent.

Chromatography is considered here as the method with highest resolution and highest variability and adaptability, therefore being essential for pDNA production. No wonder it *is* chromatography, which has to be tuned for plasmid DNA separation to make the manufacturing process move into the final clinical phases up to reaching the market. The company Boehringer-Ingelheim RCV uses a three-step chromatographic process to purify its plasmids [35]. The combination consists of HIC as the capture step, AIEX for purifying and SEC for polishing. During the first step, all RNA is removed chromatographically and not by use of enzymes as these should be avoided. The samples used during this work were the final bulk solutions after the polishing step.

Apart from the impurities, which are removed by the different selectivity principles, the chromatographic supports should also be suited for pDNA purification. They should have high binding capacities and give the necessary performance for removing impurities (and concentrating the desired substance) in a reasonable amount of time. Unfortunately, not many supports for bioapplications meet these specifications, because the largest fraction of them was developed for proteins.

One way to improve the analytical performance for pDNA chromatography is using non-porous particles; however their binding capacities compared to its porous relatives are much lower. Another very exciting new support seem to be a monolithic one, which is a continuous bed of flow-through pores, whose porosity and pore size can be controlled to a satisfying level. The experiments with methacrylate-based monoliths (ligand: diethylaminoethyl, DEAE) show, that the

binding capacities for plasmid DNA may be by more than an order of magnitude higher than with conventional media suited for protein separation. [36] To give a comparison of the size, the monolith had a pore diameter of 1.5 µm while the hydrodynamic radius of the 5kb plasmid was between 45 and 70 nm (depending on the salt concentration in the mobile phase).

Another group could show a separation of pDNA (all forms co-eluted) from all other impurities such as genomic DNA and RNA using monolithic DEAE-discs [37]. By using 15% isopropanol as an additive to the mobile phase and a linear salt gradient, a baseline separation from other impurities was achieved within a very short time. At the moment, monolithic columns are in the process of up-scaling in order to test their suitability for the industry. Their practical advantage over classical particulate supports is that they can be produced very easily in capillaries for a rapid screening and monoliths with either activated or specific ligand groups can be generated by in situ polymerization. [38]

4 Aim of the thesis

The objective of this thesis is the development of a generic method for chromatographic separation and analytical quantitation of linear, open circular, ccc and multimeric plasmid variants. The basis for this is the development of newly designed stationary phases according to chemoaffinity principles with enhanced separation characteristics. Systematic correlations between plasmid size and separation properties should be established in order to be predictable for other analytes (plasmids) beyond this work.

For this purpose different chromatographic ligands should be synthesized and immobilized on suitable stationary phases in order to be screened on their separation properties. Beside the ligand structure, other parameters such as anchor chemistry, ligand density and spacer length should be studied and optimized. At the focal point of these studies is the analytical employment of a potential separation method, including in addition to the mentioned parameters a method validation as well. In this context the precision, detection and quantitation limits as well as the recovery should be part of the method characterization. The recovery represents an important issue for the open circular form, whose concentration was found to be underestimated in mid-sized plasmids (4 – 8 kbp) in chromatography and no recovery is obtained with large plasmids on current state-of-the art methods, respectively.

If applicable, an analytically successful material with the corresponding method may be employed for preparative use by transferring the surface chemistry onto a suitable support. In this context, selectivity, loading capacity and stability of such material has to be evaluated.

This was the original aim of the project, however, as mentioned in the preface, a second general topic arose after a topoisomer separation on one of our chromatographic supports has been achieved. The objective of this second general topic was the proving of the separation itself and the determination of the fundamental separation principle. After that, a generic method should be found for chromatographic separation and analytical determination of the topological distribution in a ccc plasmid sample. Systematic correlations between plasmid size

and separation properties should be established in order to be predictable for other analytes (plasmids) beyond this work.

Further, a two-dimensional chromatographic setup should be set up for the automated determination of both, the concentration of plasmid isoforms (general topic 1) and analysis of the topoisomer distribution (general topic 2) in a single run. For both general topics, the analysis should be possible with non-purified samples as well, i.e. those from the in-process control (IPC samples) or from downstream processing. Additional purifying steps may be necessary to achieve this, however an online pre-purification is preferred in this context.

5 Results

A brief overview is given over the most important results achieved during my PhD thesis. A more detailed description of the approach, methods, results and discussion is given in the papers and in the appendices later in this book. The results here are split into two parts, according to the two general topics.

5.1 General topic 1: separation of plasmid isomers (oc, lin, ccc, others)

In the course of the work presented, three plasmids of different sizes (5 kbp, 10 kbp and 15 kbp) have been employed. A generic chromatographic method capable of base-line separation of all plasmid isoforms for all plasmids could not be found. However, many very important aspects on the way there have been discovered, which we will mention here.

One of the two main issues in plasmid analytics is the poor recovery of the open circular form. This effect can be seen in many chromatographic modes, be it anion exchange chromatography (AIEX), size exclusion chromatography (SEC) and even ion-exclusion chromatography with cation exchangers. In all cases, only the oc form shows poor recovery, the ccc and lin forms are never affected. It is not entirely clear why, however we have found possible solutions to enhance the oc recovery [39].

We have found that the silica gel surface shows better recoveries than polymethacrylate surfaces. This is due to silanol groups on the silica surface, being equally charged as the plasmid molecules (negative), when applying a suitable pH value of the mobile phase (pH > 7). To maximize the interaction with the silanol groups, a short spacer between the surface and the chromatographic ligand must be employed in order to exploit the silanol effect. The highest recoveries (up to 100% for all forms) have been found when a pH gradient was employed up to a pH near 8. This ensures an entire negatively charged silica surface and thus the elution of all plasmid forms. Such a chromatographic mode was indeed chosen as the final method for validation because of high recoveries.

In this context it has to be mentioned, that research was undertaken to explain the phenomenon of low oc recoveries. Because it was possible to elute the

oc form with a pH change, the oc must have been present in the chromatographic system intactly. With no column installed, the oc gives (nearly) full recovery as expected. Thus the column alone must be responsible for reversible adsorption. The frits after plasmid DNA containing chromatographic runs have also been tested for adsorption by ethidium bromide staining. It was found, that glass wool used at the column head between inlet frit and packing adsorbs plasmidic DNA, but stainless steel as well as a titanium-steel alloy does not. Thus, steel frits should be preferably mounted in columns intended for plasmid analysis without additional glass wool filters.

The second main issue of a chromatographic plasmid separation was an invariant elution order combined with a steady selectivity between the isoforms. The most critical analyte pair was the oc / ccc pair, which can now be separated on our novel materials very well. We are convinced, that our novel chromatographic columns provide accurate values on the oc content of plasmid-containing samples.

Further, the linear form eluted on our columns close to the oc form but before the ccc form, making the following elution order valid for all plasmids: oc < lin < ccc. However, the resolution between the linear and the oc form was found to be mainly dependent on the flow channel size of the chromatographic bed, i.e. on the particle size of a packed column or on the flow-through pore size of a monolithic column, respectively. The best results can be achieved with particular materials of about 1.5 – 2.5 µm diameter, while 1 – 1.5 µm flow-through pores work best with monolithic materials. The main issue in this context is the availability and handling of such a material. With a standardly employed, 5µm particular material, still a fair oc/lin resolution can be obtained to provide satisfying information. For comparison, on the state-of-the-art AIEX material, the elution pattern changes with plasmid size and/or gradient slope due to discrepancies in the elution time of the linear form. Such effects have not been observed on our novel materials.

The multimeric forms, denoted as “others” in the course of this work, could not be separated well from the ccc form on our columns. This comes from the broad ccc peak itself, on the end of which the multimeric forms elute. When present in usual concentration (< 5%), these “others” cannot be identified as peaks nor integrated. Hence, a combination of our novel material and method is

necessary to provide full information about the isoform distribution in a plasmid sample.

5.2 General topic 2: separation of ccc topoisomers

The power to separate ccc topoisomers of a plasmid, i.e. circular pDNA with different topology, was found during optimization of the separation in general topic 1. While changing temperature, salt concentration and buffer type, initially an unusually broad ccc band was split into about 20 discrete and slim peaks evoking a Gaussian distribution. On re-chromatography of individual isolated fractions, the peaks have not changed the elution time nor produced the Normal distribution, thus, discrete species must have been present [40].

Employing capillary gel electrophoresis (CGE) with and without chloroquine as an intercalator for natural samples, a similar distribution was obtained. The slim peaks, isolated by our novel chromatographic method, were resolved in the same manner on CGE with chloroquine. Because the CGE method for topoisomer separation was described in literature, it was a proof that our chromatography could separate the very same. Later, the presence of topoisomers was confirmed by AGE running the sample along with a topological ladder and also, the number of superhelical turns in the natural sample was determined for the 5 kbp and the 10 kbp plasmid.

To proof the presence of different topoisomers within the observed distribution, HPLC fractions from a semipreparative run were inspected by atomic force microscopy (AFM). Due to high DNA condensation, small bionanoparticles were obtained upon imaging on 3-aminopropyl-modified muscovite mica, the topology of which was unable to analyze from the images. Therefore, the clusters were relaxed in presence of chloroquine in order to see individual DNA strands throughout whole plasmid molecules [41].

The separation of topoisomers was further studied in detail and optimized, with the following conclusions: The spacer between the surface and the chromatographic ligand must be long, to provide enough distance between the silanol groups and the analyte. A salt gradient must be employed during analysis, with a superimposed isopropanol gradient being beneficial. The chromatographic ligand must have an anion exchange and a H-donor/acceptor moiety, being separated in space by a specific distance. An intercalator moiety is beneficial, but

not necessary, for separation. Also, higher temperature must be employed, although the reason for that remains unclear [42].

An analysis of plasmid samples drawn during the downstream process revealed that the topology does not change during purification. However, a change has been monitored when analyzing in-process control samples. There, the ccc plasmids present at the beginning of the fermentation have a different distribution average than the ccc plasmids present at the end. We believe, that the topoisomerase I and II activities are different at the very beginning and at the end of the manufacturing process. The biggest change in the distribution average takes place in the first few hours of fermentation, then the topology levels off. Until now, we could not reliably show if there is a night/day cycle dependency or not.

The analysis of the samples from the in-process control and downstream processing was not possible by direct injection of the cell lysate (NaOH/SDS lysis). The sample constituents, provide so much background that it is impossible to analyze the topoisomer distribution. Further, a very rapid clogging occurs with no pre-purification. Thus, a two-dimensional setup was employed for the 2D HPLC analysis.

In the first dimension, size exclusion chromatography (SEC) was used to isolate plasmidic DNA from the lysate. The pDNA fraction was then loaded onto our novel material and analyzed for topoisomers. If the plasmid amount within the cell is not sufficiently high to give well evaluable signals, a plasmid pre-concentration must precede the 2D HPLC analysis. Anyway, until now all “realistic” plasmid samples have been analyzed for their topology successfully.

In summary, new selectivities for plasmid isoform and plasmid topoisomer separation have been found and characterized on quinine-based stationary phases. Recovery, robustness and up-scaling possibilities have been improved compared to commercially available phases. Secondly, topoisomers of different linking numbers can be separated conveniently, fast and with nearly baseline resolution. In the future, isoform separation should be further optimized to provide baseline separation of all species including multimers. Atomic force microscopy should further allow us to get a more detailed view on these multimeric species as well as different topoisomers.

6 References

[1] Martinez-Robles ML, Witz G, Hernandez P, Schvartzman JB, Stasiak A, Krimer DB (2009) Nucleic Acids Res. 37:5126-5137

[2] Goldstein E, Drlica K (1984) Proc. Natl. Acad. Sci. U. S. A. 81:4046-4050

[3] Mirkin SM (2001) Encyclopedia of Life Sciences 1-11

[4] Bauer WR (1978) Annu. Rev. Biophys. Bioeng. 7:287-313

[5] Bates AD, Maxwell A (2006), DNA Topology, DNA Supercoiling, 2nd ed. Oxford University Press, New York

[6] Bauer WR, Crick FHC, White JH (1980) Scientific American 243:118-124, 126, 129-130, 132-113

[7] Fuller FB (1971) Proc. Nat. Acad. Sci. U. S. 68:815-819

[8] Bednar J, Furrer P, Stasiak A, Dubochet J, Egelman EH, Bates AD (1994) Journal of Molecular Biology 235:825-847

[9] Escude C, Sun J-S (2005) Top. Curr. Chem. 253:109-148

[10] Pulleyblank DE, Morgan AR (1975) J. Mol. Biol. 91:1-13

[11] Benevides JM, Thomas GJ, Jr. (2005) Biochemistry 44:2993-2999

[12] D'Amico ML, Paiotta V, Secco F, Venturini M (2002) J. Phys. Chem. B 106:12635-12641

[13] Depew RE, Wang JC (1975) Proc. Natl. Acad. Sci. U. S. A. 72:4275-4279

[14] Schmidt T, Friehs K, Schleef M, Voss C, Flaschel E (1999) Analytical Biochemistry 274:235-240

[15] Foret F, Křivánková, L., Boček, P. (1993), Capillary Zone Electrophoresis, Wiley-VCH, Weinheim

[16] Zhu H, Clark, S.M., Benson, S.C., Rye, H.S., Glazer, A.N., Mathies, R:A: (1994) Anal. Chem. 66:1941-1948

[17] Barron AE, Sunada, W.M., Blanch, H.W. (1996) Electrophoresis 17:744-757

[18] Schmidt T, Friehs, K., C., Flashel, E. (1996) J. Biotechnol. 49:219-229

[19] Mao DT, Levin JD, Yu L, Lautamo RMA (1998) Journal of Chromatography, B: Biomedical Sciences and Applications 714:21-27

[20] Keller W (1975) Proc. Natl. Acad. Sci. U. S. A. 72:4876-4880

[21] Schleef M (ed.) (2001), Plasmids for Therapy and Vaccination, Wiley-VCH, Weinheim

[22] Marquet M, Horn, N.A., Meek, J.A. (1997) Biopharm 5:42-50

[23] Ferreira GNM, Cabral, J.M.S., Prazeres, D.M.F. (1999) Pharm. Pharmacol. Commun. 5:57-59

[24] Tiainen P, Gustavsson, P.-E., Ljunglöf, A., Larsson, P.-O. (2007) J. Chromatography A 1138:84-94

[25] Luo D, Saltzman, W.M. (2000) Nature Biotechnol. 18:33-37

[26] Crystal RG (1995) Nature Med. 1:15-17

[27] Berger A (2000) British Medical Journal 321:424

[28] Schirmbeck R, Böhm, W., Ando, K.-I., Chisari, F.V., Reimann, J. (1995) J. Virol. 69:5929-5934

[29] Hanke T, Neumann, V.C., Blanchard, T.J., Sweeney, P., Hill, A.V., Smith, G.L., McMichael, A. (1999) Vaccine 17:589-596

[30] Reimann J, Kwissa, M., Schirmbeck, R. (1999) In: Schleef M (ed) Genetic Vaccination with Plasmid Vectors, Wiley-VCH, Weinheim

[31] Werner RG, Urthaler, J., Kollmann, F., Huber, H., Necina, R., Konopitzky, K. (2002) Pharmaceutical Technology Europe supplement issue

[32] Ferreira GNM, Cabral, J.M.S., Prazeres, D.M.F., Schleef, M. (1999) In: Schleef M (ed) Plasmid Manufacturing - An Overview, Wiley-VCH, Weinheim

[33] Durland RH, Eastman, E.M. (1998) Adv. Drug Del. Rev. 30:33-48

[34] Urthaler J, Buchinger, W., Necina, R. (2005) Acta Biochimica Polonica 52:703-711

[35] Urthaler J, Buchinger W, Necina R (2005) Chem. Eng. Technol. 28:1408-1420

[36] Zöchling A, Hahn, R., Ahrer, K., Urthaler, J., Jungbauer, A. (2004) Journal of Separation Science 27:819-827

[37] Branovic K, Forcic, D., Ivancic, J., Strancar, A., Barut, M., Gulija, T.K., Zgorelec, R., Mazuran, R. (2004) J. Chromatography B 801:331-337

[38] Hahn R, Podgornik, A., Merhar, M., Schallaun, E., Jungbauer, A. (2001) Anal. Chem. 73:5126-5132

[39] Mahut M, Schuchnigg, H., Urthaler, J., Buchinger, W., Laemmerhofer, M., Lindner, W. (2010), "Chromatographic separation of plasmid DNA isoforms with quinine-based ligands", *to be submitted*

[40] Mahut M, Laemmerhofer, M., Lindner, W. (2010) "Chromatographic separation of plasmid topoisomers of different linking numbers ", *to be submitted*

[41] Mahut M, Leitner, M., Laemmerhofer, M., Hinterdorfer, P., Lindner, W.; (2010); "Time-resolved chloroquine-induced relaxation of supercoiled plasmid DNA bionanoparticles"; *to be submitted*

[42] Mahut M, Laemmerhofer, M., Lindner, W. (2010) "Stationary phase characteristics for chromatographic separation of circular plasmid DNA topoisomers", *to be submitted*

7 Acknowledgements

First and most of all I would like to pay credit to both of my supervising professors Lindner and Lämmerhofer. We have all went through many challenges in and outside the laboratories, but I have a good feeling about what we have achieved and I am sure that this work would not be possible without any of my professors. I have been part of their working group for four years now, and I am very proud that I have received the invitation to work as a diploma and a PhD student in one of the best groups of our university.

With their knowledge, which sometimes seemed to me to be unlimited, I have overcome most of the obstacles and I have also *understood* all problems and issues that came up during this work. I am absolutely sure, that all future perspectives and aims of this project will be accomplished under their supervision and that the topic of plasmid separation will be connected with both professors within the scientific community.

I express many thanks to our company partners from Boehringer-Ingelheim RCV. Of course, I appreciate the funding of this project and the provision of instruments, but there are more important aspects to note. I would like to thank the group leaders Wolfgang Buchinger and Jochen Urthaler for introducing us, the university researchers, into the complex of difficulties in plasmid separation and for setting up and keeping up this project together with us from the beginning and during the milestone meetings, which nearly always exceeded the reserved time amount. My special thanks go to Hermann Schuchnigg, with whom we critically discussed all the details of the work and who was always keen to help me wherever it was possible.

During this work I cannot forget the help that came from my colleagues in my working group, especially Peter Frühauf's assistance with the IT infrastructure as well as everything concerning chromatographic supports from the first steps of modification up to column packing. I very much appreciate the important work of Parisa Ghazidezfuli and Elisabeth "Sissy" Haller, who have both showed big enthusiasm and motivation, and helped me prominently with agarose gel

electrophoresis and validation. Hereby I also thank the whole group of the institute for biophysics in Linz, professor Peter Hinterdorfer, Andreas “Andi” Ebner and Andreas “Andi 2“ Reiniger for making AFM measurements possible and critically reviewing our manuscript. I specially thank Michael “Mike” Leitner, who has sat with me at the AFM setup from the very beginning and showing my plasmid molecules to me for the first time.

I also thank all other group members, which make the atmosphere in our working group much better, funnier and more family-like – all those that have left us (and still drop in from time to time), all those that are still sweating here in this summer, and especially all those that are still here with me, that I know since the first laboratory course in 2002 when I began to study chemistry at the University of Vienna.

Finally my warmest thanks go to my family, especially to my parents, who made two very important and right decisions many years ago, by sending me to an Austrian school in 1990 and answering my dreams and wishes by supporting my studies of chemistry on a technical college and university-level since I was fourteen. It was hard sometimes, but it was definitely worth it.

Thank you!

8 List of publications

The manuscripts have not been published yet, but are expected to be submitted during 2010.

Manuscript 1:
Marek Mahut, Michael Leitner, Andreas Ebner, Michael Lämmerhofer, Peter Hinterdorfer, Wolfgang Lindner
“ Time-resolved chloroquine-induced relaxation of supercoiled plasmid DNA bionanoparticles “

Manuscript 2:
Marek Mahut, Hermann Schuchnigg, Jochen Urthaler, Wolfgang Buchinger, Wolfgang Lindner, Michael Lämmerhofer
“ Chromatographic separation of plasmid DNA isoforms with quinine-based ligands “

Manuscript 3:
Marek Mahut, Parisa Ghazidezfuli, Wolfgang Lindner, Michael Lämmerhofer
“ Chromatographic separation of plasmid DNA topoisomers of different linking numbers “

Manuscript 4:
Marek Mahut, Wolfgang Lindner, Michael Lämmerhofer
“ Molecular recognition principles and stationary phase characteristics for chromatographic separation of circular plasmid DNA topoisomers “

Manuscript 1

Title: Chromatographic separation of plasmid DNA isoforms with quinine-based ligands

Authors: Marek Mahut[1], Hermann Schuchnigg[2], Jochen Urthaler[2], Wolfgang Buchinger[2], Michael Lämmerhofer[1], Wolfgang Lindner[1]

[1] University of Vienna, Department of Analytical Chemistry, Waehringer Strasse 38, A-1090 Vienna, Austria
[2] Boehringer-Ingelheim RCV, Dr.Boehringer Gasse 5-11, A-1121 Vienna, Austria

Abstract:

This paper describes a novel method for separation of plasmid isoforms that are naturally present in plasmid samples: covalently closed circular (ccc), open circular (oc) and linear (lin) form. We found that silica based chromatographic support in combination with a suitable pH range of the mobile phase facilitates full recovery of all plasmid species from the chromatographic system. In this context, the spacer length between the silica surface and the chromatographic ligand must be short to promote repulsive silanol interaction. Further, the observed elution pattern (oc < lin < ccc) is constant upon changes of mobile phase, gradient slope and plasmid size. In the course of the study, parameters of the chromatographic support (particle size, porosity, spacer length) and of the mobile phase (elution type, pH, temperature, organic modifier content) have been varied to find a powerful method for plasmid isoform analysis.

The separation itself is governed by quininecarbamate-type ligands, which have not been employed for this type of chromatography before. The ligand contains a well defined arrangement of a H-donor, H-acceptor, anion exchange as well an intercalating moiety. Hence the plasmid isoforms interact with the ligand in a defined way, ensuring an invariant elution order. A quinoline ring system provides additional selectivity because the isoforms have different affinities for intercalators. Thus, we present a new concept for separation of very large biomolecules based on molecular recognition principles.

Keywords:
plasmid DNA, plasmid isoform separation, quinine carbamate

1. Introduction

Plasmid DNA is an extrachromosomal genetic unit providing its host cell with additional functionalities. Since the discovery of the great potential for use as a genetic therapeutic or a vaccine, much attention is paid to biotechnological production of these novel type of drugs [1]. From more possible isoforms, the so called covalently closed circular (ccc) form is considered to be most active for therapeutics. Pharmaceutical grade ccc plasmid DNA is often produced by fermentation in *E.coli*, followed by cell harvesting, alkaline lysis and multi-step purification of pDNA [2]. For human gene therapy, all these steps must meet regulatory guidelines, such as the absence of non-animal substances in the final product (e.g. bacterial enzymes and endotoxins) or avoiding the use of toxic reagents [3]. Additionally, a high content of the ccc form relative to other pDNA isoforms is recommended in the final formulation of the bioactive drug [4].

During upstream and downstream processing as well as in the quality control, there is a demand for a reliable analysis of the plasmid isoform

distribution. Other isoforms, that have to be monitored are the open circular form (oc), generated from the ccc form by a single nick in the DNA backbone, and the linear form (lin), which is formed when two nicks are in close vicinity. Apart from these monomeric forms, also di- and oligomeric species may be generated during fermentation [5], such as concatemers and catenanes, especially with high-copy number plasmids [6]. Capillary electrophoresis offers the highest resolving power [7], but suffers from low robustness, low sample salt-tolerance and is more time-consuming, which is why methods based on liquid chromatography are preferred. A large number of different chromatographic applications [8] and different chromatographic supports [9] [10] [11] [12] [13] [14*] are available for preparative plasmid purification of various quality preferences. However on analytical scale the choice is very much restrained to anion exchange columns, such as the DNA-NPR from Tosoh Bioscience or GenPak FAX from Waters, employing the same basis material, i.e. non-porous 2.5 µm particles composed of a hydrophilic organic polymer with diethylaminoethyl (DEAE)-based ligands.

Micropellicular stationary phases seem to be the most promising option for analytics, because of a thin retentive layer at the surface of a non-porous particle [14]. Porous supports with mid-sized pores used for small molecules do not allow the biomolecules to enter inside [15], which is consistent with our findings. Large and gigaporous materials suffer from slow mass transport and low sample recovery. Monoliths are a very promising alternative to particulate materials [16], because of excellent binding capacities and ultra-short analysis due to high resolution at fast column flow and no mass transfer limitation [17].

Although the type of stationary phase is very important as we will show later, we paid much more attention to the chromatographic ligand. Chromatographic ligands employed in ion exchange chromatography for plasmid separation are based on simple tertiary (such as DEAE) or quaternary (such as Q) amines. These rather unspecific groups separate nucleic acids according to the number of negative charges of the analyte [18] [19]. When analyte differ by tertiary structure but bear the same net charge, such as pDNA isoforms, the separation depends on charge density and hydrodynamic factors [20] (strictly speaking, the charge between the ccc, oc and lin forms differ by 1, however this can be neglected over the whole molecule). Effects, similar to slalom chromatography, can be observed which cause the pDNA isomer separation to be dependent on the flow-rate and gradient slope [21]. For this reason we chose to employ ligands able to form accurately defined interactions with the analyte and thus predictable elution properties which should be insensitive to mobile phase conditions.

Quininecarbamate was the base material for our experiments we chose for this study for two reasons. Firstly, the molecule contains a well-defined arrangement of moieties for ion-pairing, dipole-dipole interaction and hydrogen bonding [22]. Secondly, the quinoline ring represents an intercalating moiety [23] which may form π–π interactions with nucleobases, while the quinuclidine ring system projects into one of the grooves of DNA, but still binding reversibly to the double-helix [24]. Acridine yellow, an intercalating ligand, has been used for preparative ccc pDNA purification successively [25], but to our knowledge no ligand containing an intercalating moiety has been used in pDNA isoform separation for analytical purposes in the past. Dissociation from the intercalator can be facilitated by temperature increase or addition of salt [26] or an organic modifier, weakening π–π interaction.

2. Experimental

2.1 Materials and instruments

Empty stainless steel columns for HPLC with 100 mm length and 4.0 mm i.d., stainless steel frits (3 µm mesh width) and steel-glass sandwich frits (containing two 5µm stainless steel frits and three glass wool filter layers between them) were purchased form Bischoff Chromatography (Leonberg, Germany). The column were packed with the modified 5 µm and 10 µm silica stationary phases, respectively, in-house at a pressure of 600 bar. If not stated differently, sandwich frits were mounted on each side of the column. For recovery studies, an empty column with 50 mm length and 3.0 mm i.d. was also purchased from Bischoff Chromatography. HPLC analyses were carried out on an Agilent 1200 SL system (Waldbronn, Germany) equipped with a binary pump, a thermostatted autosampler (cooled to 4°C) and a DAD UV detector. Prior to analysis, all solvents were filtered (Millipore) through a 0.22 µm nylon filter (Sigma-Aldrich) and ultrasonically degassed. The pH was measured with a pH 720 meter by WTW (Weilheim, Germany). A zero dead volume (17 nL) union made from polyether ether ketone (PEEK) was purchased from Upchurch Scientific.

5 µm Kromasil® silica particles (6 µm particle size, 100Å pores, 304 m²/g specific surface area) were purchased from EKA chemicals (Bohus, Sweden). 10 µm silica particles (120Å pores, 300 m²/g), and for the pore-size-study 5 µm particles with pore sizes of 120Å (332 m²/g), 200Å (200 m²/g) and 300Å (100 m²/g) were purchased from Daiso (Osaka, Japan). 1.5 µm non-porous silica particles (3 m²/g specific surface area) were purchased from Micra Scientific (Northbrook, IL, USA) and packed by Bischoff. HPLC grade isopropanol was purchased from Carl Roth (Karlsruhe, Germany).

Three different Plasmid DNA preparations in Tris-EDTA (TE) buffer were provided and characterized [27] by Boehringer-Ingelheim RCV (Vienna, Austria), pMCP1 (4.9 kbp, 2.8 mg/ml), pAcMC1 (9.9 kbp, 1.1 mg/ml) and pGNA3 (14.5 kbp, 0.7 mg/ml), with homogeneities (ccc form contents) > 90%. Unless otherwise stated, the open circular form (50 µg/ml) was produced from each plasmid preparation by reaction with a nicking endonuclease Nt.BstNBI [28], purchased from New England Biolabs (Ipswich, MA, USA). Linear forms (50 µg/ml) were produced from each plasmid preparation by reaction with an appropriate endonuclease according to the manufacturer's instructions and supplied by Boehringer-Ingelheim RCV. Plasmid preparations enriched by the multimeric content were produced by semi-preparative size-exclusion chromatography by means of a ÄKTA system and provided by Boehringer-Ingelheim RCV.

Agarose gel electrophoresis was performed in a Sub-Cell GT apparatus from BioRad equipped to a PowerPac Basic power supply. Gels were photographed with a GelDoc XR+ system equipped with an amber filter and a CCD camera. For plasmid isoform analysis, a 0.8% agarose LE (Biozym, Hess, Germany) gel in 1x Tris-borate-EDTA (TBE) buffer was run at 200V for 2 hours at room temperature. A volume of 15µl of each sample, containing about 100 ng of DNA, was mixed with 5µl of sample buffer containing 50% glycerol (Sigma) and bromophenolblue (Merck) before being pipetted into a well on the agarose gel. Staining was performed for 2 hours at room temperature with a 0.1 mg/L ethidium bromide solution in 1x TBE, diluted from a 10 mg/ml stock solution (Sigma).

2.2 Synthesis of chromatographic ligands

Two quinine-carbamate ligands were employed in this study, one of which was anchored via a short spacer (Fig. 1a), and the other one via a long spacer (Fig. 1b) to the silica surface. The latter was synthesized and attached to the silica support as described earlier [29]. Briefly, a mercaptopropyl-modified silica was produced from bare silica and the corresponding silane by refluxing in toluene. Later, *tert*-butylcarbamoylquinine and mercaptopropyl-modified silica was refluxed in methanol in presence of AIBN as radical initiator. After washing with methanol, the silanol groups were endcapped with hexamethyldisilazane to form trimethylsilyl (TMS)-endcapped silanols. All silica materials listed in the previous section were modified with the long spaced ligand according to this procedure with respect to the different specific surface areas.

Short-spacer-containing ligand was prepared by a modified version of our procedure published earlier [30]. 10 mmol 3-isocyanatopropyl-triethoxysilane (ABCR, Karlsruhe, Germany) and 10.5 mmol quinine (Buchler, Braunschweig, Germany) were refluxed for 5 hours under nitrogen atmosphere in the presence of 25 µmol dibutyltindilaurate (Aldrich) as the catalyst. Complete conversion was monitored by IR spectroscopy for the missing isocyanate band (2267 cm^{-1}) and resulting carbamate band (1697 cm^{-1}). After cooling to about 40°C, the reaction mixture in toluene was directly used for attaching the ligand to the silica surface. Here, 11 g of bare Kromasil silica was drained before silylation by azeotropic distillation in toluene with a Dean-stark trap to remove excess of water. After flushing the apparatus with nitrogen, the ligand-containing reaction mixture was added along with 20 mg of 4-dimethylaminopyridine (Fluka) as the catalyst. The slurry was refluxed over night under nitrogen atmosphere. After filtration, the silica gel was washed with the solvent. The material was then endcapped by refluxing in toluene with 4 ml of hexamethyldisilazane (Fluka) for three hours. After filtration, the silica gel was washed with toluene and methanol. The dried material was used for column packing after sieving through a 40 µm stainless steel sieve. Elemental analysis (C, H, N) revealed a ligand density of 260 µmol/g and an endcapping group (TMS) density of 60 µmol/g.

A DEAE-carbamoyl silica material (with a short spacer) was prepared in the same manner starting from 2-(diethylamino)ethanol instead of quinine. According to elemental analysis a ligand density of 480 µmol/g and an endcapping group density of 190 µmol/g was present on the surface.

2.3 Optimized analysis method for plasmid isoform separation

For chromatographic analysis performed on 5µm Kromasil silica support, a phosphate-buffer pH-gradient from 7.2 to 7.9 in 15 minutes was used. First, a 0.5 mol/L stock solution from NaH_2PO_4 (Merck, Darmstadt, Germany) was prepared. Buffer A consisted of 50 mmol/L NaH_2PO_4 titrated to 7.2 with 5M NaOH. Buffer B consisted of 50 mmol/L NaH_2PO_4 and 20% (v/v) isopropanol titrated to 7.9 with 5M NaOH. A gradient from 0 to 100%B in 15 minutes was run during analysis. Between the analytic runs, the column was washed by a plug of sodium chloride (injection of 50µl 3M NaCl (aq.)), followed by reequilibration to 0% B for 5 minutes. The flow rate was set to 0.7 ml/min, detection wavelength to 258 nm (reference 360 nm with 100 nm bandwidth) and the temperature to 60°C (with preheating of the solvent in the 3 µl heat exchanger). Injection volume was dependent on the sample concentration (3 – 20 µl).

3. Results and Discussion

Following the ideas presented earlier in the introduction to this paper, a silica column with the long-spacer-ligand was tested for plasmid isoform selectivity at first. The first chromatogram can be seen in Fig. 2a, which shows some selectivity for the isoforms. The elution order oc < ccc < lin is not as expected from the frequently used DNA-NPR column (a pure AIEX ligand) under a similar NaCl-gradient slope shown in Fig. 2b. On the commercial DNA-NPR column the linear form coelutes with the ccc form at a rate of 50mM NaCl per minute. However, when the gradient slope is changed, the elution of the linear form changes relatively to oc and ccc. Hence, we observed three possibilities for the DNA-NPR column: oc < ccc < lin, oc < ccc ~ lin and oc < lin < ccc (data not shown). A nice overview over this phenomenon was published by Smith et al. [21]. The elution order on our columns based on quinine-carbamate however are insensitive to changes of gradient slope and thus more robust for plasmid analytics and method development. From this point of view it seemed promising to investigate the column further by optimizing each method variable to achieve better separation of the isoforms.

3.1. temperature dependence

The column temperature was found to be an essential part of the separation method. Upon rising temperature, we observed that the ccc form eluted later than both, the oc and the linear form. On the other hand, retention times of the oc and linear form have not shifted relatively to each other upon temperature change. A plot of retention curves can be seen in Fig. 3, showing that selectivity increases with rising temperature. Further studies up to 70°C, which is the highest temperature emplyed, follow this trend. The selectivity is therefore limited by the equipment, as well as the analyte and column stability. With even higher temperatures the double strands of the plasmid may start to separate, forming denatured DNA, the formation of which is not desired during analysis. For practical purposes we decided to use 60°C for plasmid analysis, which is a temperature providing very good selectivity but still avoiding DNA denaturation. However, for very AT-rich plasmids it might be safer to use a lower temperature of 55°C or 50°C.

Another effect observed during the temperature study was the unusually high broadening of the ccc peak with higher temperature starting up from 35°C (see Fig. 4). This implicates that although the selectivity α between the lin and ccc form is huge, the peak resolution R is comparably low. In fact, at 60°C a baseline separation of only R_s = 1.5 can be achieved. Later during this study it was found, that this broad peak is in fact an unresolved pattern of discrete peaks representing individual ccc topoisomers (ccc circles with different linking numbers). Our studies on the separation of these topoisomers will be published elsewhere. For the aim of this study it was however undesirable to further separate the ccc form. Thus, a method had to be found to provide the mentioned oc/lin/ccc selectivity without further resolving these topoisomers. In fact, such a method was provided later by employment of a pH gradient.

3.2. pH dependence

The effect of the buffer pH during salt-promoted elution was studied in the range between 5 and 8. In general, the retention of all isoforms decreases with increasing pH (see Fig. 5a). Below pH 6, the interaction with the stationary phase is too strong to make a complete ccc plasmid DNA elution possible with 1M NaCl

in buffer B. Use of even higher concentrations of salt is not practicable because of clogging problems, significantly reduced column lifetime, frequent system maintenance and high salt loads of the eluate.

Between pH 6 and pH 8 there is a pronounced change in the retention times, as might be expected due to an ion exchange process on a silica based weak anion exchanger. Since the pK_a values of the ligand are 10 for the quinuclidine and 4 for the quinoline moiety, no significant change of ionization of the ligand is expected in the range between 6 and 8. However, it was shown earlier, that the ζ-potential of silica particles changes dramatically in this region due to residual silanol groups [31]. According to elemental analysis data, only a part of the total number of silanols on the particle surface (which is a constant [32]) are modified by either the ligand or the endcapping group, therefore still enough silanols are present to promote silanol-analyte interactions (see table 1). In fact, on an organic polymer support with the same ligand, such a pH dependency of the retention was not observed. Secondly, on a DEAE-carbamate silica column the plasmid forms can be completely eluted from the column at pH 7.9 without NaCl, but on a DEAE-methacrylate-polymer column (both, the commercial DNA-NPR and an in-house produced monolithic column) the plasmids cannot be eluted without NaCl at a pH up to 10 (data not shown).

In this context it has to be mentioned, that the silanol activity is strongly dependent on the type of silica that is used as chromatographic support. Silanol activities may vary between different silica gels particles [33]. The implication here is that the pH dependency and thus the buffer pH value will be slightly different when the type of silica is exchanged. For example the highest resolution between all plasmid isoforms for the MICRA NPS 1.5 µm support can be found at pH 6.0. However for 5 µm Kromasil silica particles with 100 Å pores we found an optimum in the pH range around 7.

Remember that when operating the column at 50°C, we did not achieve true baseline separation (R_s > 1.5) between the ccc form and the oc and linear forms by varying the pH value (see Fig. 5b). However, at pH 7.0 the oc and the linear forms elute unretained from the column, whereas the ccc form is eluted by the NaCl gradient. Such conditions are useless for analytical applications but an interesting concept for preparative use where the ccc form is the desired product. Again, the suitable pH for such separation has to be evaluated for each silica phase separately.

3.3 particle size and pore size dependency

The particle type has proven to be very important for successful separation between the oc and linear form. In fact, we found that substantial differences were present between the 1.5 µm non-porous and 5 µm porous supports. Unfortunately, we did not have access to either 1.5 µm porous or 5 µm non-porous supports in order to deconvolute the pore size and particle size contributions, respectively. On the 5 µm support the oc form and the linear form are separated very badly, in fact only a hump of the linear form can be guessed. Employing the same conditions on the 1.5 µm support, a nice separation between the oc and linear form can be achieved, being additionally well separated from the ccc form (Fig. 6). The separation can be improved by lowering the gradient slope. Note that upon this change the elution order is not affected.

On the 5 µm chromatographic support we tested different pore sizes with the same chromatographic ligand and similar ligand densities per surface area in hope for improving the separation of the oc and linear form. However raising the

pore size from 100 to 300Å was followed by complete coelution. Also, the selectivity between the ccc form and the peak containing the oc and the linear form was lowered. Thus we may conclude, that non-porous particles provide better separation for plasmid isoforms than those with mid-sized pores. Because no significant shift in salt concentration needed for elution has been observed, the plasmids obviously do not enter the pores. That means that the vast majority of the chromatographic ligand is not used for separation and can be saved when using non-porous particles.

Comparing the 5 µm and 10 µm particles with same ligand chemistry, ligand density and pore sizes, no changes in the separation of the oc and linear form occur. However, bigger particles provide better separation between the ccc form and the peak containing the oc and the linear forms *(R* = 1.9, α = 1.84 (5µm); *R* = 2.1, α = 1.45 (10µm), conditions as in Fig.6 employing a gradient from 0 to 100% buffer B in 15 minutes). This may be an important aspect for preparative use, where usually bigger particles are employed to ensure low pressure drops over the column.

3.4 other plasmid variants

So far only monomeric forms have been considered. From the analysis performed on the commercial DNA-NPR column it is evident, that multiple other forms eluting after the ccc form are present, which are not characterized yet and summarized here as other plasmid variants. We think that they consist of dimers and/or higher multimers. On the quinine-type phases we have not been able to identify these forms so far, thus we decided to produce samples with a high content of these forms. In Fig. 7, a chromatogram of such a sample on our quinine-type phase is overlayed with a chromatogram of a natural sample containing less than 5% of the multimeric forms. The probable multimers are apparently eluting after the ccc form, such as they would on a DEAE column, but the tailing of the ccc peak rules out a reliable identification of contents below 10%.

The content of these other plasmid variants in the enriched sample is about 40%, according to an analysis performed with the DNA-NPR column. However the chromatogram in Fig. 7a shows a far less amount, about half of the expected peak area. Blank runs after the injection of that sample revealed a carry over, that has not been observed before. From that point of view, it is necessary to enhance the recovery from our quinine-type column in order to achieve reliable analyses. Recovery problems on chromatographic columns are generally associated with the open circular form, thus we might speculate, that at least parts of the “Others” consist of oc form. However, this is part of our current research in combination with atomic force microscopy (AFM) measurements.

3.5 effect of spacer length and open circular form standard

When comparing chromatographic properties of the long spacer between the surface and the ligand, to the short spacer, we obtained striking results in two aspects. Firstly, the recovery of the oc form, which has not been mentioned so far, has been significantly improved. Recoveries were estimated by comparing the area of an unknown peak to the peak area of the linear form, which was assumed to elute with full recovery. Of course, this was only a rough estimate but accurate enough for our purposes.

When a long spacer was present, the open circular form of the two bigger plasmids could not been identified reliably. Using a short spacer however we *could* identify the oc form of the 10 kb and the 15 kb plasmid in the natural sample with

low oc contents, which has not been reported before. The recoveries of the oc forms were as following: for the 5 kb plasmid full recovery was recorded, for the 10 kb plasmid we found ~ 60% recovery and for the 15 kb plasmid only 15% recovery were recorded. Although not complete, this is still a significant improvement over other columns that are currently used for plasmid isomer analysis [34].

The second important feature of the short spacer was the simplification of the elution pattern of the ccc form, and of the oc form, which will be discussed in more detail. The ccc topoisomer separation, mentioned briefly before, was significantly reduced, but not fully restrained on this column. The ccc form thus gave a broad but compact peak. For the aim of this work this is also a significant improvement. Not only the ccc form, also the open circular form has been found to consist of more species as well. This is a remarkable result since we could not find any further classification of open circular forms in the literature, however the naturally forming oc form and the one produced by enzymatic digestion behaved differently on our columns. The only possible structural difference between these two oc forms is that the naturally present species is formed by a lone single-strand break (“nick”) and that the enzymatically-produced species contains up to one nick in every enzyme-recognized sequence. For example the pMCP1 plasmid contains ten of these sequences, but because the enzyme reaction may vary depending on the actual isomer conformation [35], less nicks will be present in practice.

We decided to vary the nicking time and enzyme concentration during nicking reaction and analyze the plasmid DNA constituents by chromatography on our novel phases. When nicking the ccc form according to manufacturer’s instructions (1 hour at 55°C, followed by 20 min heat inactivation at 80°C), three peaks can be see in the chromatographic run. This is however striking, because only a single substance can be seen in AGE (apart from low amounts of the linear form and other plasmid variants). By reducing the reaction time down to one minute (reaction was stopped by addition of 10 mM EDTA), peak No. 2 and peak No. 3 disappeared to give a single peak at the retention time of the naturally occurring oc form (Fig. 8a). The same phenomenon can be seen when varying the enzyme concentration (Fig. 8b). It is very interesting that with an enzyme concentration as low as 0.005U enzyme/µg pDNA (!) still full conversion to the nicked plasmid is achieved (AGE analysis, Fig. 8d).

It is worth mentioning, that the three peaks indeed represent different species, which was proven by re-chromatography of the occurring peaks. Although the exact characteristics of the three species is not known at this point of research, it appears that only the species eluting firstly from the column is relevant for use as an analytical standard. However, the best reference is definitely the naturally generated open circular form, which can be isolated i.e. by means for preparative production of pure homogenous standards. There is not much literature providing details on nicking of the ccc form producing natural oc form, although this phenomenon is very well known [36]. In general, nicking can be induced by higher temperature, mechanical stress [37], chemical stress [38] and by UV light [39] [40]. However no systematic study has been published so far to provide procedures for creating large amounts of natural oc form (without creating substantial amounts of the linear form or even more degraded fragments) or give reliable conditions for eliminating natural oc form generation.

With increasing plasmid size, the pattern of different peaks representing different species of the open circular form, becomes even more complicated (data not shown). Larger sized plasmids have a higher probability of the presence of an enzymatic recognition sequence, such as 5’-GAGTC-3’ for the nicking enzyme

employed here. Because the naturally occurring oc form still contains only one nick, the discrepancy between itself and the enzymatically produced one is larger. In fact, in case of large plasmids such two samples do not show a common peak, which would correspond to the natural species, anymore. This is, because the probability of enzymatically nicking the plasmid *more* than one time is nearly 100%.

3.6 Mixed pH and organic modifier gradient

A short spacer provided better recoveries than the long spacer, but a generic analysis method would still be possible only for small plasmids with the mobile phase conditions employed until now (e.g. those in Fig. 7). In order to obtain full recoveries, a pH gradient seemed as a promising alternative to the salt gradient. Without NaCl, a pH gradient indeed showed full recoveries for the open circular plasmids for all plasmid sizes. We were also able to reduce the carry over to a minimum. For a good separation the pH gradient must be combined with a high column temperature (60°C) and an organic modifier gradient. As with the NaCl gradient, the elution order does not change upon temperature and gradient slope variation.

The pH range has to be slightly adjusted for every different silica support. In general, the starting pH should be between 7.0 and 7.5, rising linearly up to about 7.8. The pH value should not exceed 8.0 because of ligand bleeding. To find the optimum pH range, firstly the pH value has to be determined at which the first peak *just* elutes at t_0, then the range is set to +/– 0.3 adjacent to this value; i.e. if the oc form is retained at pH 7.4 but is not retained at pH 7.5, a range of 7.2 – 7.8 can be chosen.

The pH gradient alone does not promote separation and good recoveries, because of strong hydrophobic binding and intercalation by the ligand. For this reason an organic modifier has to be added to buffer B (no modifier in starting buffer A) creating a mixed pH/isopropanol gradient. We studied the addition of isopropanol in the range between 0 and 30% and have found equally good separations at 10 and 20% isopropanol in buffer B. Because of earlier elution and thus faster analysis, we recommend using the latter.

A characteristic of the salt-free elution is the complete disappearance of the topoisomer separation, which means that the ccc form elutes as a single and (relatively) slim peak providing better analytical results. Nevertheless the other plasmid variants, mentioned in section 3.4, still could not be separated good enough for quantification. The open circular forms produced enzymatically eluted differently from the naturally generated forms. For validation purposes, the open circular form must therefore be generated naturally from the ccc form by incubation at room or higher temperature and purified. In general, by increasing incubation temperature the open circular form is generated faster. However when working with big plasmids at elevated temperatures, the linear form is generated rapidly from the already generated oc form, which leads to a mixture of oc and linear forms. Thus, the bigger the plasmid, the lower the temperature of oc formation which has to be employed.

3.7 Other variables

Other parameters that have been studied include buffer type, flow rate and column frit material. Sodium phosphate buffer provided best results, because of its $pK_{a,2}$ close to the employed range. Triethylammounium phosphate buffer, being able to form ion pairs, has not provided any improvements. Further, the elution

order and the separation of plasmid isoforms are insensitive to flow rate variation (tested in the range between 0.3 ml/min and 1.0 ml/min), simplifying method development.

The frit material has shown to have great influence on recovery. By choosing improper materials, up to 50% of the open circular form may remain adsorbed at the column frits. In general, the bigger the plasmid size, the smaller its oc form-recovery. Usually two types of column frits are used in our laboratories, the first being a stack of pure stainless steel filters of small mesh width, the second being a sandwich frit composed of glass wool enclosed by two stainless steel filters of large mesh width on each side.

We have tested the adsorption of the individual plasmid isomers on a 50 mm x 3 mm i.d. stainless steel empty column housing with new sandwich frits, by comparing UV peak areas after plasmid injection to those obtained with no column installed (a PEEK union with zero-dead-volume was mounted instead). The results are shown in table 2, however an uncertainty of 10% must be allowed because of possible interference of the UV absorbance with other solution constituents. Nevertheless it is clear that the open circular form partly adsorbs to the frits, while the linear form as well as the ccc form elute almost completely. The ccc form preparations contain about 10% open circular form, which explains the less pronounced effect of lower UV peak areas. It is also evident, that the adsorption is greater with increasing plasmid size. Thus, for a 15 kb plasmid only 50% of the open circular form eluted from the column without any stationary phase.

Due to low recoveries obtained from the previous experiment, the columns were dismantled to test whether stainless steel, glass wool or both frit constituents adsorb DNA. All constituents were put in glass vials and incubated separately with a SYBR Gold staining solution at room temperature for 30 minutes. Afterwards the suspension was centrifuged and the supernatant was transferred to a different vial. All vials, containing solid frit constituents, the supernatants of the incubation solutions and a blank solution were illuminated by UV light in the GelDoc apparatus. The so induced fluorescence image can be seen in Figure 9 with the correspondent intensities shown in table 2. Stainless steel frits, or more general, metal frits adsorb DNA minimally. Because the supernatant of the metal frit incubation solution shows some fluorescence, bound DNA is desorbed easily. Metal frits therefore do not represent a critical point for plasmid DNA recovery.

Both glass-wool filters on the other hand fluoresce very intensively caused by adsorbed DNA, according to previous results mainly by the open circular isoform. The adsorption is reversible, shown by substantial fluorescence of the supernatant. In practice this means that a non-negligible amount of plasmid DNA is adsorbed on a glass-wool filter and may be released continuously during HPLC analysis or column washing (“frit bleeding”).

To prove the innocuousness of the metal frits, the empty housing was again equipped with stainless steel frits. On each side of the column five metal filters were installed, in order to have the same thickness as the steel/glass-wool sandwich. The recoveries can be seen in table 1. No adsorption of DNA can be discovered, nor any trend (such as decreasing recovery with increasing plasmid size) can be deduced from the data. Therefore, metal frits should be installed on HPLC columns intended for use in plasmid DNA analytics.

4. Conclusion

We have found that large biomolecule separation carried out by stationary phases employing molecular recognition principles are more robust and better

suitable for method development as well as up- and downscaling. On stationary phases with quinine-based ligand, the elution order of plasmid isoforms (open circular < linear < ccc) is insensitive to variation of flow rate, gradient slope, plasmid size as well as particle and column dimensions. We have found that the nature of the support has great influence on separation, especially that negatively charged silanol groups force complete recoveries of the open circular form, which remain a major issue when using organic polymers. Complete recoveries of all forms can be achieved in our opinion on such mixed-mode phases only.

Our stationary phases work best with a pH gradient in the range around pH 7 in combination with a short spacer between the quinine-based ligand and the surface. Both these characteristics promote full recoveries, minimal carry over effects as well as the absence of topoisomer separation of the covalently closed circular form. Specific ionic and hydrophobic interaction between the analyte and the ligand is attenuated gradually by a superimposed isopropanol gradient. HPLC columns containing our materials provide best separations at elevated temperatures with an optimum at 60°C, which does not cause any sample degradation during the time scale of an analysis run.

Particle size is a very important parameter for separation between the open circular and the linear form (the “loose” forms). However it does not affect separation between these loose forms and the ccc form. For preparative scale applications, which focus on the therapeutic active ccc form, upscaling is not an issue with our materials. The porosity seems to have little influence on the separation, but generally small pores (< 120 Å) give better results. Of course, non-porous materials are optimal because of low ligand consumption, maximum binding capacity (plasmids do not interact with the surface within the pores) and best performance.

An interesting conclusion of this study was the fact, that the open circular form, which is generated naturally from the ccc form by UV light or mechanical and chemical stress, differs from that generated enzymatically by an nicking enzyme. Chemically these species differ by the number of nicks, i.e. breaks in the phosphodiester bond, but these discrepancies were thought to be negligible over the whole molecule. However, the natural species shows a single peak on our supports, whereas the enzymatically produced species shows a reproducible pattern of multiple peaks. In general, the complexity of this pattern grows with plasmid size. Although we haven’t been able to identify any chromatographic discrepancies on other (commercially available) columns, we would like to stress the use of naturally produced open circular forms as a standard for quantification.

In the course of this study we have also looked at other possible causes for low plasmid recovery. We have found that open circular plasmids adsorb tightly, but reversibly, on glass-wool, which is part of some frits used at both ends of an HPLC column. Thus, usage of such filters in column frits should be avoided and, when possible, they should be replaced by metal frits, which do not show significant adsorption, for reliable results.

5. Acknowledgement

We greatly appreciate the financial support and the provision of the HPLC system by Boehringer-Ingelheim RCV (Vienna, Austria).

6. Figures

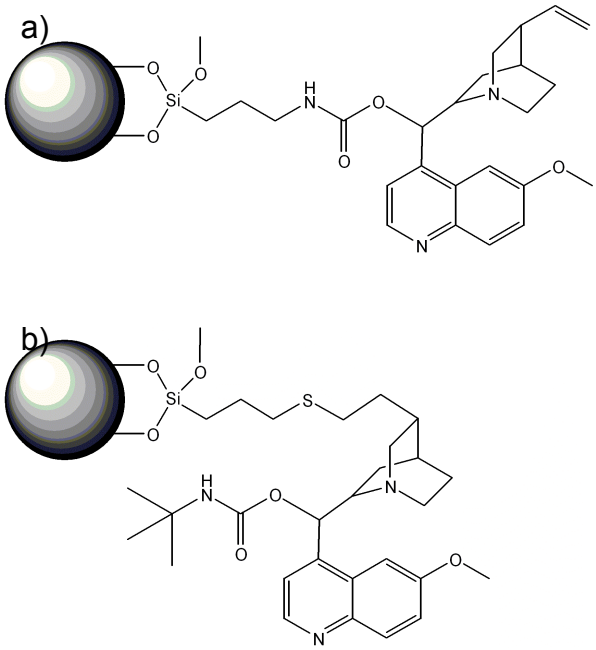

Figure 16: Structure of Quinine-type chromatographic ligands employed in this study, (a) with short spacer and (b) with long spacer

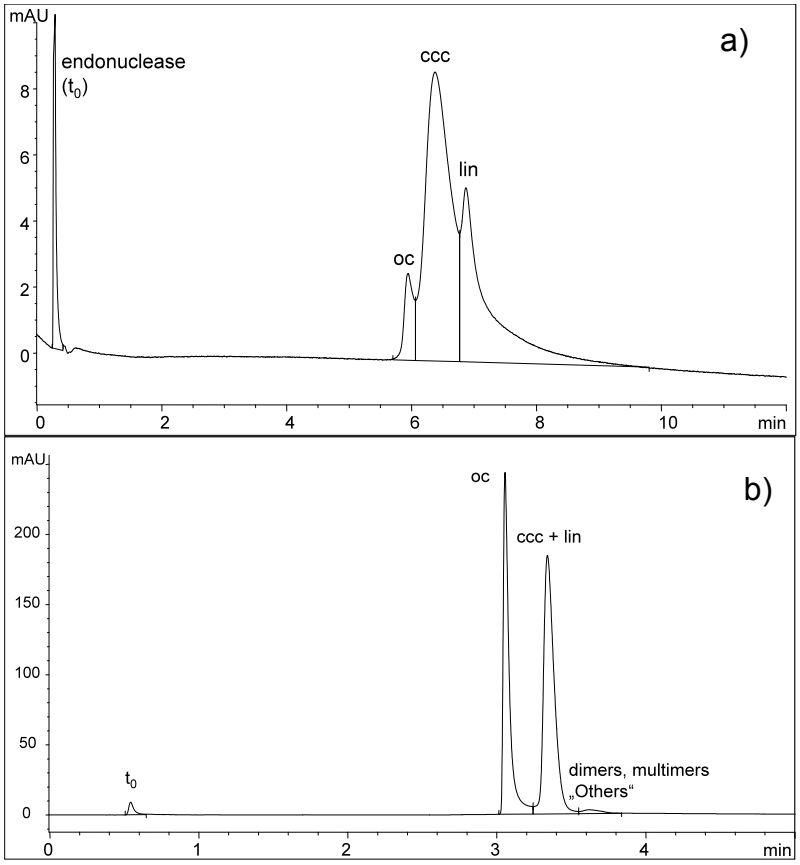

Figure 17: Chromatograms of spiked plasmid samples (pMCP1, 1 µl inj.) on a quinine carbamate column with short spacer attached to MICRA NPS 1.5 µm (a) and a DNA-NPR 2.5 µm (DEAE AIEX) column (b) at ambient temperature. Conditions: (a) 50 mM phosphate buffer pH 7.5, linear gradient from 0 to 600mM NaCl in 15 minutes, 1.0 ml/min, 25°C, det. 258 nm: (b) 20 mM TrisHCl pH 9.0, linear gradient from 500 to 750mM NaCl in 5 minutes, 25°C, det. 258 nm, 1.0 ml/min

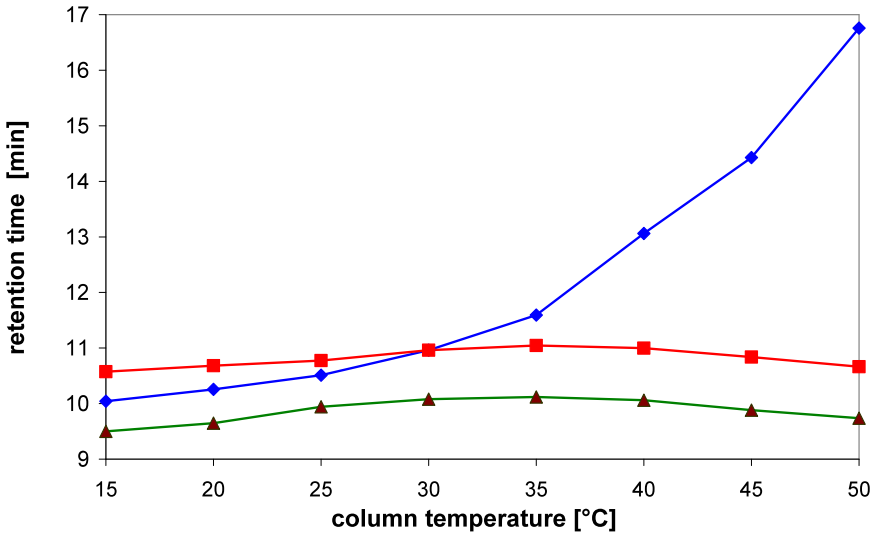

Figure 18: plot of the peak retention times against the column temperature for oc (▲), linear (■) and the ccc (♦) form. Conditions: quinine-carbamate with long spacer on MICRA, 1.0 ml/min, 50mM phosphate pH 6.0, linear gradient 0 – 1000 mM NaCl in 25 min, inj. 1 µl spiked pMCP1

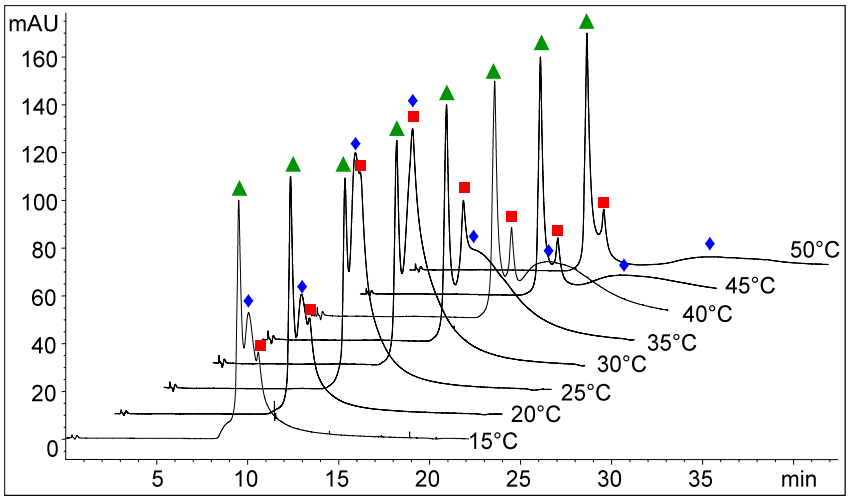

Figure 19: An overlay of chromatograms (10% offset for y and x-axis, respectively) from the temperature study in the range between 15°C and 50°C in 5°C steps, showing the peak maxima for oc (▲), linear (■) and the ccc (♦) form. Conditions as in Fig. 3

Table 1: Amount of modified silanols of different supports with short and long spaced quinine-type ligand. Note that all supports contain enough free silanol groups after modification to promote weak ion exchanger properties. The density of modified silanols is calculated as the sum of the endcapping group plus the anchor group (long spaced ligand) or the ligand (short spaced ligand), respectively. The total silanol number is calculated from the Zhuralev constant (4.6 OH groups/nm²).

support	ligand	density per mass of modified silanols	specific surface area	surface coverage of modified silanols	ratio of modi to total silan
5µm Kromasil 100Å	short spaced	581 µmol/g	304 m²/g	1.91 µmol/m²	25%
5µm Daisogel 120Å	long spaced	1366 µmol/g	332 m²/g	4.11 µmol/m²	54%
5µm Daisogel 200Å	long spaced	906 µmol/g	200 m²/g	4.53 µmol/m²	59%
5µm Daisogel 300Å	long spaced	480 µmol/g	100 m²/g	4.80 µmol/m²	63%
1.5 µm Micra non-porous	short spaced	DATA FROM MICHI!	3 m²/g	0.00 µmol/m²	0%
1.5 µm Micra non-porous	long spaced	10.4 µmol/g	3 m²/g	3.48 µmol/m²	46%

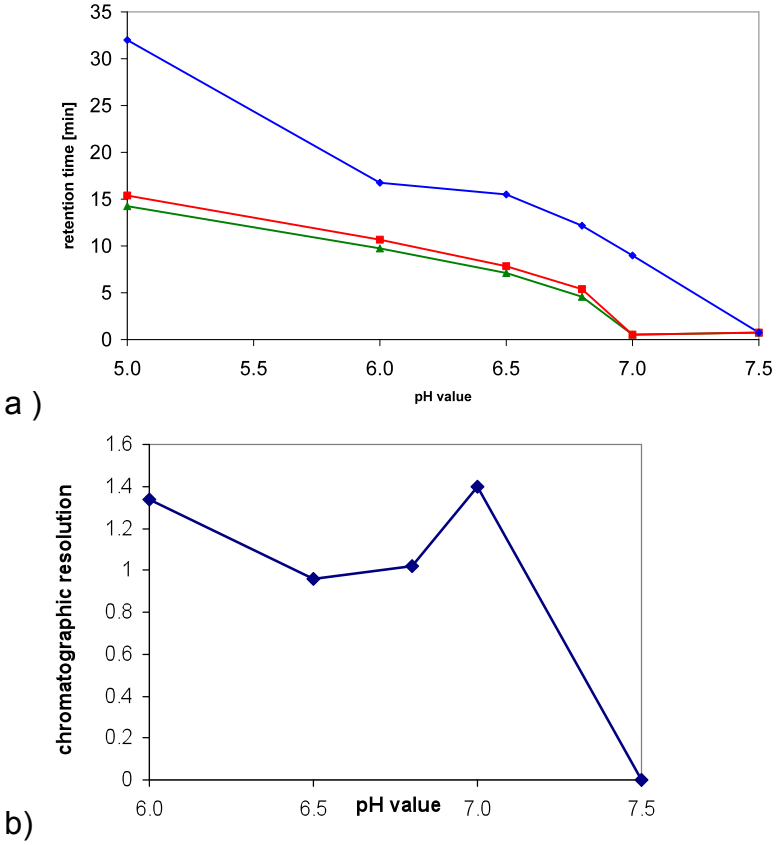

Figure 20: pH dependence of the retention times for oc (▲), linear (■) and the ccc (♦) form (a) and the resolution R_s between the peaks of the oc and ccc form, respectively (b). Conditions: quinine-carbamate with long spacer, 0.9 ml/min, 50°C, 50mM phosphate, linear gradient 0 – 1000 mM NaCl in 25 min, inj. 1 µl spiked pMCP1

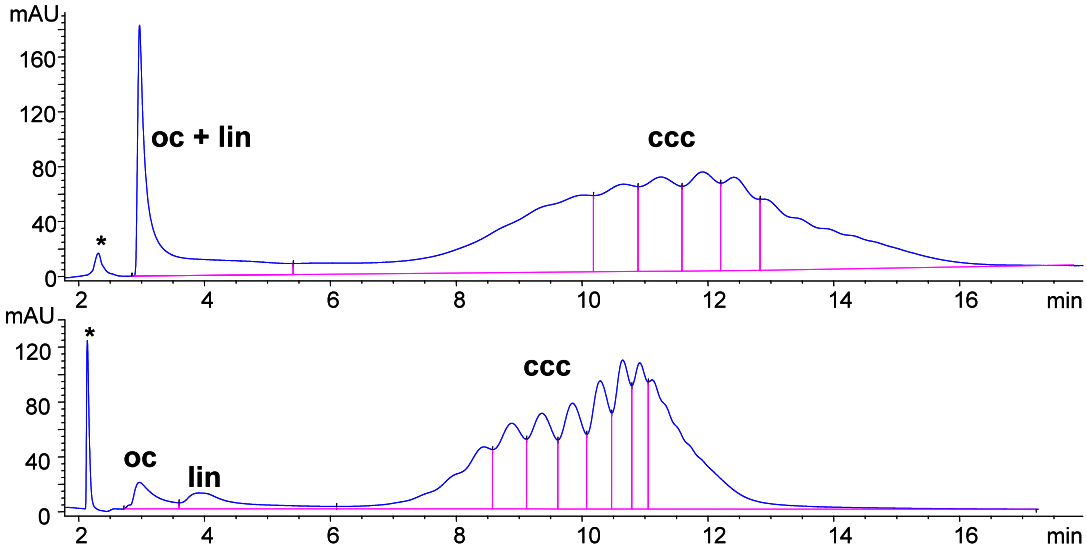

Figure 21: Chromatograms of a pMCP1 sample spiked with linear form on a 5 µm 100 Å porous Kromasil (a) and MICRA 1.5 µm non-porous support (b). The oc and linear forms coelute on Kromasil, but are separated nicely on 1.5 µm non-porous silica. The ccc form is further separated into topoisomers, which will be described in detail elsewhere. Peaks marked with an asterisk containing the lin-forming endonuclease. Conditions: quininecarbamate with long spacer, buffer A: 50mM phosphate pH 7, buffer B: A + 0.6M NaCl & 30% isopropanol, 60°C, 0.7 ml/min, 3 µl inj. spiked pMCP1; linear gradient 10 – 35%B in 15 min.

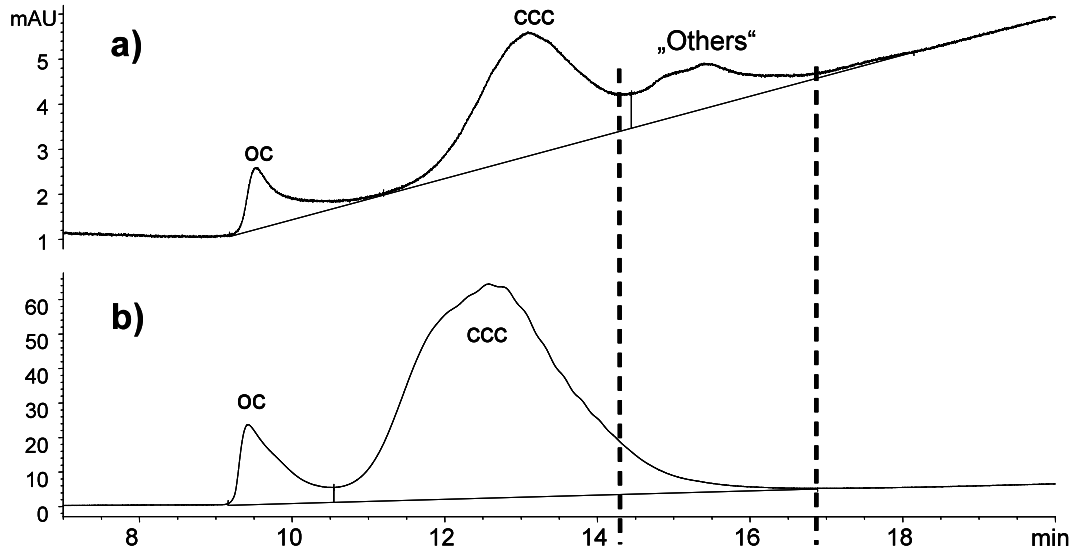

Figure 22: overlayed chromatograms from pMCP1 plasmid runs with a high (a, 40% Others according to analysis with DNA-NPR) and low (b, 5% Others) content of other plasmid variants, showing the elution window of these multimeric species. Conditions: quininecarbamate with long spacer on Kromasil; buffer A: 50mM phosphate pH 7, buffer B: A + 0.6M NaCl & 10% isopropanol, 60°C, 0.7 ml/min, linear gradient 0 – 100%B in 15 min

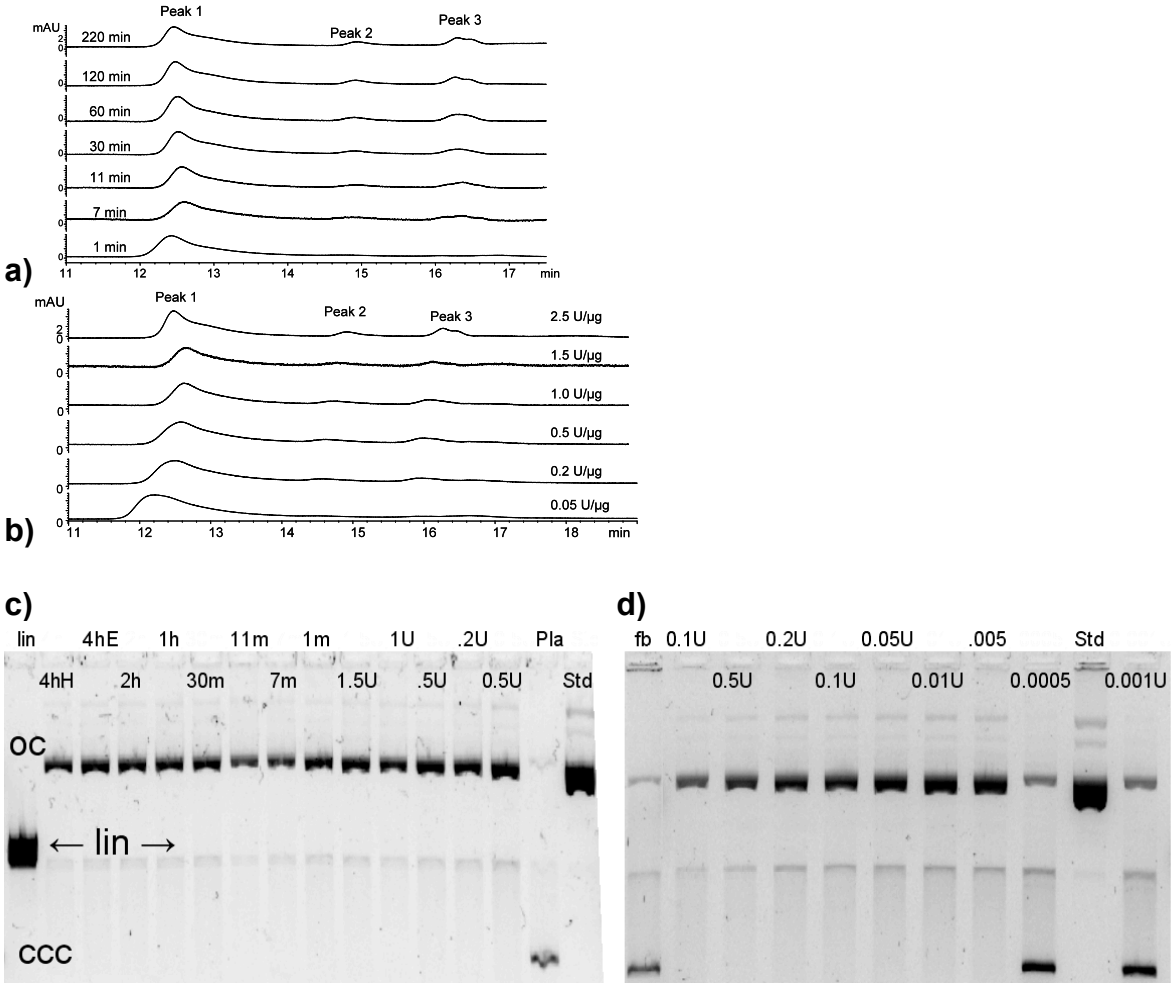

Figure 23: Chromatograms (a), (b) and AGE analysis (c), (d) of enzymatically nicked pMCP1 plasmid. We varied the time (a), (c) as well as the biocatalyst concentration (b),(d) during enzymatic reaction.

Abbreviations: "fb": plasmid preparation with high ccc amount; "4hH/4hE": 4h long enzymatic digest followed by heat (H) or EDTA-promoted (E) enzyme inactivation; "m": minutes reaction time; "U": Units enzyme per µg plasmid DNA; "Pla": placebo (without enzyme); "Std" open circular form produced according to manufacturer's description. Chromatographic conditions as in Fig.7, Electrophoretic conditions: 1x TBE, 3h @ 120V, staining with SYBR Gold for 2h at rt. The chromatograms in (a) and (b) were aligned to the absorbance of the Peak 1.

Table 2: Comparison of recoveries of individual plasmid isoforms from an empty HPLC column housing, equipped with a glasswool/steel sandwich frit and a steel-only frit, respectively. Recovery is calculated here as the quotient between the UV peak area with and without an empty column. In the latter case the connection capillaries were connected through a zero-dead-volume union, made of PEEK. The oc and linear forms are pure preparations, whereas the ccc form contains a certain amount of the open circular form. Each value is an average over three individual measurements.

	steel & glass wool frit	steel-only frit
5kbp		
ccc	90% ± 1%	96% ± 1%
oc	80% ± 1%	89% ± 1%
lin	90% ± 1%	92% ± 1%
10 kbp		
ccc	86% ± 1%	92% ± 1%
oc	62% ± 1%	98% ± 3%
lin	92% ± 2%	91% ± 0.3%
15 kbp		
ccc	82% ± 2%	92% ± 1%
oc	56% ± 2%	96% ± 3%
lin	98% ± 2%	95% ± 3%

Table 3: Fluorescence intensities with subtracted blank values from Figure 9. Solid metal frits SF1, SF2 and MF1 do not show any fluorescence.

sample name	fluorescence intensity (arbitrary units)	% of total fluor.intensity
GW1	133373	45.6
GW2	88488	30.2
GW1-S	43024	14.7
GW2-S	14451	4.9
SF1-S	6137	2.1
MF1-S	4739	1.6
SF2-S	2514	0.9

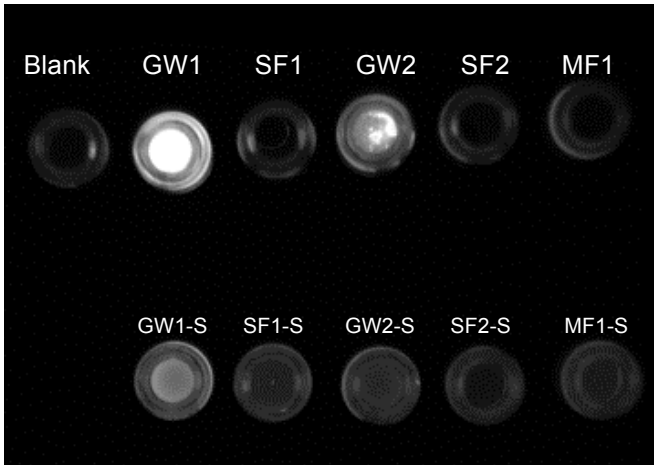

Figure 24: Image of UV induced fluorescence of the DNA-SYBRGold complex of different HPLC frit constituents: GW (glass wool filter); SF (stainless steel frit); 1 and 2 denote the top and the end of the column, respectively; MF (metal frit of the DNA-NPR column); -S denotes the supernatant (dye containing incubation solution). Glass wool adsorbs most of the DNA, that is not recovered from an empty HPLC column.

7. References

[1] Schleef, M., *Plasmids for Therapy and Vaccination*, Wiley-VCH, Weinheim 2001.

[2] Urthaler, J., Ascher, C., Woehrer, H., Necina, R., *Journal of Biotechnology* 2007, *128*, 132-149.

[3] Urthaler, J., Buchinger, W., Necina, R., *Chemical Engineering & Technology* 2005, *28*, 1408-1420.

[4] FDA, U., in: Administration, F. a. D. (Ed.), *Considerations for Plasmid DNA Vaccines for Infectious Disease Indications*, Rockville, MD 2007.

[5] Lahijani, R., Hulley, G., Soriano, G., Horn, N. A., Marquet, M., *Human Gene Therapy* 1996, *7*, 1971-1980.

[6] Hallet, B., Vanhooff, V., Cornet, F., in: Funnell, B. E., Phillips, G. J. (Eds.), *Plasmid Biology*, ASM Press, Washington, D.C. 2004, pp. 145-180.

[7] Schmidt, T., Friehs, K., Schleef, M., Voss, C., Flaschel, E., *Analytical Biochemistry* 1999, *274*, 235-240.

[8] Diogo, M. M., Queiroz, J. A., Prazeres, D. M. F., *Journal of Chromatography, A* 2005, *1069*, 3-22.

[9] Wu, L., Pang, G.-c., *Chromatographia* 2007, *66*, 151-157.

[10] Tiainen, P., Gustavsson, P.-E., Mansson, M.-O., Larsson, P.-O., *Journal of Chromatography, A* 2007, *1149*, 158-168.

[11] Sousa, F., Tomaz, C. T., Prazeres, D. M. F., Queiroz, J. A., *Analytical Biochemistry* 2005, *343*, 183-185.
[12] Danquah, M. K., Forde, G. M., *Journal of Chromatography, B: Analytical Technologies in the Biomedical and Life Sciences* 2007, *853*, 38-46.
[13] Prazeres, D. M. F., Schleup, T., Cooney, C., *Journal of Chromatography, A* 1998, *806*, 31-45.
[14*] Urthaler, J., Schlegl, R., Podgornik, A., Strancar, A., Jungbauer, A., Necina, R., *Journal of Chromatography, A* 2005, *1065*, 93-106
[14] Huber, C. G., *Journal of Chromatography, A* 1998, *806*, 3-30.
[15] Rozing, G. P., *Journal of Chromatography A* 1989, *476*, 3-19.
[16] Jungbauer, A., *J. Chromatogr., A* 2005, *1065*, 3-12.
[17] Hahn, R., Panzer, M., Hansen, E., Mollerup, J., Jungbauer, A., *Separation Science and Technology* 2002, *37*, 1545-1565.
[18] Sykora, D., Svec, F., Frechet, J. M. J., *J. Chromatogr., A* 1999, *852*, 297-304.
[19] Wieder, W., Bisjak, C. P., Huck, C. W., Bakry, R., Bonn, G. K., *Journal of Separation Science* 2006, *29*, 2478-2484.
[20] Onishi, Y., Azuma, Y., Kizaki, H., *Analytical Biochemistry* 1993, *210*, 63-68.
[21] Smith, C. R., DePrince, R. B., Dackor, J., Weigl, D.*, et al.*, *Journal of Chromatography, B: Analytical Technologies in the Biomedical and Life Sciences* 2007, *854*, 121-127.
[22] Piette, V., Lammerhofer, M., Lindner, W., Crommen, J., *Chirality* 1999, *11*, 622-630.
[23] Allison, R. G., Hahn, F. E., *Antimicrobial Agents and Chemotherapy* 1977, *11*, 251-257.
[24] Estensen, R. D., Krey, A. K., Hahn, F. E., *Molecular Pharmacology* 1969, *5*, 532-541.
[25] Vincent, W. S., III, Goldstein, E. S., *Analytical Biochemistry* 1981, *110*, 123-127.
[26] Danko, P., Kozak, A., Podhradsky, D., Viglasky, V., *Journal of Biochemical and Biophysical Methods* 2005, *65*, 89-95.
[27] Urthaler, J., Buchinger, W., Necina, R., *Acta Biochimica Polonica* 2005, *52*, 703-711.
[28] Morgan, R. D., Calvet, C., Demeter, M., Agra, R., Kong, H., *Biological Chemistry* 2000, *381*, 1123-1125.

[29] Mandl, A., Nicoletti, L., Lammerhofer, M., Lindner, W., *J. Chromatogr., A* 1999, *858*, 1-11.
[30] Laemmerhofer, M., Lindner, W., *Journal of Chromatography, A* 1996, *741*, 33-48.
[31] Sanchez Munoz Orlando, L., Hernandez Ever, P., Lammerhofer, M., Lindner, W., Kenndler, E., *Electrophoresis* 2003, *24*, 390-398.
[32] Zhuravlev, L. T., *Reaction Kinetics and Catalysis Letters* 1993, *50*, 15-25.
[33] Zhuravlev, L. T., *Colloids and Surfaces, A: Physicochemical and Engineering Aspects* 2000, *173*, 1-38.
[34] Molloy, M. J., Hall, V. S., Bailey, S. I., Griffin, K. J.*, et al.*, *Nucleic Acids Research* 2004, *32*, e129/121-e129/110.
[35] Linial, M., Shlomai, J., *J. Biol. Chem.* 1988, *263*, 290-297.
[36] Giacomoni, P. U., *Journal of Photochemistry and Photobiology, B: Biology* 1995, *29*, 83-85.
[37] Levy, M. S., O'Kennedy, R. D., Ayazi-Shamlou, P., Dunnill, P., *Trends in Biotechnology* 2000, *18*, 296-305.
[38] Muiras, M. L., Giacomoni, P. U., Tachon, P., *Mutation Research, DNAging: Genetic Instability and Aging* 1993, *295*, 47-54.
[39] Jiang, Y., Ke, C., Mieczkowski, P. A., Marszalek, P. E., *Biophysical Journal* 2007, *93*, 1758-1767.
[40] Boullard, A., Giacomoni, P. U., *Journal of Photochemistry and Photobiology, B: Biology* 1988, *2*, 491-501.

Manuscript 2

Title: Chromatographic separation of plasmid DNA topoisomers of different linking numbers

Authors: Marek Mahut, Parisa Ghazidezfuli, Wolfgang Lindner, Michael Lämmerhofer

University of Vienna, Department of Analytical Chemistry, Waehringer Strasse 38, A-1090 Vienna, Austria

Abstract:

In this paper we present an analytical method for efficient separation of topoisomers of circular plasmid DNA by liquid chromatography. The separation is governed by quinine-carbamate ligands on a silica support in combination with optimized mobile phase conditions, which include elevated temperature, salt elution gradient and a superimposed isopropanol gradient. With these conditions, we were able to split covalently closed circular (ccc) bands from all studied plasmids in the range between 2.7 and 14.5 kbp into a pattern of discrete narrow peaks, the areas of which formed a Gaussian distribution. By analyzing collected HPLC fractions by capillary gel electrophoresis (CGE) under topoisomer-resolving conditions, the separation could be reproduced proving the identity of the separated species. Further, the number of superhelical turns was determined for one particular HPLC fraction containing a single topoisomer by means of agarose gel electrophoresis. Because of high loadability of our columns, this method might be also very useful for preparative isolation of topoisomers.

Keywords:
plasmid DNA, plasmid topoisomer separation, linking numbers, quinine carbamate

1. Introduction

Circular plasmid DNA is believed to have great potential in modern gene therapy and vaccination [1]. The so called covalently closed circular (ccc) form exists, when both strands of the double helix are intact, while the open circular (oc) form is formed by single strand nicking from the ccc form [2]. An inherent property of ccc plasmids is supercoiling, which is the coiling of the axis of the double helix around itself [3]. It is mathematically described by the linking number *Lk*, an topologically invariant integer which cannot be altered by deformation [4]. The actual *Lk* of a certain plasmid molecule is dependent on the number of base pairs (bp) per turn of the double helix, *h*. Under standard conditions (0.2 M NaCl, pH 7, 37°C [5]), often the value 10.5 bp/turn is taken (h^0). The linking number is thus obtained by dividing the number of base pairs, *N*, by h^0. When bringing the ends of the DNA in close vicinity in order to close a circle without twisting them against each other, probably the ends will not precisely match each other. Thus, a slight twisting will be required to join the ends together, which is negligible over the whole molecule. This small angular displacement is denoted as ω ($-0{,}5 \leq \omega \leq 0{,}5$). The so obtained closed circle has a standard linking number (Lk_m) which can be described by

$$Lk_m = \frac{N}{h^0} + \omega \cdot \qquad \text{(Eqn. 1)}$$

Supercoiling consists of two quantities, twist (*Tw*) and writhe (*Wr*), which are interconvertible but the sum of both is invariant for a certain topoisomer. Mathematically this can be expressed as *Lk* = *Tw* + *Wr*. The twist quantity is changed, e.g. by introducing a turn on one end of a cut double helix, while keeping the other fixed ("twisting one end against the other"), followed by resealing both strands; this corresponds to a change of *h*. The writhe quantity describes the coiling of the central axis of the double helix [6], but is often referred to as the number of superhelical turns. However, this is not strictly correct as the writhe quantity is not an integer.

The linking number for a given ccc plasmid molecule can be only changed by cutting one or both strands and swivelling them around each other. In a cell, this is the function of a set of enzymes called topoisomerases [7], which catalyze a topoisomer equilibrium depending on solution conditions. The energy difference between adjacent topoisomers around Lk_m is smaller than thermal energy fluctuations, leading to a Gaussian distribution of topoisomers [8]. From the topoisomer concentration in a mixture the free energy difference ΔG between any topoisomer Lk_x and the most intense topoisomer Lk_m can be calculated by

$$\Delta G(Lk_{x-m}) = -RT \cdot ln\frac{[Lk_x]}{[Lk_m]} \qquad \text{(Eqn. 2)}$$

with R being the gas constant and *T* the absolute temperature. Using Hooke's law and the parameter ω, equation 2 can be rearranged to yield

$$\frac{1}{\Delta Lk} ln\frac{[Lk_x]}{[Lk_m]} = -\frac{K}{RT}\Delta Lk - \frac{2K\omega}{RT} \qquad \text{(Eqn. 3)}$$

where $[Lk_x]$ is the concentration of a certain topoisomer, $[Lk_m]$ is the concentration of the highest abundant topoisomer and K is an elastic constant.

Topoisomer distributions can be currently analyzed by electrophoretic techniques only. In 1975 it was found by Depew and Wang, that the electrophoretic mobility of supercoiled plasmids is determined by differences in the writhe value, which translates into different hydrodynamical radii [9]. Topoisomers differing by discrete linking numbers differ also by discrete values of writhe and will hence form separate bands [10]. However, due to relatively small differences in the tertiary structure of naturally supercoiled plasmids, often only a single ccc band is formed in conventional electrophoresis. The key to the separation of highly supercoiled plasmids lies in the conversion of writhe into twist, which can be easily done by adding an intercalator to the running buffer, such as ethidium bromide or chloroquine [11] [12]. Depending on the concentration of the intercalator, the primary negative writhe is lowered, i.e. superhelical turns are removed at the expense of increasing twist, until a sufficiently low writhing number is gained in order to achieve separation. The exact limit of separation is dependent on the electrophoretic resolution, but from our experience topoisomers with up to about 20 superhelical turns can be separated by our AGE method.

A molecule with no writhing (*Wr* ~ 0) is the slowest migrating band in a series of topoisomers, because adjacent topoisomers with one supercoil, will have a smaller hydrodynamical radius and migrate faster. Topoisomers of same absolute writhing values but with opposite sign, e.g. *Wr* = +1 and *Wr* = –1, migrate as a single band [13]. The intercalator concentration, needed to reduce the writhe below the limit of separation, has to be determined for each plasmid sample

separately, because it depends on the plasmid size and superhelicity. In general, a big-sized plasmid will need a higher intercalator concentration than a small one.

To our knowledge no analytical method exists for determination of topoisomer distribution by chromatographic means. Although selectivity for ccc plasmid topoisomers was found on RP-18 column based on hydrophobicity, no reasonable resolution between adjacent topoisomers could be achieved [14]. Herein we present the first chromatographic deconvolution of a natural distribution of supercoiled topoisomers of various plasmids. We also like to stress the name “topology analysis” for our method, since various authors refer to this name or similar, when separating isoforms (but not topological isomers) meaning the three forms linear, oc and ccc (as a whole).

2. Experimental

2.1 Materials and instruments

Empty stainless steel columns for HPLC with 4.0 mm i.d. and 120 mm length, and steel-glass sandwich frits (containing two 5µm stainless steel frits and three glass wool filter layers between them) were purchased form Bischoff Chromatography (Leonberg, Germany). Columns with our modified 5µm silica stationary phase were packed in-house at a pressure of 600 bar. Sandwich frits were mounted on each side of the column. HPLC analyses were carried out on an Agilent 1200 SL system (Waldbronn, Germany) equipped with a binary pump, a thermostatted autosampler (cooled to 4°C) and a DAD UV detector. Prior to analysis, all solvents were filtered by a glass filtration unit (Millipore) through a 0.22 µm nylon filter (Sigma-Aldrich) and ultrasonically degassed. The pH was measured with a pH 720 meter by WTW (Weilheim, Germany).

5 µm particles with 120Å pores (332 m²/g specific surface area) were purchased from Daiso (Osaka, Japan). HPLC grade isopropanol was purchased from Carl Roth (Karlsruhe, Germany). Three different Plasmid DNA preparations in Tris-EDTA (TE) buffer were provided by Boehringer-Ingelheim RCV (Vienna, Austria), pMCP1 (4.9 kbp, 2.8 mg/ml), pAcMC1 (9.9 kbp, 1.1 mg/ml) and pGNA3 (14.5 kbp, 0.7 mg/ml), with homogeneities (ccc form contents) > 90% [14*]. Eukaryotic topoisomerase I (Topo I) from wheat germ (10 Units/µl), pUC19 plasmid DNA, pBR322 plasmid DNA and a 10 mg/ml stock solution of ethidium bromide (EtBr) were purchased from Sigma. pET-40b(+) and pBACsurf-1 plasmids were purchased from Novagen (Madison, WI, USA). Chloroquine diphosphate was purchased from Fluka. When stated, samples were dialyzed against water for salt removal by a VSWP cellulose ester membrane (25 mm diameter, 25 nm pores) purchased from Millipore (Billerica, MA, USA). The discs were put on the water surface with the shiny side up and a volume of up to 300 µl was loaded onto the disc surface carefully. After floating for 15 to 30 minutes at 4°C, the samples were recovered with a pipette and used for further analyses.

Capillary gel electrophoresis was performed in a ^{3D}CE instrument from Agilent. A DB-17 coated capillary with 100 µm i.d. was purchased from J&W Scientific (Folsom, CA), cut to a length of 32 cm and a detection window was made by removing the polyimide coating with a razor blade (effective length 24.5 cm). For topoisomer analysis [15], the capillary was filled with Tris-borate-EDTA (TBE, 89 mM boric acid, 89 mM Tris, 2 mM EDTA, titrated to pH 9.0 with NaOH) buffer containing 0.1% hydroxypropylmethylcellulose (HPMC, 86 kDa) purchased from Acros organics (Geel, Belgium). For complete homogenization of the buffer, the solution was stirred for 24 h after addition of the biopolymer and afterwards let

to stand for another 24 h without disturbing at room temperature [10]. For gaining higher resolution of highly supercoiled ccc plasmids, an intercalator was added to the electrophoresis buffer [13], in our case 12 µl and 20 µl of a 5 mg/ml aqueous chloroquine diphosphate solution to 4 ml of electrophoresis buffer to give a final concentration of 15 µg/ml and 25 µg/ml chloroquine, respectively. Samples were introduced by electrokinetic injection at -5 kV for 4 seconds. Electrophoresis was performed in negative mode at 3.3 kV for 25 minutes at 25°C, with UV detection at 258 nm. Before injection, the capillary was flushed with water for 3 minutes and then preconditioned with running buffer for 5 minutes.

Agarose gel electrophoresis was performed in a Sub-Cell GT apparatus from BioRad equipped to a PowerPac Basic power supply. Gels were photographed with a GelDoc XR+ system equipped with an amber filter and a CCD camera. An agarose gel for topoisomer separation was produced by cooling 200 ml solution of 0.6 to 1.0% (w/v) agarose LE (Biozym, Hess, Germany) and 0 to 10 µg/L ethidium bromide in 1x Tris-borate-EDTA (TBE, 89 mM tris, 89 mM boric acid, 2.5 mM EDTA) buffer. A volume of 15µl of each sample, containing about 100 ng of DNA, was mixed with 5µl of sample buffer containing 50% glycerol (Sigma) and bromophenolblue (Merck) in 1 x TBE before being pipetted into a well on the agarose gel. The agarose gel containing the plasmid samples was run at 200V for 2 hours at room temperature. Staining was performed for 2 hours at room temperature with a 1 x SYBR Gold solution (Molecular Probes, Eugene, USA) in 1 x TBE, diluted from a 10.000 x stock solution.

The topoisomer ladder was produced according to the procedure described by Keller [16]. To a mixture of 25 µl 2 x reaction buffer (20mM TrisHCl, 0.4M NaCl, 0.4 mM EDTA·Na_2, 0.1 mM dithiothreitol, 1% glycerine, pH 7.9), 7.5 µl 0.18 µg/µl pMCP1 (1.3 µg) solution, and 0.5 µl topoisomerase (5 Units, corresponds to 4 Units/µg), following volumes of a 10 mg/ml EtBr solution were added and the reaction volume was filled up with water to a total volume of 50 µl (final EtBr-concentration is given in the brackets): 0 µl (0 M EtBr), 2 µl ($1 \cdot 10^{-6}$ M EtBr), 4 µl ($2 \cdot 10^{-6}$ M EtBr), 6 µl ($3 \cdot 10^{-6}$ M EtBr), 8 µl ($4 \cdot 10^{-6}$ M EtBr), 12 µl ($6 \cdot 10^{-6}$ M EtBr). After incubation for 30 minutes at 37°C in a thermomixer (Eppendorf, Hamburg, Germany), 50µl of a saturated aqueous phenol (Riedel de Haën) solution was added. After addition of an equal volume of chloroform and vigorous mixing, a three-phase sytem was formed with an interphase containing denatured proteins. After removal of the organic phase, the aqueous mixture was extracted another two times with chloroform. For AGE analysis, 2 µl of the top aqueous layer were mixed with 13 µl water and 5 µl of sample buffer and the total volume was pipetted into a well of the agarose gel.

2.2 Synthesis of stationary phase

The chromatographic ligand 9-(*O*-allylcarbamoyl)quinine was prepared by a modified version of our procedure published earlier [17]. 30 mmol dihydroquinine (Buchler, Braunschweig, Germany) were dissolved in dry dichlormethane (Sigma). After addition of 33 mmol allyl isocyanate (Fluka) and two drops of dibutyltindilaurate (Aldrich) as the catalyst, the solution was refluxed for 6 hours under nitrogen atmosphere. Complete conversion was monitored by tlc (hexane : ethyl acetate : triethylamine = 3 : 6 : 1, $R_{f,\ product}$ 0.4, $R_{f,\ educt}$ 0.0). After solvent evaporation, the raw material was crystallized from toluene/hexane and washed with cold hexane, yielding 11 g (27 mmol, 90%) of white crystals.

The ligand was attached to 3-mercaptopropyl-modified silica produced from 3-mercaptopropyl-methyldimethoxysilane and bare silica, which was drained

before silylation by azeotropic distillation in toluene with a Dean-stark trap as described elsewhere [18]. In a second step, the silanol groups were endcapped with hexamethyldisilazane to form trimethylsilyl (TMS)-endcapped silanols. Later, 9-(*O*-allylcarbamoyl)quinine and 3-mercaptopropyl-modified silica was refluxed in methanol in presence of AIBN as radical initiator. Washed and dried silica material was used for column packing after sieving through a 40 µm stainless steel sieve. Elemental analysis (C, H, N, S) revealed a ligand density of 320 µmol/g. Compared to the thiol concentration on the silica surface (615 µmol/g) measured spectrophotometrically [19], 52% of thiols were modified.

2.3 Optimized analysis method for plasmid isoform separation by chromatography

For chromatographic analysis a mixed salt and organic modifier gradient was used. First, a 0.5 mol/L stock solution from NaH_2PO_4 (Merck, Darmstadt, Germany) was prepared. Buffer A consisted of 50 mmol/L NaH_2PO_4 titrated to 7.0 with 5M NaOH. Buffer B consisted of 50 mmol/L NaH_2PO_4, 0.6 mol/L NaCl and 10% (v/v) isopropanol titrated to 7.0 with 5M NaOH. A gradient from 0 to 100%B in 15 minutes was run during analysis. Between the analytical runs, the column was washed by a plug of sodium chloride (injection of 50µl 3M NaCl (aq.)), followed by reequilibration to 0% B for 5 minutes. The flow rate was set to 0.7 ml/min, detection wavelength to 258 nm (reference 360 nm with 100 nm bandwidth) and the temperature to 60°C (with preheating of the solvent in the 3 µl heat exchanger). Injection volume was dependent on the sample concentration (10 to 50 µl).

3. Results and Discussion

Chromatographic columns containing quinine carbamate ligands attached to silica were successfully used in our group for separating isoforms of plasmid DNA, i.e. ccc, oc and linear forms [20]. For this isoform separation, a short-spaced linker between the silica surface and the chromatographic ligand was employed, in combination with a mixed pH and isopropanol gradient. By salt-promoted elution and linker extension from 4 to 8 bonds between the carbamate nitrogen and silicon atom (see fig. 1), the originally broad band of the ccc form split into a set of discrete and narrow peaks (fig. 2). The separation may be enhanced by decreasing the gradient slope, which was important for semipreparative fractionation and isolation of single peaks, i.e. individual topoisomers of different linking numbers *Lk*. Topoisomers of bigger sized plasmids (over 10 kbp) usually need shallow gradients as well in order to obtain a good separation.

The identity of the separated species was indicated by plotting peak areas of adjacent peaks in a histogram, thus assuming that adjacent peaks belong to topoisomers differing by one superhelical turn, i.e. one unit of writhe. Such a histogram is shown in figure 3 for two different plasmids, pMCP1 and pAcMC1 with sizes of 4.9 kbp and 9.9 kbp, respectively. The peak areas of the 9.9 kbp plasmid shown in fig.3b were fitted to a Gaussian distribution using Sigma Plot and the following equation

$$f(x) = a \cdot e^{-\frac{1}{2}\cdot\left(\frac{x-x_0}{b}\right)^2} \qquad \text{(Eqn. 4)}$$

where a, b and x_0 were parameters to be fitted and x_0 is the deviation between Lk_0 and Lk_m and must be between -0,5 and +0,5. The curve fitting in Fig.

4a shows a very good correlation indicating that the peak area distribution is indeed Gaussian. Another way of plotting the data in order to obtain linear regression is according to equation 3, defined in the introduction section. The data obtained from chromatographic runs can be displayed by plotting the expression on the left side (for $[Lk_x]$ and $[Lk_m]$ the peak areas are taken) on the y-axis against the linking number difference ΔLk, counted from the most abundant topoisomer Lk_m [21]. Such plot is shown in Fig. 4b for the 9.9 kbp plasmid, overlaid by a linear curve, which fits well to our data set. Small discrepancies may originate from incomplete resolution and peak tailing, which causes some error when integrating individual peaks. Because of good correlation of the linear regression, it can be assumed that the Gaussian distribution obtained by chromatography with the quinine carbamate ligand originates from ccc topoisomers having different linking numbers.

Various other commercial and non-commercial plasmids in the range between 2.7 and 14.5 kbp have been injected into our chromatographic system to verify the universal applicability of our method. All plasmids in this study have been separated into its ccc topoisomers, as can be seen in figure 5. Merely the linear elution gradient has to be adapted to the plasmid size. While small plasmids below 6 kbp can be separated with a gradient of 0 to 100%B in 15 minutes, corresponding to 40 mM NaCl / min, bigger plasmids are better separated with 10 mM NaCl / min or even less. However, by raising the start concentration of buffer B, the analysis can be carried out in less than 20 minutes (for exact elution conditions for some plasmids see caption of fig. 5).

Mobile phase optimization

We studied the following parameters in order to optimize mobile phase conditions for maximum resolution between the most abundant topoisomer and the adjacent topoisomer eluting later: buffer pH value, temperature and organic modifier (isopropanol) concentration in the eluting buffer, the results of which can be found in table 1. The buffer pH was studied in the range between 6.0 and 7.7. Below pH 6, the retention is very strong, thus high salt content of the elution buffer would be necessary, which in turn might cause clogging and leaking problems. Over pH 7.7, plasmid DNA is not retained on the stationary phase due to repulsive silanol interactions and loss of actual ion-exchange capacity. Highest topoisomer resolution is obtained at pH 7.0. Because of relatively small retention at this pH, topoisomers elute from the column at a relatively low salt content, being beneficial for semipreparative fractionation and further analyses of the eluates.

Temperature was found to be an extremely important parameter, which we studied in the range between 20°C and 65°C. The selectivity for topoisomer separation is only present at temperatures above 45°C, while at lower temperatures the topoisomers comigrate as a single, narrow ccc peak. We found highest resolution at 60°C, but the exact influence of this parameter on separation is unclear. It is however safe to assume that the obtained peak distribution profile has not originated from DNA denaturation, since at 45°C the double-helix is still intact.

Topoisomer separation on our quinine carbamate stationary phase can be carried out successfully by employing a linear gradient of only one component, sodium chloride. Without a salt, no topoisomer separation is possible, i.e. the ccc form elutes as a single band. However, better results can be achieved by adding isopropanol, an organic solvent known to modify hydrophobic interactions and π–π stacking. We found best results when adding the organic solvent only to the elution

buffer B, while buffer A is purely aqueous. Therefore, a mixed salt and isopropanol gradient is run during chromatography. We optimized the content of the organic modifier in buffer B in the range between 0 and 30%, because higher concentrations may cause solubility problems. We found highest resolution at 10% isopropanol, however when topoisomer separation is better than necessary, the isopropanol content may be increased to 20% to speed up the separation. At this level, the resolution is decreased by about 10%, but the analysis time can be halved and the eluted substances are significantly less contaminated with salt in preparative runs.

Analysis of isolated topoisomers

Individual topoisomers were isolated by collecting eluates after UV detection, during six semi-preparative runs injecting the maximum possible volume of 100 µl each. The eluates were concentrated by removing 60 – 80% of the solvent volume by blowing a stream of nitrogen gas into the eluate-containing vial. The samples were dialyzed to remove a large part of salts to exclude possible interferences due to high ionic strength. By re-chromatographing the isolated fractions with the same conditions that were used for fractionation, discrete peaks were recorded at the retention time of their collection. In figure 6, an overlay of one semi-preparative run and three isolated fractions is shown. Note that the isolated fractions give single peaks, showing that they consist of discrete species and that the Gaussian peak distribution is not a dynamic phenomenon induced by the chromatographic process. After incubation of the isolated fractions at different temperatures (-20°C, +4°C and room temperature) for several days, still a single peak is obtained in the chromatogram with an additional peak being the open circular form, which is formed naturally during thermal and mechanical stress from the ccc form (data not shown). This phenomenon is a further proof of the topoisomer presence, since the topology and thus the complete distribution could be only formed by adding topoisomerases. Secondly, the emerging peak for the open circular form increasing with time can only be formed from the ccc form (in the absence of specific enzymes).

We have analyzed the isolated fractions with capillary gel electrophoresis containing chloroquine in the running buffer. Without chloroquine, the selectivity based on tertiary DNA structure, i.e. between topoisomers, is very low because of their very similar hydrodynamical radius. Thus, a separation can only be guessed when zooming into the broad peak containing fractions isolated before (fig. 7). In the electropherograms, the open circular form served as a reference having no writhe, i.e. no superhelical turns. By adding 15µg/ml chloroquine to the running buffer, the number of negative superhelical turns was decreased below the limit of separation, and the ccc band was split into two peaks corresponding to the two fractions in the mixture (fig. 8a). The migration order C < A < oc indicated that the topoisomer in fraction A is less supercoiled than the one in C, which would be true if both topoisomers are still negatively supercoiled. By adding more chloroquine to the running buffer, both topoisomers were migrating closer to the oc form than previously, proving that the writhe was still negative (fig. 8b). From these results the elution order on our stationary phases can be deduced, namely that less (negatively) supercoiled ccc topoisomers migrate earlier than those with higher supercoiling.

For complete characterization of the separated topoisomers, we have determined the number of superhelical turns in one of the isolated fractions. According to the Method by Keller [16], a topoisomer ladder has been constructed

with topoisomers having a superhelicity between a relaxed reference state and the isolated sample, as described in the experimental section. The topoisomers have been separated by means of agarose gel electrophoresis containing various amounts of ethidium bromide in the gel and the running buffer (fig. 9). This ensured, that the writhe of all species in the topoisomer ladder was decreased below the limit of separation at some point. By comparing the densitometric traces the number of superhelical turns in the isolated fraction could be determined (fig. 10). Fraction X contains a topoisomer with 26 ± 2 superhelical turns. Following figure 6 and the rule, that topoisomers with higher supercoiling elute later from the chromatrographic column, fractions A – C have following numbers of superhelical turns: 29 ± 2 (A), 32 ± 2 (B), 36 ± 2 (C). Finally it can be deduced, that the topoisomer distribution in the natural sample of the pMCP1 plasmid is centred around the topoisomer with a writhe of 30 ± 2.

It has to be added that once such a topoisomer is provided for a certain plasmid, it can serve as a reference point for future analysis. Because the isolation of such material is relatively easy and does not need special equipment apart from the chromatographic column, sufficient quantities can be produced in short time for analytical purposes as individual topoisomer standards. Additionally, semi-preparative runs have shown excellent loading capacities. Due to injection volume restriction of our system, we were only able to inject volumes up to 100 µl. This however corresponded to a load of 285 µg plasmid DNA on a porous 120 x 4.0 mm column. As plasmids do not enter the pores, the available surface area is less than one square meter for the whole column. Thus, with a single analytical column alone milligram quantities of an *individual* topoisomer can easily be isolated after 30 – 50 runs. Compared to electrophoresis, chromatography in general allows much faster and easy-to-handle isolation of single topoisomers. For example, one chromatographic run allows two orders of magnitude greater yields than an electrophoretic run. Furthermore, chromatography is characterized by much easier upscalability.

4. Conclusion

During optimization of mobile phase conditions for plasmid isoform separation, i.e. open circular (oc), linear (lin) and covalently closed circular (ccc) plasmid isoforms, conditions were found where the broad ccc band started to separate into a set of discrete and narrow peaks. When plotting the areas of the separated peaks in a histogram, a Gaussian distribution is obtained, which is typical for plasmid topoisomer distribution. By re-chromatographing the eluted peaks, the chromatogram matched the eluted fraction, thus showing that a discrete species is present and that the observed separation is not induced by the chromatographic process.

To verify the identity of the species, fractions were collected after chromatographic separations and desalted by dialysis. Under conditions, where ccc topoisomers are separated according to literature, the collected fractions could be separated by electrophoresis by both variants, capillary gel electrophoresis and agarose gel electrophoresis. With the latter, the number of superhelical turns of a single topoisomer from a chromatographic fraction could be determined. Thus, we showed that our chromatographic method in combination with electrophoretic techniques is suitable for producing larger quantities of defined, well-characterized single topoisomers or their mixtures on one hand. Secondly, rapid analysis of the topoisomer distribution can be performed by referencing the retention times to a topoisomer standard with defined superhelicity. In combination with size-exclusion

chromatography in two-dimensional HPLC, fast analysis (< 13 minutes) of heavily contaminated samples, such as cell lysates, can be easily accomplished (*manuscript in preparation*).

The key to the presented separation of topoisomers with different numbers of superhelical turns is the quinine carbamate-based chromatographic ligand along with the specified mobile phase conditions. With this stationary phase, a powerful method was developed for liquid chromatography, which is considered more robust than electrophoresis. Secondly, chromatographic methods can be easily upscaled for preparative applications or coupled to different devices for further analysis. In the near future we will focus on a more detailed study of the biomolecules in connection with atomic force microscopy and on possible biological implications.

5. Acknowledgement

We greatly appreciate the financial support and the provision of the HPLC system by Boehringer-Ingelheim RCV (Vienna, Austria).

6. Figures

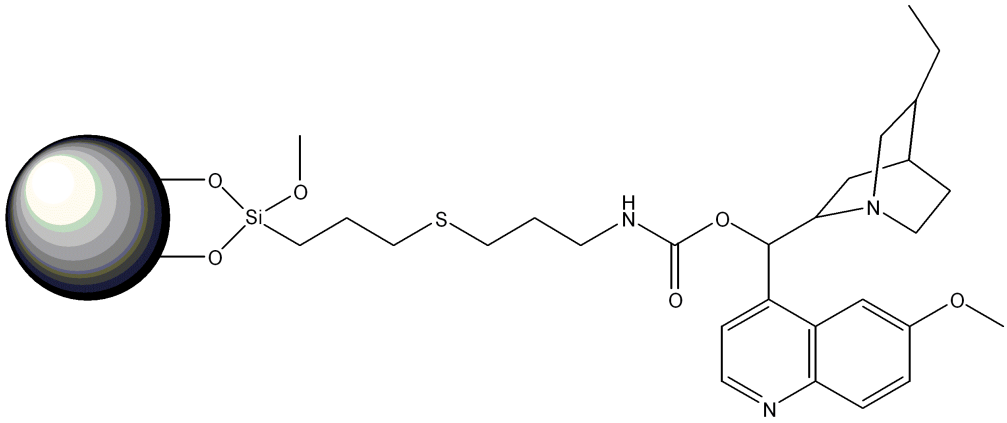

Figure 1: Quinine carbamate ligand attached to silica via a long thioether linker employed in this study. A short linkage, for comparison studies, lacks the thiopropyl moiety. The quinoline ring may intercalate into the double helix while the quinuclidine and the carbamate groups, separated by a specific distance, bind into grooves of the DNA, providing the basis for molecular recognition.

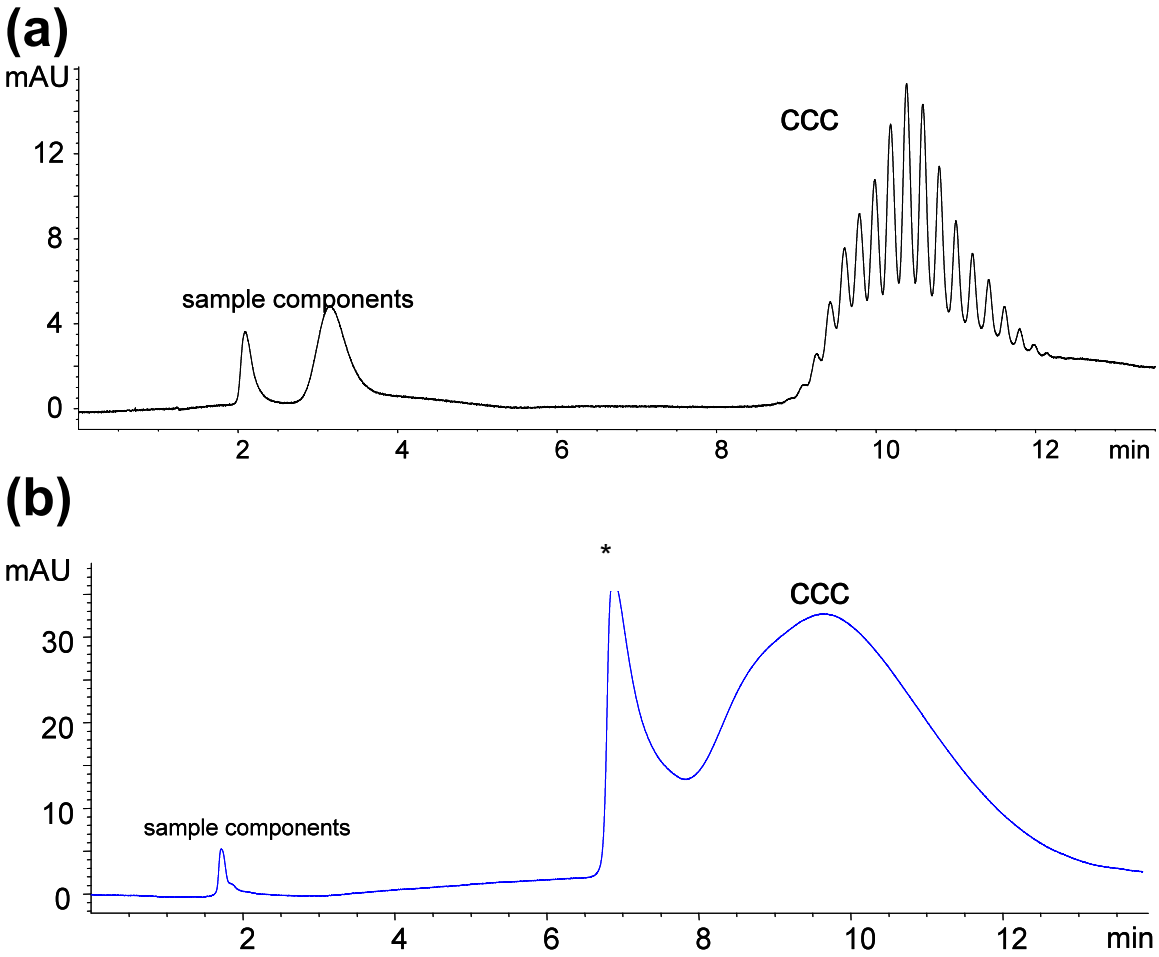

Figure 2: Chromatograms of pMCP1 plasmid (4.9 kbp) on quinine carbamate columns attached to 5µm porous silica surface via long (a) and short (b) linker (for short linker see ref. [20]). Note that both columns provide selectivity for ccc topoisomers, however, while the short linker gives an unresolved ccc band, the elongated linker provides a nice separation of single topoisomers with different linking numbers. Conditions: A: 50mM phosphate buffer pH 7.0, B: A + 0.6M NaCl + 10% isopropanol, linear gradient from 0 to 100%B in 15 minutes, 60°C, 0.7 ml/min, inj. of 8 µg pDNA each, det. 258 nm. Peaks marked with "sample components" do not contain DNA according to DAD-UV spectra. Sample in (b) contains a substantial amount of the oc form (*), whereas the sample in (a) has a high ccc form contents.

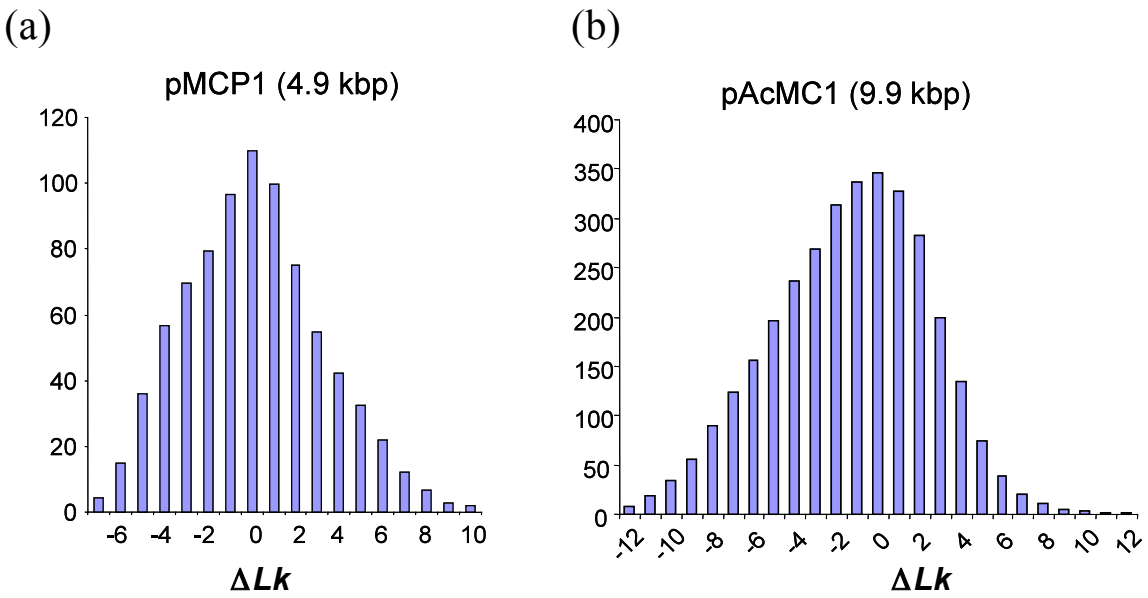

Figure 3: Histograms plotting adjacent topoisomer-peak areas (mAU·s) against the linking number for the pMCP1 (data from Fig. 2a) and pAcMC1 plasmids. The highest abundant topoisomer is set as Δ*Lk* = 0. Conditions: (a) as in Fig. 2., (b) as in fig. 2 with a gradient from 0 to 100%B in 60 minutes.

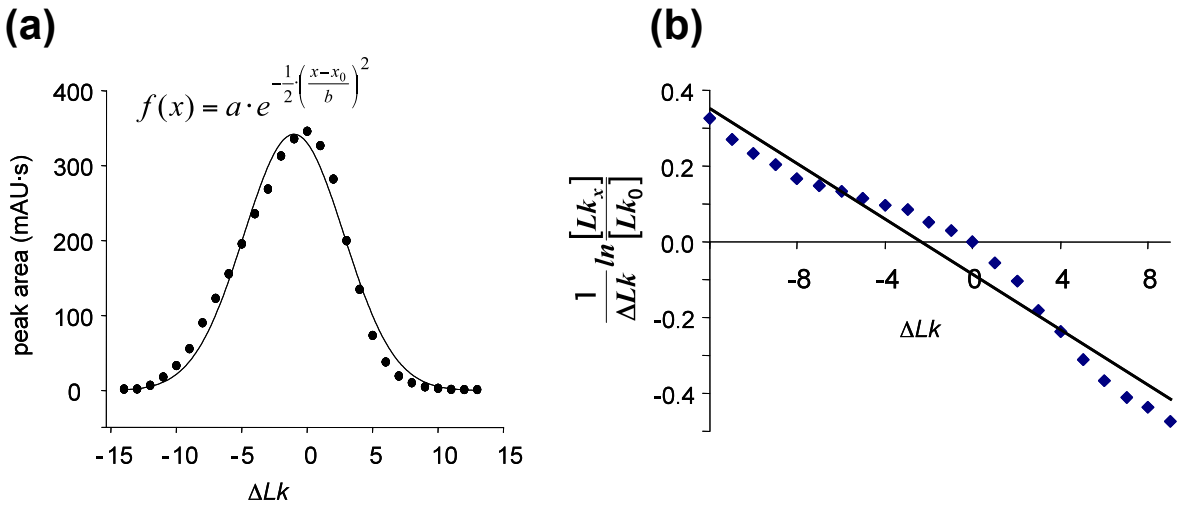

Figure 4: (a) Curve-fitting to experimental data of the histogram in Fig. 3b (●) with a Gaussian distribution (—) shows a good correlation (R^2 = 0.988). The fit was performed with Sigma Plot software to the equation shown in the upper left corner for three independent variables (a, b, x_0). (b) Plot following equation 3 showing a linear correlation (R^2 = 0.964, trendline shown in the plot). Both fits, the Gaussian distribution in (a) and the linear curve in (b), are associated with the topoisomer distribution in a natural sample and thus provide an indirect evidence of the presence of these species within the peaks obtained by our chromatographic method.

a) **b)**

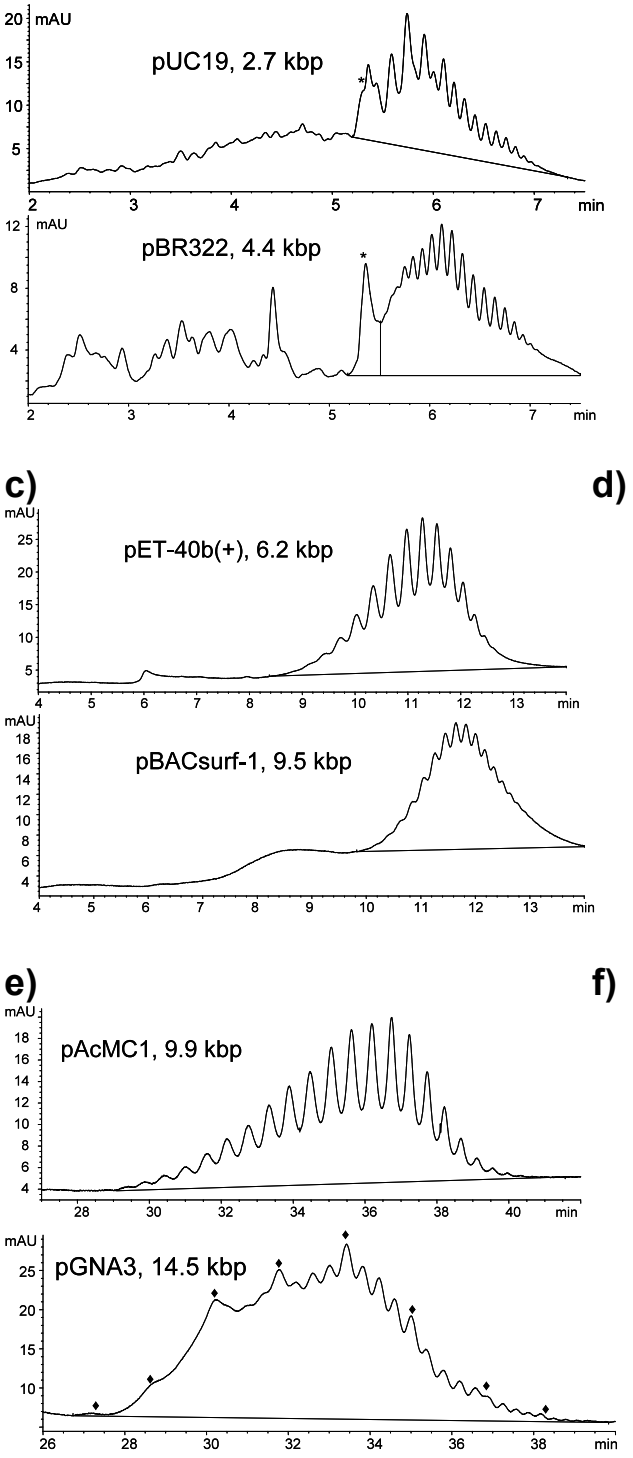

Figure 5: Various commercial (a – d) and non-commercial (e, f) ccc plasmid preparations separated on the quinine carbamate stationary phase of fig. 1. Ccc forms of all plasmids, marked by a baseline, could be separated into topoisomers, showing the universal applicability of the method. With increasing plasmid size the gradient slope must be decreased in order to achieve good separation. The asterisks in (a) and (b) mark the open circular form. Plasmid pGNA3 in (f) had a smaller plasmid as by-product – its topoisomers are marked with a diamond mark. Conditions: A: 50mM phosphate buffer pH 7.0, B: A + 0.6M NaCl + 30% isopropanol pH 7.0, 60°C, 0.7 ml/min, det. 258 nm.; (a),(b) 0 – 100%B in 15 min, inj. 0.8 µg (a) and 0.5 µg (b) pDNA; (c),(d), 5 – 30%B in 15 min, inj. 2.0 µg pDNA each; (e),(f) 0 – 75%B in 45 min, inj. 3 µg (e) and 8 µg (f)

Table 1: Optimization of mobile phase conditions for three parameters: pH value of phosphate buffer, temperature and isopropanol content in the elution buffer B. The value out of each parameter, yielding the highest resolution between the most abundant topoisomers, is written in bold letters. This study

was carried out with 8 µg pMCP1 plasmid DNA per injection, employing a linear gradient 0 – 100%B in 15 min (pH, temperature) and 0 – 100%B in 60 min (isopropanol content), respectively. Buffer B always contained 0.6 mol/L NaCl.

buffer pH value (buffer A and buffer B),
temperature (60°C) and isopropanol content of the elution buffer (30%) are kept constant

pH	number of separated topoisomers	retention time of highest abundant topoisomer	resolution between most abundant topoisomers	peak width of most abundant topoisomer
6.0	18	10.01 min	0.46	0.184 min
6.5	18	8.18 min	0.55	0.188 min
7.0	18	7.42 min	**0.61**	0.220 min
7.5	15	4.12 min	0.38	0.430 min
7.7	8	2.81 min	0.22	0.680 min

temperature
pH value of buffer (7.0) and isopropanol content of the elution buffer (30%) are kept constant

temp. in °C	number of separated topoisomers	retention time of highest abundant topoisomer	resolution between most abundant topoisomers	peak width of most abundant topoisomer
20	0	--- no separation of topoisomers ---		
35	0	--- no separation of topoisomers ---		
40	0	--- no separation of topoisomers ---		
45	7	6.24 min	0.05	1.330 min
50	13	6.01 min	0.23	0.490 min
55	13	6.18 min	0.68	0.197 min
60	14	6.24 min	**0.89**	0.102 min
65	14	6.08 min	0.52	0.097 min

organic modifier (isopropanol, IPA) content
pH value of buffer (7.0) and temperature (60°C) are kept constant

% IPA	number of separated topoisomers	retention time of highest abundant topoisomer	resolution between most abundant topoisomers	peak width of most abundant topoisomer
0	20	11.00 min	0.67	0.372 min
10	22	22.33 min	**0.99**	1.000 min
20	21	14.86 min	0.90	0.640 min
30	19	10.76 min	0.68	0.385 min

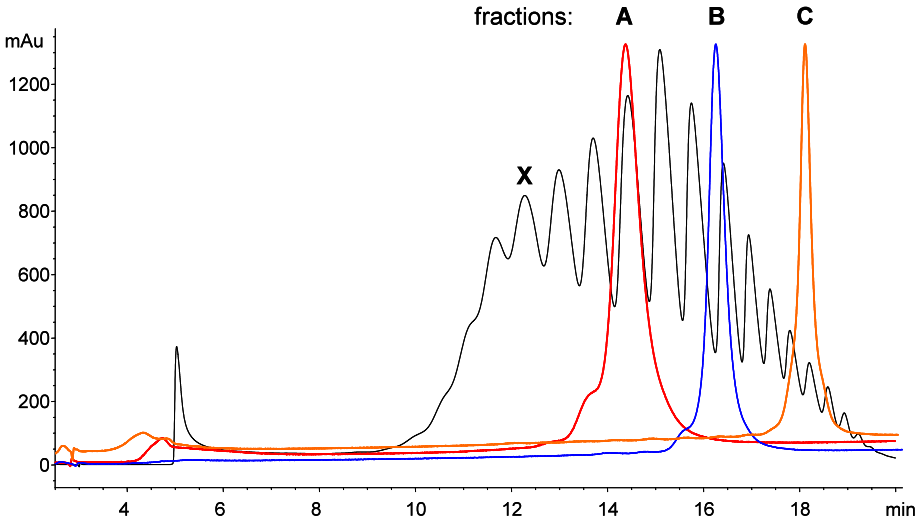

Figure 6: Chromatogram of a semi-preparative run after injecting 285 µg pMCP1 onto a 120 x 4.0 mm column with 5 µm porous (120 Å) silica containing quinine carbamate ligand of fig. 1, during which three fractions (A, B, C) were isolated. 20 µl of the isolated aliquots were re-injected and the corresponding chromatograms overlayed in the diagram (y-axis scaled to preparative run). Correspondingly, the ccc peak distribution in the pMCP1 sample must consist of discrete peaks (i.e. topoisomers). Fraction X was used for determination of the number of superhelical turns. Conditions:

A: 50mM phosphate buffer pH 7.0, B: A + 0.6M NaCl + 30% isopropanol pH 7.0, 60°C, 0.7 ml/min, det. 258 nm.; linear gradient 10 – 35%B in 30 min

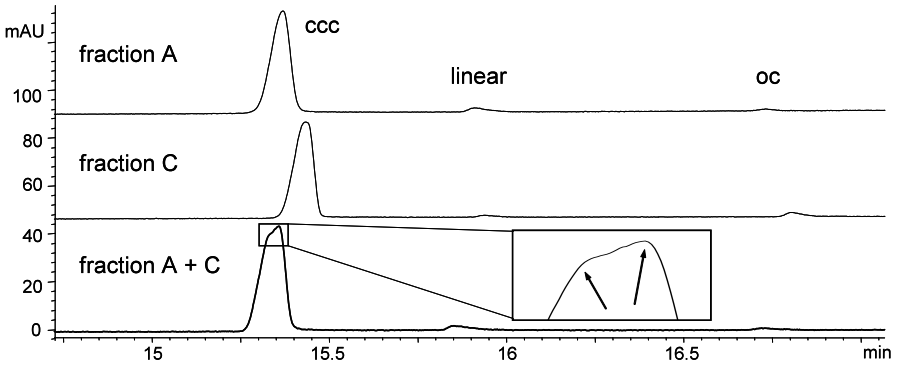

Figure 7: CGE electropherograms of isolated ccc fractions (pMCP1 plasmid) without intercalator. Individual topoisomers cannot be separated well. However, a minute selectivity may be present which is indicated by the arrows in the zoomed inset, marking two topoisomers differing by 7 superhelical turns. Conditions: TBE buffer pH 9 + 0.1% 86 kDa hydroxypropylmethylcellulose, -3.3 kV, inj. -5 kV for 4 sec., 25°C, UV det. 258 nm

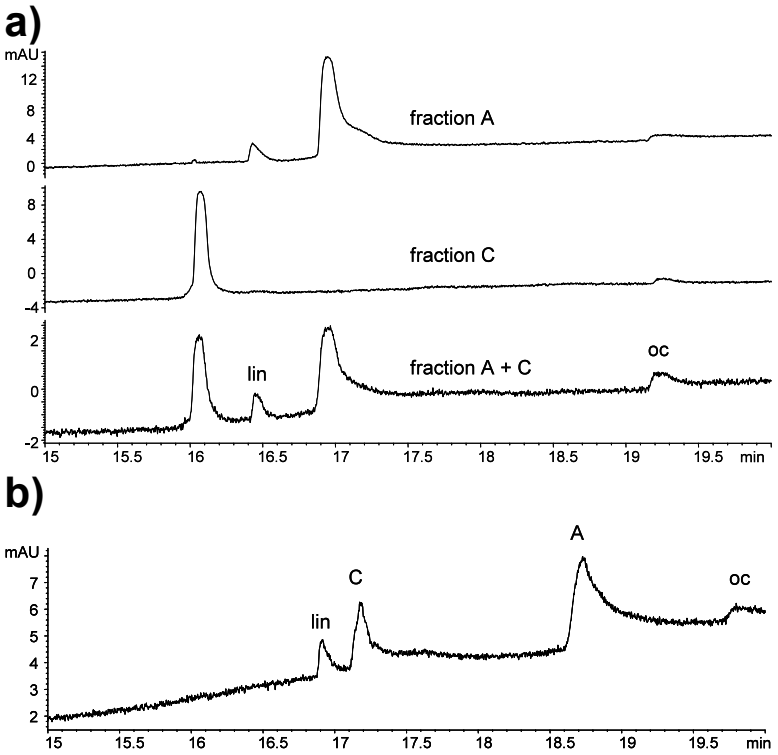

Figure 8: CGE electropherograms of isolated ccc fractions (pMCP1 plasmid) with various intercalator concentrations in the running buffer. Topoisomers in both fractions are naturally negatively supercoiled, i.e. have negative writhe. Due to chloroquine addition in (a), topoisomer in fraction A now has less negative superhelical turns and migrates closer to the open circular form, which has no writhe, than the other topoisomer. By increase of the chloroquine concentration, migration times of both topoisomers are even more closer to the open circular form, confirming that topoisomer in fraction A is less (negatively) supercoiled than topoisomer in fraction C. This also defines the elution order during our chromatographic conditions. Conditions as in Fig. 7, containing 15 µg/ml (a) and 25 µg/ml (b) chloroquine diphosphate in the running buffer.

a) **b)**

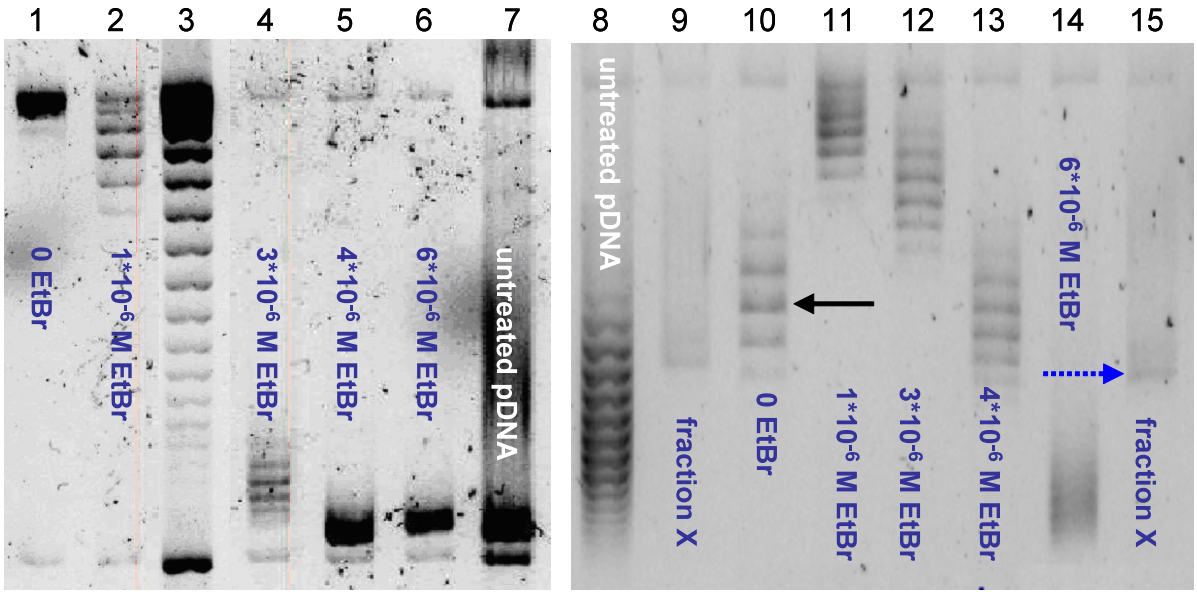

Figure 9: Photographs of agarose gels stained with SYBR-Gold, run with 0 (a) and with 5 µg/L ethidium bromide present in the running buffer. On gel (a), lanes 4 – 7 contain topoisomers of the pMCP1 plasmid, the writhe of which is above the limit of separation. Also the sample, which is enzymatically relaxed without ethidium bromide (lane 1), could not be separated. However all these samples can be separated on gel (b), which also contains fraction X marked by the dotted arrow (lanes 9 and 15), isolated by chromatography. The straight-lined arrow marks the reference point having no writhe in lane 10. Lane 2 contained the standard produced in the presence of $2*10^{-6}$ M EtBr.

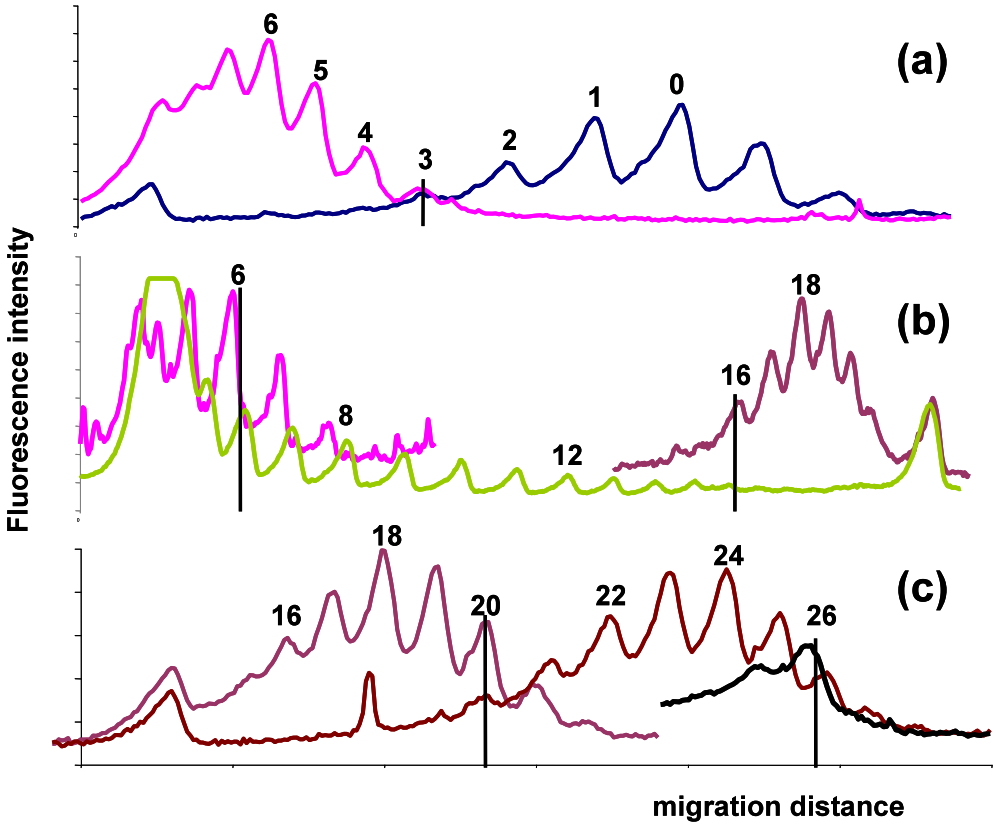

Figure 10: Overlays of densitometric tracings of lanes from figure 9, showing an example of AGE data analysis. Adjacent peaks differ by one superhelical turn, thus the difference between the unknown topoisomer and the $3*10^{-6}$ M EtBr standard (meaning the highest abundant species) in lane 12 is 8 supercoils (c). The difference between standards 1 and $3*10^{-6}$ M EtBr is 12, determined by overlaying lanes 2, 3, and 4 (b). Finally, standard $1*10^{-6}$ M EtBr differs from the reference point with zero writhe by 6 superhelical turns (c). The values sum up to 26 superhelical turns (6 + 12 + 8) for fraction X.

7. References

[1] Schleef, M., *Plasmids for Therapy and Vaccination*, Wiley-VCH, Weinheim 2001.

[2] Giacomoni, P. U., *Journal of Photochemistry and Photobiology, B: Biology* 1995, *29*, 83-85.

[3] Bauer, W. R., Crick, F. H. C., White, J. H., *Scientific American* 1980, *243*, 118-124, 126, 129-130, 132-113.

[4] Mirkin, S. M., *Encyclopedia of Life Sciences* 2001, 1-11.

[5] Bauer, W. R., *Annual Review of Biophysics and Bioengineering* 1978, *7*, 287-313.

[6] Fuller, F. B., *Proc. Nat. Acad. Sci. U. S.* 1971, *68*, 815-819.

[7] Bjornsti, M.-A., Osheroff, N., *DNA Topoisomerase Protocols*, Humana Press, Totowa, New Jersey 1999.

[8] Pulleyblank, D. E., Shure, M., Tang, D., Vinograd, J., Vosberg, H. P., *Proceedings of the National Academy of Sciences of the United States of America* 1975, *72*, 4280-4284.

[9] Depew, R. E., Wang, J. C., *Proc. Natl. Acad. Sci. U. S. A.* 1975, *72*, 4275-4279.

[10] Mao, D. T., Levin, J. D., Yu, L., Lautamo, R. M. A., *Journal of Chromatography, B: Biomedical Sciences and Applications* 1998, *714*, 21-27.

[11] Mayan-Santos, M.-D., Martinez-Robles, M.-L., Hernandez, P., Krimer, D., Schvartzman, J. B., *Electrophoresis* 2007, *28*, 3845-3853.

[12] Reyes-Dominguez, Y., Contreras-Ferrat, G., Ramirez-Santos, J., Membrillo-Hernandez, J., Gomez-Eichelmann, M. C., *Journal of Bacteriology* 2003, *185*, 1097-1100.

[13] de Carmejane, O., Schwinefus, J. J., Morris, M. D., *Proceedings of SPIE-The International Society for Optical Engineering* 1999, *3602*, 346-354.

[14] Kapp, U., Langowski, J., *Analytical Biochemistry* 1992, *206*, 293-299.

[14*] Urthaler, J., Buchinger, W., Necina, R., *Chemical Engineering & Technology* 2005, *28*, 1408-1420.

[15] Raucci, G., Maggi, C. A., Parente, D., *Analytical Chemistry* 2000, *72*, 821-826.

[16] Keller, W., *Proc. Natl. Acad. Sci. U. S. A.* 1975, *72*, 4876-4880.

[17] Laemmerhofer, M., Lindner, W., *Journal of Chromatography, A* 1996, *741*, 33-48.
[18] Mandl, A., Nicoletti, L., Lammerhofer, M., Lindner, W., *J. Chromatogr., A* 1999, *858*, 1-11.
[19] Nogueira, R., Laemmerhofer, M., Maier, N. M., Lindner, W., *Analytica Chimica Acta* 2005, *533*, 179-183.
[20] Mahut, M., Schuchnigg, H., Urthaler, J., Buchinger, W.*, et al.*, *to be submitted* 2010.
[21] Bates, A. D., Maxwell, A., *DNA Topology*, Oxford University Press, New York 2006, pp. 55-65.

Manuscript 3

Title: Molecular recognition principles and stationary phase characteristics for chromatographic separation of circular plasmid DNA topoisomers

Authors: Marek Mahut, Wolfgang Lindner, Michael Lämmerhofer

University of Vienna, Department of Analytical Chemistry, Waehringer Strasse 38, A-1090 Vienna, Austria

Abstract:

Chromatographic separation of circular plasmid topoisomers of different linking numbers was earlier shown to be possible on silica stationary phases with a quinine carbamate ligand. In this paper we present a study on stationary phase conditions with a focus on ligand structure to derive structure-separation relationships for topoisomer recognition. Two main parts of the quinine carbamate molecule, quincorine and quinoline moiety, were attached individually onto silica support. While the quinoline carbamate showed no selectivity, the quincorine carbamate was able to resolve the topoisomer pattern of the covalently closed circular (ccc) plasmid form. Thus, intercalation is obviously not an essential part of molecular recognition during the chromatographic process. We found that the key elements necessary for the selectivity of the *tert*-butylcarbamoyl-quincorine stationary phase are 1) the presence of a rigid weak anion-exchange/H-acceptor site, 2) the presence of a second H-acceptor site, 3) the distance between these two sites. Additionally, greater rigidity of the ligand molecule is advantageous, which implies that ligands attached through the 9-carbamoyl moiety to the silica support provide higher chromatographic resolution. The silica support providing best analytical results are small non-porous particles, such as the 1.5 µm Micra material. Because of the size of plasmid molecules, these do not enter small mesopores, so standard employed supports with pore sizes below 120 Å still provide reasonable separation. As a result of our study, an ideal stationary phase for ccc topoisomer separation is discussed along with a detailed study of the chromatographic selector structure and its interactions with circular plasmids having different degrees of supercoiling.

Keywords:

plasmid DNA, plasmid topoisomer separation, quinine, quincorine, molecular recognition of plasmid topoisomers

1. Introduction

Native samples of covalently closed circular (ccc) plasmids consist of a series of individual topoisomers, which differ by various degrees of supercoiling [1]. These topological isomers (topoisomers) have different linking numbers [2], and thus a different number of superhelical turns [3]. We have recently described the first chromatographic separation of such topoisomers of native plasmid DNA [4], which was previously only possible with electrophoretic methods [5]. The key element in the separation was a quinine carbamate ligand attached to 5 µm porous silica support. In this study we present a detailed study of the ligand optimization by varying individual structural elements.

Groove-binders, intercalators and triplex-helical forming agents are main groups of DNA binding molecules, which may recognize DNA specifically [6]. Quinine (QN) belongs to a group of anti-R-plasmid substances, such as ethidium

bromide, quinacrine and chloroquine, which change the superhelical density of DNA *in vitro* indicating an intercalative binding [7]. The quinoline ring of QN is thought to satisfy the criteria for this behaviour [8]. Data obtained by photometric titration suggest a second binding site, which is thought to be an electrostatic interaction between the tertiary aminogroup of quinuclidine and a groove of the DNA-helix [9]. Our chromatographic ligand bears additionally a carbamate moiety, the role of which for topoisomer recognition turns out to be important which is thoroughly described in this paper.

In a second part, we focus on the characteristics of the chromatographic support, the morphology of which has also great influence in DNA separation [10]. In general, micropellicular stationary phases, such as with a solid core and a thin retentive layer, are thought to have best separating performance for large biomolecules such as plasmid DNA [11]. We have therefore compared different types of silica supports as well as stationary phase characteristics such as ligand density, pore size and length of the linker between the support phase and the ligand. The consideration of these findings for the improvement of the separation materials and the combination of the most effective stationary phase parameters has led to the design of an optimized stationary phase for topoisomer separation. The key element, however, remains the chromatographic ligand, the general essential structure of which for topoisomer recognition could be discovered herein by structure-topoisomer separation relationship studies. A detailed description of all pivotal structural elements and their proposed interaction modes is given.

2. Experimental

2.1 Materials and instruments

5 µm silica particles with 120Å pores (332 m²/g specific surface area), 200Å (200 m²/g specific surface area) and 300Å (100 m²/g specific surface area) were purchased from Daiso (Osaka, Japan). 3 µm silica particles with 3100Å pores were purchased from Akzo Nobel and 1.5 µm non-porous silica particles “Micra NPS” (3 m²/g specific surface area) were purchased from Micra Scientific (Northbrook, IL, USA). Columns with our modified 5 µm silica stationary phases (SP) were packed in-house at a pressure of 600 bar into stainless steel columns with 4.0 mm i.d. and various lengths between 100 and 150 mm, while columns with our modified 1.5 µm silica stationary phase were packed by Bischoff Chromatography (Leonberg, Germany) into stainless steel columns with 4.6 mm i.d. and 33 mm length. On both column types, steel-glass sandwich frits (containing two 5µm stainless steel frits and three glass wool filter layers between them, purchased form Bischoff Chromatography) were mounted on each side of the column. HPLC analyses were carried out on an Agilent 1200 SL system (Waldbronn, Germany) equipped with a binary pump, a thermostatted autosampler (cooled to 4°C) and a DAD UV detector. Prior to analysis, all solvents were filtered by a glass filtration unit (Millipore) through a 0.22 µm nylon filter (Sigma-Aldrich) and ultrasonically degassed. The pH was measured with a pH 720 meter by WTW (Weilheim, Germany). HPLC grade isopropanol was purchased from Carl Roth (Karlsruhe, Germany). Three different Plasmid DNA preparations in Tris-EDTA (TE) buffer were provided by Boehringer- Ingelheim RCV (Vienna, Austria), pMCP1 (4.9 kbp, 2.8 mg/ml), pAcMC1 (9.9 kbp, 1.1 mg/ml) and pGNA3 (14.5 kbp, 0.7 mg/ml), with homogeneities (ccc form contents) > 90% [11*].

2.2 Ligand synthesis for SP 1 – SP 4

2.2.1 Quinine-based ligands (for SP1 and SP2a–d): The ligand 9-(*O*-allylcarbamoyl)quinine of the SP 1 material was prepared according to our procedure published earlier [12]. For the synthesis of SP 2a, anhydrous quinine was directly used for attachment to the thiol-modified silica support. 9-(*O-tert*-butylcarbamoyl)quinine for SP 2b as well as 9-(*O-tert*-butylcarbamoyl)cinchonidine for SP 2c, starting from cinchonidine instead of quinine, were synthetized according to our procedure published earlier [13]. 9-(*O-n*-butylcarbamoyl)quinine for SP 2d was prepared in the same manner starting from *n*-butylisocyanate (Aldrich) instead of *tert*-butylisocyanate.

2.2.2 ((2S,4S,5S)-8-vinylquinuclidin-2-yl)methyl tert-*butylcarbamate (tBuCQCl)(for SP 3a):* 1.1 g (6.6 mmol) quincorine (Buchler) was dried by azeotropic distillation in toluene using a Dean-Stark trap. To 15 ml of the dry solution, 0.87 ml (7.6 mmol) *tert*-butylisocyanate and 5 µl dibutyltindilaurate was added. The reaction mixture was refluxed under nitrogen atmosphere and the progress was monitored by tlc (hexane : ethyl acetate : triethylamine = 3:6:1). After 5 h the reaction was complete (no educt at R_f 0.35) and the reaction mixture was concentrated *in vacuo*. The raw product was filtrated through a short silica column (eluent: ethyl acetate with 10% triethylamine) and the solvent removed. The product was obtained in 96% yield as a yellowish oil, which does not crystallize.
ATR FT-IR (cm^{-1}): 2927, 1713, 1528, 1454, 1265, 1215, 1087, 910; ^1H NMR (TMS, $CDCl_3$): 0.86 (dd, 1H), 1.30 (s, 9H), 1.50 (m, 2H), 1.73 (sext, 1H), 1.85 (ddt, 1H), 2.30 (m, 1H), 2.69 (m, 2H), 3.03 (m, 2H), 3.22 (dd, 1H), 3.87 (t, 1H), 4.03 (dd, 1H), 4,84 (s *(br)*, 1H, N-**H**), 5.02 (m, 1H), 5.05 (dt, 1H), 5.89 (ddd, 1H); positive ESI-MS (m/z): 267.5 ([$M+H^+$], 100%), 168.4 (62%, loss of carbamate group)

2.2.3 1-tert-*butyl-3-(((2S,4S,5S)-8-vinylquinuclidin-2-yl)methyl)urea (for SP 3b):* 500 mg (3 mmol) quincorine-amine (Buchler) was dried by azeotropic distillation in toluene using a Dean-Stark trap. To 9 ml of the dry solution, 0.4 ml (3.4 mmol) *tert*-butylisocyanate and 5 µl dibutyltindilaurate was added. The reaction mixture was refluxed under nitrogen atmosphere and the progress was monitored by tlc (hexane : ethyl acetate : triethylamine = 3:6:1). After 8 h the reaction was complete and the reaction mixture was concentrated *in vacuo*. The raw product was filtrated through a short silica column (eluent: ethyl acetate : methanol : triethylamine = 9:1:1) and the solvent removed. The product was obtained in 55% yield as a yellowish oil, which crystallizes after a few days.

ATR FT-IR (cm^{-1}): 3331 (broad, NH), 2961, 1643, 1556, 1451, 1390, 1361, 1271, 1215, 913; ^1H NMR (TMS, $CDCl_3$): 1.07 (1H, m), 1.31 (9H, s), 1.69 (1H, ddt), 1.88 (1H, sext), 2.01 (1H, ddt), 2.48 (1H, m), 2.73 – 2.82 (2H, m), 3.03 (1H, t), 3.08 (1H, m), 3.17 (1H, m), 3.31 (1H, dd), 3.49 (1H, d (br.)), 4.75 (1H, s *(br)*, NH), 5.10 (1H, d), 5.13 (1H, d), 5.83 (1H, ddd), 6.38 (1H, s *(br.)*, NH); positive ESI-MS (m/z): 266.6 ([$M+H]^+$, 100%), 193.4 (46%), 167.6 (76%)

2.2.4 N-*(((2S,4S,5S)-8-vinylquinuclidin-2-yl)methyl)pivalamide (for SP 3c):* 500 mg (3 mmol) quincorine-amine (Buchler) were dissolved in 3 ml dry THF and 0.44 ml triethylamine (3.15 mmol) under nitrogen atmosphere. At -10°C (ice/NaCl), 0.40 ml (3.15 mmol) pivaloyl chloride was slowly added. During reaction, triethylammoniumchloride precipitated from the solution. After 4 h the cooling bath was removed, the mixture filtrated and the filter cake was washed with THF. After removing the solvent, the residue was dissolved in dichloromethane. The organic

phase was washed 2x with sat. aqueous $NaHCO_3$ and once with water, dried over $MgSO_4$ and concentrated. The raw product was filtrated through a short silica column (eluent: ethyl acetate : methanol : triethylamine = 9:1:1) and the solvent removed. The product was obtained in 71% yield as yellowish crystals.

ATR FT-IR (cm^{-1}): 3355 (br.), 2932, 2866, 1638, 1531 (br.), 1481, 1455, 1365, 1204, 1051, 909; ^1H NMR (TMS, $CDCl_3$): 0.92 (1H, ddt), 1.18 (9H, s), 1.51 (2H, m), 1.73 (1H, sext), 1.90 (1H, ddt), 2.30 (1H, m), 2.56 – 2.66 (2H, m), 2.77 – 2.93 (3H, m), 3.17 (1H, dd), 3.53 (1H, ddd), 5.03 (1H, dt), 5.04 (1H, dt), 5.88 (1H, ddd), 6.39 (1H, s *(br.)*, NH); positive ESI-MS (m/z): 251.4 ($[M+H]^+$, 100%)

2.2.4 N_1*-methyl* O-tert-*butylcarbamoyl-quincorinium chloride (for SP 3d):* 600 mg (2.25 mmol) *t*BuCQCl were dissolved in toluene followed by removal of the solvent *in vacuo*. This procedure was repeated three times to obtain a dry educt, which was then dissolved in 10 ml absolute THF in nitrogen atmosphere and cooled down to 0°C (ice bath). 0.17 ml (2.7 mmol) methyl iodide were added to the stirred solution. After 30 min the cooling bath was removed and the solution was stirred at rt and monitored by tlc (ethyl acetate with 10% triethylamine). After removing the solvent, the iodide salt of the desired product was obtained as white crystals.
The iodide salt was dissolved in 7 ml ethanol in a light-protected flask and 0.97 g AgCl (6.75 mmol) were added. The suspension was stirred for 3 days at rt, forming a yellowish precipitate which is insoluble in ammonia (→ AgI). The suspension was filtered through a por.5 filter and the filter cake was washed 2 x with ethanol. The filtrate was concentrated and dried *in vacuo* to yield the product in 93% yield as a white powder.

ATR FT-IR (cm^{-1}): 3216, 2969, 2936, 1726, 1534, 1265, 1216, 1100, 922, 774, 733, 670 (the last two signals are chloride-specific); ^1H NMR (MeOH-d_4): 1.35 (9H, s), 1.72 (1H, dddd), 2.09 (2H, m), 2.18 (1H, sext), 2.35 (1H, t *(br.)*), 2.97 (1H, m), 3.11 (3H, s, N^+-CH_3), 3.43 (1H, m), 3.50 (1H, ddd), 3.76 (1H, dd), 3.78 (1H, m), 3.84 (1H, m), 4.40 (2H, s *(br.)*), 5.29 (1H, dt), 5.33 (1H, dt), 6.02 (1H, ddd); positive ESI-MS (m/z): 182.5 (81%), 281.2 (87%, $[M–Cl]^+$), 283.4 (100%), 597.4 (26%)

2.2.5 Two-step synthesis of (6-methoxyquinolin-4-yl)methyl allylcarbamate (for SP 4)

a) Synthesis of (6-methoxyquinolin-4-yl)methanol
100 ml absolute THF and 13.5 ml (13.5 mmol) of a 1M lithiumaluminumhydride solution in THF (Aldrich) were put in a dry flask under nitrogen atmosphere. 2.5 g quininic acid (produced in-house) were slowly added over 60 minutes, during which the solution turned from colourless over yellow to dark brown. After stirring for 2 hours at rt, the reaction was quenched by slow addition of water under release of hydrogen gas to give an orange coloured suspension. After filtration the solution was concentrated and separated via flash silica chromatography (dichloromethane:methanol = 20:1). The raw product was purified via preparative reversed phase HPLC using a 10µm Gemini C18 column (Phenomenex) under isocratic conditions with acetonitrile/water (23:77) mobile phase. After evaporation of the solvent 466 mg (9%) of the product were obtained. Although the yield was very low, the amount produced from two batches was sufficient for production of SP 4, thus the reaction yield was not optimized.

ATR FT-IR (cm^{-1}): 3175, 2839, 1509, 1241, 1226, 1087, 1069, 1025, 850; ^1H NMR (TMS, $CDCl_3$): 1.35 (9H, s), 1.72 (1H, dddd), 2.09 (2H, m), 2.18 (1H, sext), 2.35 (1H, t *(br.)*), 2.97 (1H, m), 3.11 (3H, s, N^+-CH_3), 3.43 (1H, m), 3.50 (1H,

ddd), 3.76 (1H, dd), 3.78 (1H, m), 3.84 (1H, m), 4.40 (2H, s *(br.)*), 5.29 (1H, dt), 5.33 (1H, dt), 6.02 (1H, ddd)

b) Synthesis of (6-methoxyquinolin-4-yl)methyl allylcarbamate
516 mg (2.95 mmol) of 4-hydroxymethyl-6-methoxy-quinoline was dissolved in 40 ml dichloromethane under nitrogen atmosphere. After addition of 285 µl (3.25 mmol) allylisocyanate and 2 µl dibutyltindilaurate as a catalyst the solution was refluxed for 6 hours. Afterwards the solvent was removed and the raw product was purified by flash silica chromatography (dichloromethane:methanol = 30:1) yielding 727 mg (98%) of the desired product.

ATR FT-IR (cm^{-1}): 3235, 3051, 2931, 1709, 1246, 1228, 1134, 850; ^1H NMR (TMS, $CDCl_3$): 3.87 (t (*br*), 2H), 3.93 (s, 3H), 5.06 – 5.18 (dd & s, 2H,), 5.22 (dd, 1H), 5.56 (s, 2H), 5.87 (ddt (*br*), 1H), 7.17 (d, 1H), 7.39 – 7.35 (m, 2H), 8.03 (d, 1H), 8.70 (d, 1H); positive ESI-MS (m/z): 273.5 $[M+H]^+$ (100%), 190.3 (76%)

2.3 Synthesis of stationary phases

Stationary phases SP 1 to SP 4 (Fig. 1a and 1b) were synthesized in close analogy to our method published before [12]. In a first step, 5µm (120Å) bare particulate silica was dried before silylation by azeotropic distillation in toluene with a Dean-stark trap followed by conversion to 3-mercaptopropyl-modified silica particles, produced by refluxing with 3-mercaptopropyl-methyldimethoxy-silane (Fluka) in toluene. All chromatographic ligand precursors for SP 1 to SP 4 contained one allyl group which has been used for attaching to the thiol-modified stationary phase by radical addition in the presence of AIBN (Merck) during refluxing in methanol. In the last step, the remaining reactive silanol groups were endcapped with hexamethyldisilazane (Fluka) to form trimethylsilyl (TMS)-endcapped silanols. Washed and dried silica material was used for column packing after sieving through a 40 µm (5 µm silica particles) or 25 µm (Micra particles) stainless steel sieve, respectively, purchased from Retsch (Haan, Germany). Elemental analysis (C, H, N, S) revealed ligand densities between 210 and 330 µmol/g on 5 µm silica particles. Compared to the thiol concentration on the silica surface (650 µmol/g) measured spectrophotometrically [14], 34 – 54% of thiols were modified.

Three SP 1 phases with different ligand densities were also synthesized, employing different equivalents of 9-(*O*-allylcarbamoyl)quinine to the surface thiol concentration during radical addition. Equimolar amounts lead to a maximum ligand density of 310 µmol/g. This corresponds to a ratio of surface thiol modification of ca. 50%, which is close to the maximum load we have practically achieved for any other ligand (54%) and cannot be exceeded by use of higher educt concentration. Starting with 0.35 molar equivalents of 9-(*O*-allylcarbamoyl)quinine, a ligand density of 190 µmol/g was obtained, corresponding to a ratio of 28% modified thiol groups. Employment of 0.18 molar equivalents of the ligand precursor, a ligand density of 110 µmol/g was obtained, corresponding to a ratio of 16% modified thiol groups.

For the pore size study, SP 2b was synthesized employing 5 µm particulate silica with two different pore sizes of 200Å (200 m^2/g specific surface area) and 300Å (100 m^2/g specific surface area) purchased from Daiso. Gigaporous silica material (3 µm, 3100Å) was also 3-mercaptopropyl-modified to yield 16µmol/g active thiols, followed by radical addition with with 9-(*O*-allylcarbamoyl)quinine to give SP 1 with a ligand density of 6 µmol/g. The gigaporous material was packed into 100 x 4.0 stainless steel columns in-house at a pressure of 230 bar. One

batch of SP 2b was also produced starting from 10 µm silica particles with 120Å pores purchased from Daiso.

Stationary phases SP 5 and SP 6 (Fig. 1c) were synthesized according to our method published earlier [13]. SP 5 was obtained starting from quinine powder, purchased from Buchler (Braunschweig, Germany), and 3-isocyanatopropyl-triethoxysilane (ABCR, Karlsruhe, Germany). The resulting carbamoylsilane was attached to dry 5 µm (120Å) bare silica, achieving a ligand density of 260 µmol/g and an trimethylsilyl-endcapping group (TMS) density of 60 µmol/g. SP 6 was prepared in the same manner starting from 2-(diethylamino)ethanol (Aldrich) instead of quinine. According to elemental analysis on 5µm (120Å) silica particles a ligand density of 480 µmol/g and an endcapping (TMS) group density of 190 µmol/g was present on the surface. Stationary phases SP 2b and SP 5 were also synthesized with non-porous 1.5µm Micra NPS material giving ligand densities of 9 µmol/g.

2.4 Screening method for plasmid topoisomer separation on different stationary phases

For chromatographic analysis a mixed salt and isopropanol gradient was used. First, a 0.5 mol/L stock solution from NaH_2PO_4 (Merck, Darmstadt, Germany) was prepared. Buffer A consisted of 50 mmol/L NaH_2PO_4 titrated to 7.0 with 5M NaOH. Buffer B consisted of 50 mmol/L NaH_2PO_4, 0.6 mol/L NaCl and 10% (v/v) isopropanol titrated to 7.0 with 5M NaOH. A gradient from 0 to 100%B in 60 minutes was run during analysis. Between the analytical runs, the column was washed by a plug of sodium chloride (injection of 50µl 3M NaCl (aq.)), followed by reequilibration to 0% B for 5 minutes. The flow rate was set to 0.7 ml/min, detection wavelength to 258 nm (reference 360 nm with 100 nm bandwidth) and the temperature to 60°C (with preheating of the solvent in the 3 µl heat exchanger). Injection volume was dependent on the sample concentration (3 to 20 µl).

3. Results and Discussion

Ligand structure requirements for molecular recognition of DNA topoisomers

Topoisomers of covalently closed circular (ccc) plasmid DNA with different linking numbers could be successfully separated on stationary phase SP 1 (see fig. 2a). We have decided to fragment the ligand and vary individual molecule parts to find the key interaction sites for the observed chromatographic selectivity. Thus, we synthesized a set of ligands and attached them to 5 µm porous silica particles to result 12 different stationary phases (see fig. 1). All three plasmids (4.9 kbp, 9.9 kbp and 14.5 kbp) were analyzed on all columns employing the same mobile phase conditions. In general, ccc topoisomers originating from smaller plasmids are better separated than those from larger plasmids, providing more data on less-efficient stationary phases. Results for the pMCP1 plasmid (4.9 kbp) are summarized in Table 1. Because of gradient elution, a retention factor is not defined and thus a selectivity factor according to IUPAC guidelines cannot be calculated. Selectivity is instead calculated as the difference in retention times $t_{R1} - t_{R2}$.

We initially assumed that intercalation may be involved in the separation process, and that the quinoline moiety is crucial for topoisomer selectivity. However the quincorine carbamate phase SP 3a, which lacks the aromatic ring,

still shows reasonable selectivity (fig. 2b). The intercalation process itself is obviously not necessary for selectivity, however because of higher peak resolution (R_s = 1.32 with and R_S = 0.26 without quinoline) the quinoline ring obviously enhances the separation. Anyhow, plasmid DNA elutes from columns containing quinine carbamate ligands at lower elution strength (40 – 50% buffer B) than from those with quincorine-based ligands (60 – 80 % buffer B) with same ligand chemistry and comparable ligand densities, being 327 ± 10 µmol/g for quinine-based ligands and 260 µmol/g ± 40 for quincorine-based ligands. If intercalation would be present, a shift to significantly later elution would be expected due to multivalency interaction. Also, because intercalation is a multi-step and relatively slow process [15] accompanied by rearrangement of DNA [6], significantly broader peaks would be expected as a result of such binding mode [16]. We may therefore assume, that intercalation is not or very weakly taking place during our chromatographic process, but a rather weak global interaction with fast kinetics instead. Greater retention of pDNA from quincorine-based columns lead also to incomplete elution of the injected plasmid amount. Blank runs with no injection, recorded after runs where pDNA was injected, showed a carry over between 2 and 5%. On quinine-based columns such phenomena were not observed, therefore these columns are more suitable for analyses.

What can reliably be extracted from all the structure variations, is that the presence of the carbamate group is crucial for topoisomer separation, which is shown on SP 2a containing the unmodified quinine ligand attached via the allyl group of quinuclidine. On this phase, the open circular and linear forms coelute, but are separated from the ccc form eluting as a single peak (containing all topoisomers). The carbamate group might be exchanged by an urea moiety (SP 3a → SP 3b) without losing selectivity. However the presence of an additional amide H-donor functionality leads to broader peaks of individual topoisomers, which in turn decreases the peak resolution dramatically. In fact, it is possible to carry out topology analysis on the SP 3a phase containing the carbamate moiety with plasmids up to 5 kbp (see fig. 2b), but on phase 3b containing the urea moiety the resolution achieved is too low for such analysis.

The key element of the carbamate and urea moieties is the amide nitrogen atom adjacent to the *tert*-butyl group, possessing H-donor and H-acceptor properties. When removing this structure element (SP 3b → SP 3c), the topoisomer selectivity is lost completely. On the other hand, phase SP 3c possesses another amide H-donor functionality at a different position (see fig. 1b), being three bonds away from the quinuclidine-nitrogen, and therefore the ligand is not capable anymore of separating topoisomers. This leads to the conclusion that additionally to the necessary presence of an amide H-donor functionality, the distance between this amide H-donor functionality and the tertiary amine of the quinuclidine bicycle must equal five bonds. The tertiary amine of quinuclidine may act as an anion exchanger with a pKa of 9.8 [17], but also as a H-acceptor to form H-bond mediated ionic interactions. Such ionic interactions are directed and in order to be formed, they require geometrically defined structural restraints.

Upon quaternization of the tertiary amine of the quinuclidine ring by methylation but keeping the carbamate group unmodified (SP 3d) the topoisomer separation is lost. Because quaternary ammonium groups are permanently charged but do not exhibit H-acceptor properties, it seems likely that the lack of the latter property causes also a loss of selectivity. However steric effects may be in any case involved. It is important to note that the retention of pDNA is slightly increased, which is derived from different elution condition, being 62% eluting

buffer B (370 mM NaCl) for phase SP 3a and 68% (410 mM NaCl) for phase SP 3d. That indicates that there exists a different binding mechanism to the proposed topoisomer recognition based on the interplay of the H-donor and H-acceptor. Because of increased sodium chloride concentration needed for elution, we suggest a dominant ion-exchange interaction to be present between the tertiary or quaternary (for SP 3d) amine, respectively, of the quinuclidine ring and the phosphate groups of the DNA backbone. As such, ionic interactions of this type are not directed such as H-mediated ionic interactions, and therefore do not provide geometrically restrained selectivity, which is obviously necessary for topoisomer recognition.

Rigidity and conformational stability of the ligand is a very important parameter influencing the peak width of individual topoisomers and thus the chromatographic separation. Because the tertiary amine is incorporated into an already rigid bicyclic system, we have studied this effect on the amide H-donor functionality of the carbamate. The *tert*-butyl group attached to the carbamate (SP 2b) is more bulky and rigid [18] and provides narrower peaks which leads to significantly improved resolution over phase SP 2d containing a *n*-butyl group instead. Please keep in mind that the distance between the amide and the tertiary aminogroup was kept constant. When the linker between the support and the ligand is attached at the carbamate site (SP 1), this group becomes more rigid, again leading to narrower peaks compared to the linker attachment to the vinyl group of quinuclidine (SP 2b). In this case however, the resolution of the phase SP 2b is still higher due to superior selectivity at the same gradient slope. In practice, both stationary phases SP 1 and SP 2b provide similarly good results on topology analysis resolving equal numbers of topoisomers. We prefer using phase SP 1 due to shorter analysis times.

When comparing *tert*-butylcarbamoyl quinine (SP 2b) and *tert*-butylcarbamoyl quincorine (SP 3a), which differ in the quinoline ring moiety at position 9, the quinine-based ligand provides smaller peak widths of individual topoisomers and thus better resolution. This may also be attributed to increased conformational stability of the quinine-type ligand. From NMR studies it is known that when quinine carbamate is protonated, which applies for our mobile phase conditions, it exists almost exclusively as a single conformer [19]. This anti-open conformer forms a defined cleft with the quinoline ring [20], which is not so well defined for quincorine-based ligands, providing a possible explanation of higher chromatographic resolution of ccc topoisomers on quinine-based ligands.

A ligand with complete rotational and torsional freedom of the tertiary amine (SP 6) but bearing all other key elements that were described earlier, lacks any ccc topoisomer selectivity. In addition, a selectivity between the open circular and the ccc form, which was present on all other stationary phases in this study, is also absent on phase SP 6. The elution of pDNA from this stationary phase requires the highest amount of sodium chloride in the elution buffer amongst all phases studied. This may however be attributed to the highest ligand density of 480 µmol/g among all ligands studied, whereas all other phases had ligand densities below 330 µmol/g.

From combination of the presented results a general ligand structure for topoisomer recognition can be concluded, which is shown in fig. 3. The molecular recognition principle is based on a sterically-defined arrangement of an H-donor (amide group) and an H-acceptor (quinuclidine nitrogen). It is interesting, that a similar arrangement of structural elements can be found in minor groove binders such as netropsine [21] or hairpin polyamides designed for specific sequence

recognition [22]. Minor grove binders bind preferentially to A·T base pairs [23], groove binders in general bind to double-stranded DNA sequence-specifically, while hydrogen bonding and other noncovalent interactions are thought to be key modulators for molecular recognition [24]. A binding model between an A·T base pair and a hairpin polyamide, which satisfies our proposed structural requirements, suggests the formation of two hydrogen bonds to the N3 of the purine and the O2 of the pyrimidine, respectively [25].

We have also tested phases SP 2b and SP 5 with a different stereochemistry, starting from quinidine (QD) instead of quinine (QN). These stereochemical variants are “pseudo-enantiomers” with a configuration of 8S, 9R for quinine and 8R, 9S for quinidine [12]. These phases are known to possess enantiomer selectivity for derivatized amino acids, while the elution order observed on the QN phase is inverted on the QD phase [26]. However, we did not observe any elution differences for ccc topoisomers on these phases, so the overall selectivity is beyond classical stereoselectivity observed for small chiral entities. One may attribute the phenomena observed hence more as “topological selectivity for large (bio)molecules”.

Characteristics of the chromatographic support

The ligand density is an important parameter for the separation of ccc topoisomers. The maximum density of 9-(*O*-allylcarbamoyl)quinine that can be attached to the support via radical addition was found to be at about 50% of the available thiols, and thus depends on the surface concentration of reduced thiols of the thiopropyl-linker. This corresponded to a maximum ligand density of 310 µmol per gram stationary phase SP 1. Two more phases bearing the same ligand with a different density, 190 µmol/g and 110µmol/g, respectively, were tested for topoisomer separation. As can be seen in fig. 4, the separating power and the pDNA retention is reduced significantly when decreasing ligand density. Thus, highest possible ligand densities provide best separation. While a decrease in separation efficiency due to ligand bleeding compared to newly synthesized columns may be a general issue on silica-based stationary phases, selectivity, however, remains unaffected by the change of ligand density, as can be seen from table 2.

The pore size influences the peak resolution dramatically, which we tested on different 5µm silica supports having pore sizes of 120Å, 200Å and 300Å. These supports were 3-mercaptopropyl-modified, following by attachment of 9-(*O*-allylcarbamoyl)quinine leading to phase SP 1. All three stationary phases had comparable ligand densities per surface area. The results are shown in Table 3. Selectivities on all supports are very similar, however the peak widths change dramatically when expanding the pore diameter from 120Å to 200Å, therefore losing peak resolution. The data in Table 3, presented for the smallest plasmid (4.9 kbp) in our study, indicate that a partial or full penetration of the analytes into the pores, suggested by some authors for the supercoiled form [27], does not take place in the pore size range studied because of decreasing retention with increasing pore size. This is in agreement with data obtained on a dimethylaminoethyl-based silica stationary phase with a similarly sized plasmid pBR322 (4.3 kbp), which does not enter pores of 1000Å, but notable retention due to pore penetration is observed at pore sizes of 4000Å [28]. Chromatographic runs on a 3µm gigaporous (3100Å pores) support with a stationary phase type SP 1 show lower chromatographic performance than 5 µm silica particles with mesopores. Only 11 topoisomers of the pMCP1 plasmid can be separated,

compared to 22, and only 8 topoisomers of the pAcMC1 plasmid are separated, compared to 30 on the 5 µm (120Å) support employing the same mobile phase conditions. Gigaporous materials, which allow the penetration of large biomolecules are thus not practicable for analytical applications, because of lower performances which is well-known from the separation of large proteins [29].

We observed interesting phenomena on non-porous 1.5µm “Micra” silica particles, modified to give phases SP 5 and SP 2b, respectively. Contrary to the results obtained on 5 µm porous silica, on the Micra support phase 2b has not shown any topoisomer separation at all employing same mobile phase conditions (see table 4). Although the ccc form eluted as a broad peak, probably due to some topoisomer selectivity, individual topoisomers were neither visible nor quantifiable. Remember that phase 2b provided best results on the 5 µm porous support. However, phase 5 in combination with the nonporous Micra support and optimized mobile phase conditions provided best chromatographic performance resolving 22 topoisomers of the pMCP1 plasmid, which is also the maximum number achieved on the 5 µm porous support. The reason for this discrepancy is unclear, however the outer surface of the Micra particles is significantly different from that on 5 µm porous particles being more acidic [30]. Also the term non-porous is not entirely correct, because the spherical silica particles are not perfectly even, as might be concluded from the term “non-porous”. The surface is roughened to provide a thin retentive layer [31].

Silica particles based on the identical production protocol with a larger diameter (10 µm) but equal pore size of 120Å provide smaller resolution between ccc topoisomer peaks because of increasing peak width. The selectivities remained unchanged, indicating that the molecular recognition principle of topoisomer separation is independent on the particle morphology. The optimal column length is dependent on the particle type. For 5 µm silica particles, column lengths of 10 cm and longer (4.0 mm i.d.) provide best separations, however no significant increase in resolution was found when using columns longer than 10 cm. When using 1.5 µm non-porous particles, column lengths of only 3 cm (4.6 mm i.d.) were sufficient for best separation.

4. Conclusion

Earlier published results showed that quinine carbamate phases were able to separate circular plasmids topoisomers with different linking numbers. Stationary phases from fig. 1 were screened for ccc topoisomer separation employing the same chromatographic conditions with three plasmids of different sizes, to elucidate the key structural elements for such type of separations. Various ligands were attached to the silica support, being either structural variations of the quinine carbamate ligand, or fragments thereof. The quinoline moiety, which may intercalate into the double-helix, is not necessary for topoisomer separation, which was shown by topoisomer separation achieved on a quincorine carbamate stationary phase. Quincorine is a molecule containing the same structural elements and stereochemistry as quinine, but lacks the 6-methoxyquinoline ring. Thus despite our initial hypothesis, intercalation is barely involved in the molecular recognition process leading to topoisomer selectivity, although the aromatic ring system increase resolution and decrease plasmid retention. The latter effect avoids run-to-run carry over and decreases salt contamination in the eluting fractions.

Unmodified, i.e. not carbamoylated quinine lacks the topoisomer selectivity showing that the carbamate moiety, possessing H-donor properties at the amide-

nitrogen, is essential. The carbamate structure was explored in more detail by varying individual atoms, while attaching the ligand to the silica support via the vinyl group of the quinuclidine ring. Upon changing the *tert*-butyl group to *n*-butyl, the peak width of individual topoisomers is significantly increased, causing lower peak resolution. We suggest that this effect is due to different rigidity of the carbamate group, which is higher in the case of the more bulky *tert*-butyl group. This was supported by the fact that quinine carbamate attached to the support via the carbamate itself showed smallest peak widths.

Absence of the amide nitrogen of the carbamate group, or the change of its distance to the quinuclidine part, leads to a complete loss of topoisomer separating power. Thus, only the specific distance of five bonds (or four atoms) between the amide nitrogen of the carbamate group and the tertiary amine nitrogen of quinuclidine promotes the desired selectivity. Because the spatial distance is so important, it makes sense that ligands with rigid key-moieties provide better separation. Additionally we may speculate that this effect also accounts for higher performance of the quinine ligands over quincorine-based ones, however this is part of future research in our group. A diethylaminoethyl (DEAE) carbamate ligand with a flexible tertiary amine structure in contrast to the rigid quinuclidine bicycle shows no ccc topoisomer selectivity, nor any selectivity for the isomeric plasmid forms, i.e. ccc, oc and linear forms being present on all other stationary phases from fig. 1. These results are in contrast with results on commercial DEAE-containing nonporous organic polymer-based stationary phases used for isoform separation, and lead to speculation, that it is not the ligand alone, that promotes this kind of separation on these phases, but rather an interplay of the ligand with the morphology and surface chemistry of the chromatographic support. Again, this is part of ongoing research, which should provide more insight into the interaction of plasmid molecules with different supports, but we would like to stress the fact, that not the ligand alone, but the stationary phase as a whole has to be considered when separating such large biomolecules. In this context, polyvalency type binding events, which are largely dependent on the surface morphology, may need to be considered and thus may play a chromatographically important role.

From different silica supports we found that non-porous particles of small diameter provide best separation. Because of their limited availability and more laborious packing procedure, compared to very frequently used porous silica supports with mid-size diameter between 3 and 7 µm, small non-porous supports might be replaced by the porous supports. In this case, a shallower gradient might be employed on porous supports to achieve similar resolution. In case of a porous support, the pores should be about 100 Å or less, because larger pores show significantly increased peak widths and thus reduced peak resolution. Because we observed a shift to smaller retention times when increasing the pore size from 100 to 200 and 300 Å (keeping the ligand density per area constant), this effect is not due to partial penetration of pores. With small pore sizes, most of the ligand molecules bound to the support are not used for separation because they are present within the pores. According to elemental analyses, on a 1.5 µm non-porous supports providing highest resolution the ligand consumption is 50 times less than on a 5 µm porous support. Our ongoing research showed further, that particulate supports provide better analytical results than silica monoliths and our current work is focused on organic polymer based supports.

5. Acknowledgement

We greatly appreciate the financial support and the provision of the HPLC system by Boehringer-Ingelheim RCV (Vienna, Austria). We also thank Peter Frühauf for valuable assistance with column packing.

6. Tables and Figures

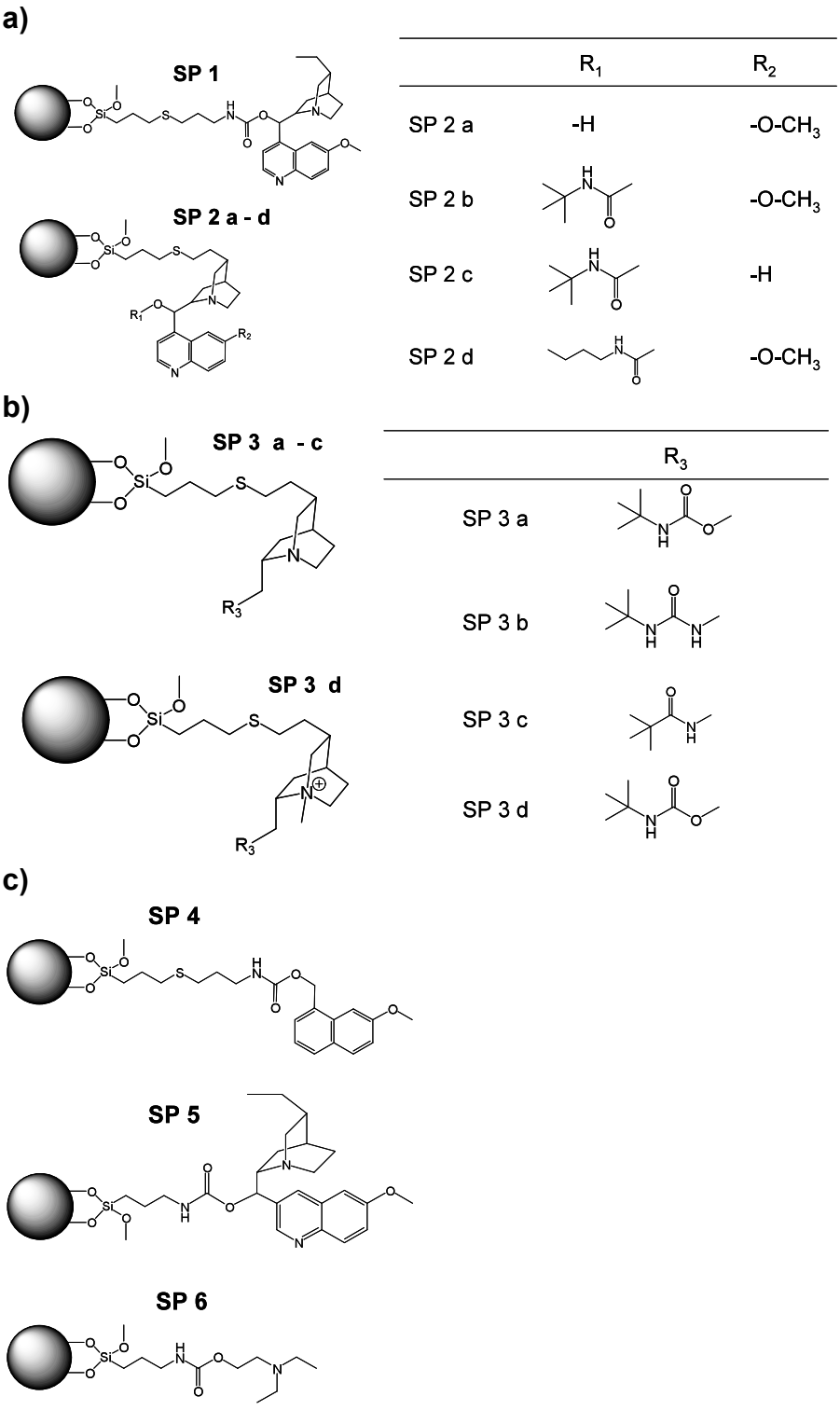

Figure 11: Structures of all chromatographic ligands attached to silica stationary phases employed during this study. SPs 1, 2 and 5 are based on quinine and SPs 3 are based on quincorine, which is a derivative of quinine. SP 4 contains the quinoline moiety of the quinine carbamate structure of SP 1. SPs 5 and 6 contain a short linkage between the ligand and the chromatographic support, while all other supports are connected via a long thioether-linkage to the chromatographic ligand.

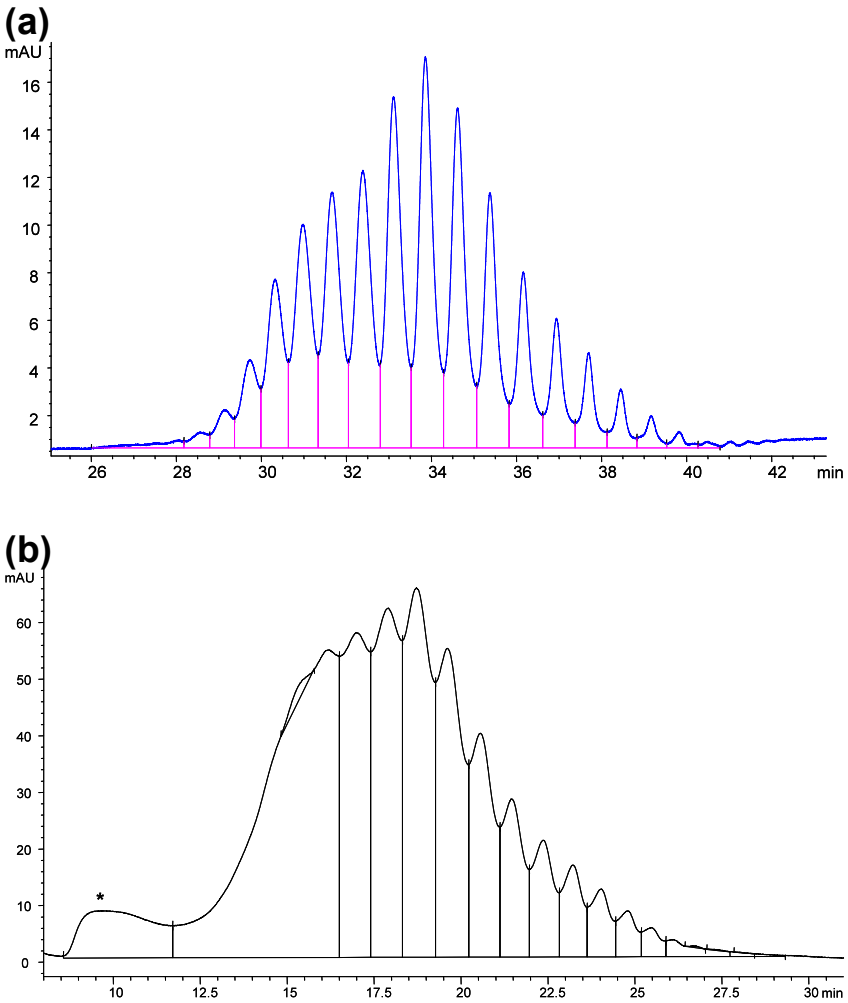

Figure 12: Topology analysis: Separation of ccc topoisomers in a sample containing native 4.9 kbp pMCP1 plasmid DNA on SP 1 (a) and SP 3a (b) (support: 5 µm silica particles with 120 Å pores). The highest abundant topoisomer has 30 negative superhelical turns according to previously published results [4]. Conditions: buffer A: 50 mM phosphate pH 7, buffer B: A + 0.6 M NaCl + 10%IPA, 60°C, 0.7 ml/min, 28 µg inj., det. UV 258 nm, linear gradient from 0 to 100%B in 60 min (a) and from 60 to 100%B in 24 min (b). The asterisk in (b) marks the open circular form.

Table 2: Parameters of chromatographic separation of ccc topoisomers (pMCP1 plasmid) on different types of stationary phases shown in fig. 1 on 5 µm porous silica support, employing same mobile phase conditions. Only structures based on quinine carbamate and quincorine carbamate possess the desired selectivity. Stationary phases SP 1 and SP 2b provide best topoisomer resolution. Although at the gradient slope chosen for this study, phase SP 2b provides slightly enhanced resolution, phase SP 1 allows shorter analysis times by 25% due to narrower peaks. Conditions: buffer A: 50 mM phosphate pH 7, buffer B: A + 0.6 M NaCl + 10%IPA, 0 – 100%B in 60 min, 60°C, 0.7 ml/min, 8 µg inj., det. UV 258 nm

Type of stationary phase	number of separated ccc topoisomers	% buffer B at elution of highest abundant topoisomer	resolution between most abundant topoisomers	peak width of most abundant topoisomer	selectivity ($^{\Delta}t_R$ of most abundant topoisomers)
SP 1	22	58%	1.23	0.36 min	0.76
SP 2a	0	87%	0.00	2.7 (total ccc)	0.00
SP 2b	22	47%	1.32	0.43 min	1.02
SP 2c	20	48%	0.64	1.40 min	0.79
SP 2d	19	39%	0.80	0.67 min	0.78
SP 3a	18	62%	0.26	2.30 min	0.61
SP 3b	13	76%	0.07	not quantifiable	0.75
SP 3c	0	80%	0.00	3.5 (total ccc)	0.00
SP 3d	0	68%	0.00	4.0 (total ccc)	0.00
SP 4	0	53%	0.00	4.8 (total ccc)	0.00
SP 5	5	49%	< 0.06	not quantifiable	not quantifiable
SP 6	0	92%	0.00	1.72 (total ccc)	0.00

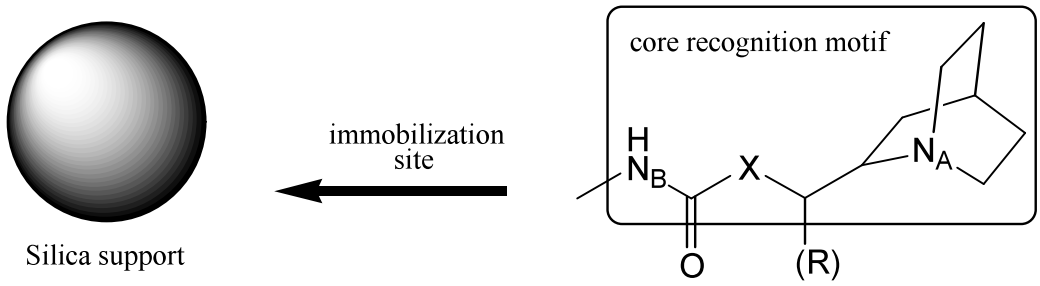

Figure 13: General structure of a chromatographic ligand with selectivity for ccc topoisomers having different linking numbers. The arrow should represent a suitable linker between the particulate silica support and nitrogen atom N_B, which increases the rigidity of the functional group. X may be –NH– or –O–, however the latter shows higher peak resolution. (R) may be –H in quincorine-based ligands or –quinoline in quinine-based ligands.

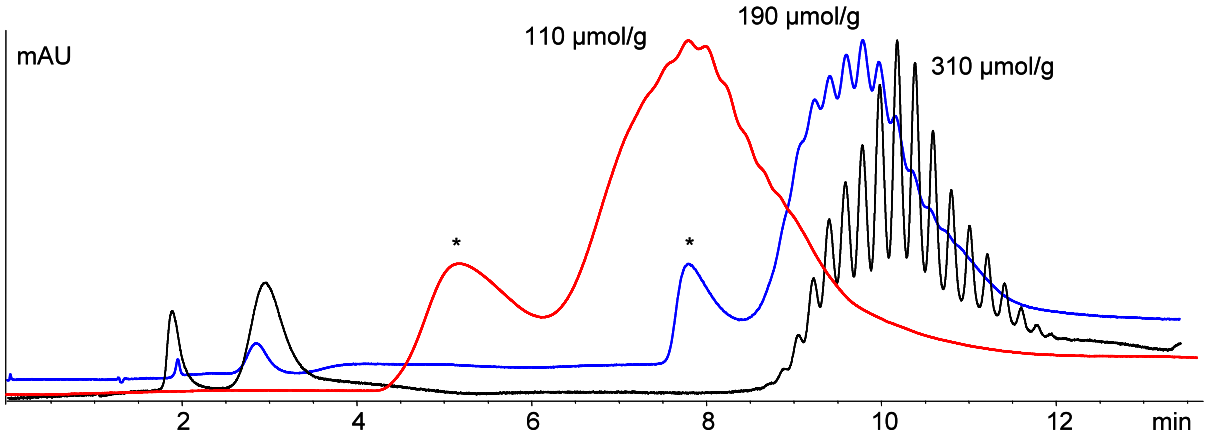

Figure 14: Chromatograms showing the ccc topoisomer separation of the pMCP1 plasmid in dependence of the ligand density in µmol ligand per gram support (data obtained from elemental analysis) on phase SP 1. With decreasing ligand density the peak width is increasing thus providing less peak resolution leading to a smaller number of individual topoisomer peaks. The overall retention is decreasing with smaller ligand density from 10.4 min (310 µmol/g) to 9.8 min (190 µmol/g) and 7.7 min (110 µmol/g). Peaks marked with an asterisk denote open circular plasmids. Conditions: buffer A: 50 mM phosphate pH 7, buffer B: A + 0.6 M NaCl + 10%IPA, 0 – 100%B in 15 min, 60°C, 0.7 ml/min, 8 µg inj., det. UV 258 nm

Table 3: Parameters of chromatographic separations of ccc topoisomers (pMCP1 plasmid) on stationary phase SP1 with different ligand densities, calculated from chromatograms shown in fig. 4. While the selectivity is largely unaffected, the peak widths increase dramatically with decreasing ligand density resulting in low peak resolution. Conditions: buffer A: 50 mM phosphate pH 7, buffer B: A + 0.6 M NaCl + 10%IPA, 0 – 100%B in 15 min, 60°C, 0.7 ml/min, 8 µg inj., det. UV 258 nm

ligand density on phase SP1	number of separated ccc topoisomers	% buffer B at elution of highest abundant topoisomer	resolution between most abundant topoisomers	peak width of most abundant topoisomer	selectivity ($^{\Delta}t_R$ of most abundant topoisomers)
310 µmol/g	20	62%	0.91	0.14 min	0.21
190 µmol/g	12	59%	0.20	0.45 min	0.19
110 µmol/g	8	45%	0.03	not quantifiable	0.19

Table 4: Parameters of chromatographic separations of ccc topoisomers (pMCP1 plasmid) on stationary phase SP2b on 5 µm particulate silica support with various pore sizes. The selectivity is largely unaffected, but the peak widths increase dramatically by expanding the pores from 120Å to 200Å and 300Å, respectively. The retention of pDNA decreases slightly by increasing the pore size. Conditions: buffer A: 50 mM phosphate pH 7, buffer B: A + 0.6 M NaCl + 30%IPA, 0 – 100%B in 60 min, 60°C, 0.7 ml/min, 8 µg inj., det. UV 258 nm.

nominal pore size	number of separated ccc topoisomers	% buffer B at elution of highest abundant topoisomer	resolution between most abundant topoisomers	peak width of most abundant topoisomer	selectivity ($^{\Delta}t_R$ of most abundant topoisomers)
120Å	17	25%	0.98	0.22 min	0.35
200Å	14	24%	0.36	0.96 min	0.37
300Å	13	21%	0.30	1.20 min	0.36

Table 5: Comparison of separations parameters of ccc topoisomers (pMCP1 plasmid) between 5 µm porous (120Å) and 1.5 µm non-porous silica support for two stationary phases SP 2b and SP 5, which differ mainly in the length of the linker between the support and the ligand. On the 5 µm porous support, the *extended* linker provides the necessary peak resolution for topology analysis, while the *short* linker shows no topoisomer resolution (although selectivity is provided, but can not be quantified). However on the non-porous 1.5 µm Micra support the *short* linkage provides topoisomer resolution, while the *extended* linkage is not capable of resolving individual peaks (again, selectivity is present but can not be quantified). Employing same mobile phase conditions, the widths of individual topoisomer peaks are much smaller on the non-porous Micra support than on 5 µm porous particles. Conditions: buffer A: 50 mM phosphate pH 7, buffer B: A + 0.6 M NaCl + 30%IPA, 0 – 100%B in 15 min, 60°C, 0.7 ml/min, 8 µg inj., det. UV 258 nm.

Type of stationary phase	number of separated ccc topoisomers	% buffer B at elution of highest abundant topoisomer	resolution between most abundant topoisomers	peak width of most abundant topoisomer	selectivity ($^{\Delta}t_R$ of most abundant topoisomers)
SP 2b - 5 µm	13	31%	0.29	0.304 min	0.10
SP 5 - 5 µm	0	26%	0.00	not quantifiable	not quantifiable
SP 2b - 1.5µm	0	19%	0.00	not quantifiable	not quantifiable
SP 5 - 1.5 µm	20	35%	0.89	0.055 min	0.12

7. References

[1] Bates, A. D., Maxwell, A., *DNA Topology*, Oxford University Press, New York 2006.

[2] Bauer, W. R., Crick, F. H. C., White, J. H., *Scientific American* 1980, *243*, 118-124, 126, 129-130, 132-113.

[3] Depew, R. E., Wang, J. C., *Proc. Natl. Acad. Sci. U. S. A.* 1975, *72*, 4275-4279.

[4] Mahut, M., Ghazidezfuli, P., Lindner, W., Laemmerhofer, M., *To be submitted* 2010.

[5] Keller, W., *Proc. Natl. Acad. Sci. U. S. A.* 1975, *72*, 4876-4880.

[6] Lane, A. N., Jenkins, T. C., *Quarterly Reviews of Biophysics* 2000, *33*, 255-306.

[7] Allison, R. G., Hahn, F. E., *Antimicrobial Agents and Chemotherapy* 1977, *11*, 251-257.

[8] Pritchard, N. J., Blake, A., Peacocke, A. R., *Nature* 1966, *212*, 1360-1361.

[9] Estensen, R. D., Krey, A. K., Hahn, F. E., *Molecular Pharmacology* 1969, *5*, 532-541.

[10] Diogo, M. M., Queiroz, J. A., Prazeres, D. M. F., *Journal of Chromatography, A* 2005, *1069*, 3-22.
[11] Huber, C. G., *Journal of Chromatography, A* 1998, *806*, 3-30.
[11*] Urthaler, J., Buchinger, W., Necina, R., *Chemical Engineering & Technology* 2005, *28*, 1408-1420.

[12] Laemmerhofer, M., Lindner, W., *Journal of Chromatography, A* 1996, *741*, 33-48.
[13] Mandl, A., Nicoletti, L., Lammerhofer, M., Lindner, W., *J. Chromatogr., A* 1999, *858*, 1-11.
[14] Nogueira, R., Laemmerhofer, M., Maier, N. M., Lindner, W., *Analytica Chimica Acta* 2005, *533*, 179-183.
[15] Monaco, R. R., *Journal of Nucleic Acids* 2010, *2010*, 4.
[16] Fornstedt, T., Zhong, G., Guiochon, G., *Journal of Chromatography A* 1996, *742*, 55-68.
[17] Sanchez Munoz Orlando, L., Hernandez Ever, P., Lammerhofer, M., Lindner, W., Kenndler, E., *Electrophoresis* 2003, *24*, 390-398.
[18] Franco, P., Lammerhofer, M., Klaus, P. M., Lindner, W., *J. Chromatogr., A* 2000, *869*, 111-127.
[19] Maier, N. M., Schefzick, S., Lombardo, G. M., Feliz, M.*, et al.*, *Journal of the American Chemical Society* 2002, *124*, 8611-8629.
[20] Krawinkler, K. H., Maier, N. M., Sajovic, E., Lindner, W., *Journal of Chromatography A* 2004, *1053*, 119-131.
[21] Corradini, R., Sforza, S., Tedeschi, T., Marchelli, R., *Chirality* 2007, *19*, 269-294.
[22] Chaires, J. B., *Current Opinion in Structural Biology* 1998, *8*, 314-320.
[23] Wittung, P., Kim, S. K., Buchardt, O., Nielsen, P., Norden, B., *Nucleic Acids Res.* 1994, *22*, 5371-5377.
[24] Haq, I., *Archives of Biochemistry and Biophysics* 2002, *403*, 1-15.
[25] Wade, W. S., Mrksich, M., Dervan, P. B., *Journal of the American Chemical Society* 1992, *114*, 8783-8794.
[26] Lämmerhofer, M., Pell, R., Mahut, M., Richter, M.*, et al.*, *Journal of Chromatography A* 2010, *1217*, 1033-1040.

[27] Ferreira, G. N. M., Prazeres, D. M. F., Cabral, J. M. S., Schleef, M., in: Schleef, M. (Ed.), *Plasmids for Therapy and Vaccination*, Wiley-VCH, Weinheim 2001, pp. 214-228.
[28] Colpan, M., Riesner, D., *Journal of Chromatography A* 1984, *296*, 339-353.
[29] Willoughby, N. A., *Journal of Chemical Technology & Biotechnology* 2009, *84*, 145-150.
[30] Laemmerhofer, M., Tobler, E., Lindner, W., *J. Chromatogr., A* 2000, *887*, 421-437.
[31] Billen, J., Desmet, G., *Journal of Chromatography A* 2007, *1168*, 73-99.

Manuscript 4

Title: Imaging of chloroquine-induced relaxation of supercoils in condensed plasmid DNA by atomic force microscopy

Authors: Marek Mahut[1], Michael Leitner[2], Michael Lämmerhofer[1], Peter Hinterdorfer[2], Wolfgang Lindner[1]

[1] University of Vienna, Department of Analytical Chemistry, Waehringer Strasse 38, Vienna, Austria
[2] Johannes Kepler University Linz, Institute for Biophysics, Altenbergerstrasse 69, A-4040 Linz, Austria

Abstract:

Herein we report on the in vitro change of DNA conformation of plasmids bound to a 3-aminopropyl-modified mica surface and monitoring the events by atomic force microscopy (AFM). In our study, we used an intercalating drug, chloroquine, which decreases the twist of the double-helix and thus alters conformation of the whole DNA molecule. During our experiments, a chloroquine solution was added while imaging a few highly condensed plasmid nanoparticles in solution. AFM images recorded after the drug addition clearly show a time-resolved relaxation of these bionanoparticles into a mixture of loose DNA strands filling the entire image. To verify, that this effect is not induced by the AFM tip, the imaging direction has been rotated by 90° during measurements.

Keywords:

Atomic force microscopy, DNA condensation, plasmid DNA, chloroquine, bionanoparticles

1. Introduction

Plasmids are either linear or circular DNA molecules, providing its host cell with additional functionalities, such as antibiotic resistance. In most cases, plasmids exist in cells as covalently closed circles (ccc). Usually, plasmids *in vivo* are underwound comparing to the relaxed state of B-DNA. A cell can regulate its supercoiling by a set of enzymes called topoisomerases. These enzymes introduce nicks into DNA strands and wind the strands around each other, thus changing topological properties of the DNA molecule. Only by such nicking procedure the topology can be altered. The topology is described by the linking number, which is a fundamental property of a

plasmid. Supercoiling, which is the difference of the linking number compared to a relaxed DNA circle, is mathematically split into two parts, twist and writhe [1].

When imaging plasmids with atomic force microscopy, the property that is usually connected with supercoiling is the writhe of the DNA. The twist of the helix, in turn, is a property that cannot be resolved or directly determined with current AFM equipment. Under usual conditions, supercoiling is partitioned to about 75% writhe and 25% twist [2]. With no topoisomerases present, a change in twist must be necessarily followed by a change of writhe and *vice versa*. Intercalators alter the twist of the DNA [3] (see also Fig. 1) which in turn leads to a change in writhe which can be monitored by AFM [4]. This effect, for example, is used for separating plasmid topoisomers in gel electrophoresis [5] [6].

Muscovite mica is the most common substrate for DNA adsorption in AFM because of its perfectly planar surface. Alike DNA, the surface is negatively charged. For this reason, the analyte is deposited either in presence of divalent cations on bare mica [7], or onto surface-modified mica plates. Two main modification strategies are used, amino-terminal silanization such as with APTES [8] or polyamino acid coating such as poly-L-lysine [9]. Both modification strategies show a more or less pronounced compaction of plasmid DNA compared to bare mica. In our experience, mica silanization produces smoother surfaces and thus better image quality than polyamino acid coating, which is why we have chosen to use APTES modified mica.

Because of our interest in studying topological properties of plasmids and their interactions with other molecules, we believe that AFM has great potential in providing further insight and information in this field. To date, most imaging studies on polynucleic acids with AFM are carried out in air, which means, that a liquid sample is dried onto a (mica) surface and imaged in air. Thus the DNA is no longer in its natural environment and additionally, no further processes with the imaged molecule are possible. However, by using a liquid cell, DNA can be imaged in solution, a Tris-EDTA (TE) buffer, for example, which guarantees the maintaining of the physiological conformation. Additionally, other solutions containing any molecules, can be added to the imaging buffer. With this technique, a new approach for studying interactions with DNA binders, or real-time conformation changes, is established. In this paper we present our first study on the time-resolved imaging of plasmid conformation change by adding an intercalator drug, chloroquine, with AFM.

2. Experimental

3-aminopropyltriethoxysilane (APTES), tris, triethylamine and sodium dihydrogenphosphate were purchased from Sigma-Aldrich at the highest purity available. Chloroquine diphosphate was purchased from Fluka. Plasmid DNA pMCP1 (4.9 kb) in TE buffer, containing > 90% supercoiled form, was supplied by Boehringer-Ingelheim RCV (Vienna, Austria). Water used in the experiments was prepared by a MilliQ unit from Millipore. Whenever mentioned, small sample volumes were dialyzed against water in Slide-A-Lyzer Mini dialysis units (Pierce) with a molecular-weight cutoff of 10,000 Da for 2 hours.

APTES-modification of mica surface

Two different modification methods, gas- and liquid phase reaction, were employed in this study. Gas-phase modification was carried out in close analogy to the protocol published by Ebner et al. [10]. A desiccator (5 L) was flooded with argon gas to remove air and moisture. Then two small plastic trays (e.g. the lids of Eppendorf reaction vials) were placed inside the desiccator, 30 µL of APTES and 10 µL of triethylamine were separately pipetted into two trays, the AFM tips were placed nearby on a clean inert surface (e.g. Teflon), and the desiccator was closed. After 120 min of incubation, APTES and triethylamine were removed, the desiccator was again flooded with argon gas for 5 min, and the tips were left inside for 2 days in order to “cure” the 3-aminopropylcoating.

For liquid-phase reaction, a 0.1% (w/v) solution of APTES in water was freshly prepared and used for modification within an hour. A 40 µl drop of this solution was placed in the centre of a freshly cleaved mica surface. After 10 min incubation the mica surface was washed 15 times with water in order to remove the unbound silane completely. The surface was dried by holding the mica plate into a stream of argon.

Sample preparation and addition of chloroquine

A commercially available AFM liquid cell (Molecular Imaging, Tempe, USA) with a volume of about 650 µl was placed onto the 3-aminopropyl-modified mica surface on a sample plate. In the case of gas-phase modified mica, 300 µl water and 30 µl of a 0.1 µg/µl dialyzed plasmid solution was placed into the liquid cell and incubated for 30 minutes at room temperature. After washing 5 times with water and removing the washing liquid, 300 µl water were added to the liquid cell.

In the case of liquid-phase modified 3-aminopropyl-modified mica, a 40 µl drop of a 0.03 ng/µl non-dialyzed plasmid solution was placed into the liquid cell and incubated for 15 minutes at room temperature. After washing 5 times with water, 500 µl 20 mmol/L aqueous Tris buffer (pH 7.5) were added to the liquid cell.
While imaging, 15 µl of a 0.5 mg/ml aqueous chloroquine solution was added directly to the imaging buffer on the sample plate. In a blank experiment, 4 µl of a 0.27 M aqueous NaH_2PO_4 solution was added. Both was done by means of a pipette connected to a glass microcapillary pipette via a plastic tubing.

AFM imaging

AFM technical information

3. Results and Discussion

Plasmid DNA was bound to 3-aminopropyl-modified mica produced in both ways, gas-phase and liquid-phase reaction, described in the previous section. Also in both cases, the biomolecules were condensed into highly ordered structures. Because of the absence of salts, compaction agents or enzymes, 3-aminopropyltriethoxysilane is the only substance in the sample being able to compact DNA. Thus, it can be deduced that this reagent alone is responsible for any compaction of plasmids. However, substantial differences in the structure of condensed plasmids have been observed between gas-phase and liquid-phase produced 3-aminopropyl-modified mica.

Relaxation on gas-phase produced 3-aminopropyl-modified mica

On gas-phase silanized mica, plasmids were highly condensed into nano-particle-like clusters (Fig. 2). Even at smaller scale, one is not able to identify individual double-strands. However, the clusters are not spherical as can be seen from the cross section of such a condensed structure showing some peaks and valleys (Fig.3). The width of these nanoparticles is around 40 nm, with heights around 4 nm. The extent of condensation is striking, being evocative of plasmid clusters obtained with highly condensing agents such as polyamino acids [11] [12], polyethylenimine [13] or metal complexes [14]. Open-circular form, marked by an arrow in Fig. 3, and linear form (not shown) of the same plasmid is not condensed under these conditions.

Although unexpected, such condensation can be explained by either dissociation of the 3-aminopropyl-modification or surface diffusion. It is known that APTES in solution can induce condensation of plasmid DNA into toroid and rod structures [15]. Hoh & Fang [16] suggest a formation of surface adsorbed silanols, i.e. with three silanol groups. These non-covalent bound molecules may potentially oligomerize to form multivalent cations which are known to condense DNA [17]. Anyway, such a high condensation would be very advantageous for this study, because any relaxation step is very pronounced and unambiguously identified.

Actually, after addition of chloroquine (final concentration 24 µg/ml, 0.05 mM), these highly condensed structures started to relax whereupon individual DNA strands were visible in the vicinity of the clusters. In Fig.4 a time-resolved transformation of such a cluster into a majority of relaxed plasmid molecules is shown. Many of these molecules have a shape of a star, hereby marking a common origin, i.e. the DNA nanoparticle.

After half an hour (Fig. 4e), an almost complete relaxation can be observed. The bigger scan size image is utterly different to the overall image before chloroquine addition. Because the imaging position on the mica surface has changed, it can be deduced that the relaxation was not induced by the AFM tip.

To proof this, another plasmid cluster on a different mica, prepared in the same manner, has been imaged just after addition of chloroquine (Fig. 5a). In this figure, a long individual double strand is “released” from the cluster in the imaging direction, as marked by the arrow. Afterwards, the scanning orientation of the AFM tip has been rotated by 90 degrees. In the following image (Fig. 5b), another similar strand can be seen parallel to the one before, marked by a dashed arrow. Because the orientation of the strand is orthogonal to the AFM tip movement, it could not have been induced by this tip. This shows that the relaxation of the plasmid DNA cluster is a chloroquine-induced effect.

Because chloroquine was added as a diphosphate salt, we checked if the observed relaxation can be promoted by the addition of phosphate salt alone. A blank test was performed adding the corresponding molar amount of sodium dihydrogenphosphate instead of the chloroquine salt. No relaxation of plasmid nanoparticles was observed upon addition of phosphate. From these experiments it is clear that the observed phenomenon is specifically due to chloroquine.

It is also worth noticing, that no reclustering takes place, i.e. no positive supercoiling occurs. Once the circular plasmid molecule gets relaxed, it does not change its condensation status. This is also true if the chloroquine solution is added to the imaging buffer twice or more often. However, if a sufficient concentration of such an intercalating substance is added to DNA in solution, primarily negatively supercoiled plasmids become positively supercoiled [18] [19] [20], forming plectonemic or toroidal structures [21]. In our case the plasmids are tightly bound to the surface via ionic interaction, which is the reason why their twist cannot be altered by an intercalating drug anymore and we do not observe further condensation. This hypothesis is supported by the fact that, at the position of a former cluster, a star shaped origin of individual double strands is present. Once DNA comes in contact with the 3-aminopropyl surface, it is very tightly bound and does not diffuse on the surface, nor changes its coiling.

In contrast to our findings, a similar study has been published by Pope et al. using freshly cleaved, unmodified mica [22]. There, a pBR322 plasmid has been deposited onto the mica surface from a HEPES buffered $NiCl_2$ solution. After addition of ethidium bromide as an intercalator (final concentration 1.1 mM) during imaging, refolding (positive supercoiling) has been observed at some parts of the plasmid molecule. However two very important differences have to be mentioned which both arise from the nature of the unmodified mica surface. Firstly, plasmids deposited on mica show no signs of supercoiling whatsoever because of high DNA mobility on the surface. Secondly, in the regions of weaker binding the tertiary DNA structure bound to the surface may change. With 3-aminopropyl-modified mica, such changes are not possible.

Relaxation on liquid-phase produced 3-aminopropyl-modified mica

Silanized mica produced in liquid phase shows generally a rougher surface, which is why the image quality on the same instrument is little lower as with gas-phase produced ones. The latter are thought to have a uniform, single layer of the modified siloxane on the surface. However, the siloxanes seem to be bound labile, i.e. not by all three possible silanol groups. On the other hand we found that liquid-phase produced 3-aminopropyl-modified mica has increased binding capacity for DNA and the plasmid binding generally proceeds faster.

Supercoiled plasmid DNA bound to liquid-phase produced 3-aminopropyl-modified mica is much less condensed than on the ones produced in gas phase, because discrete strands can be seen in most parts of a molecule (see Fig.6). A further difference is the overall shape, being rod-like on liquid-phase produced mica, whereas the other silanization type produced highly condensed clusters. However, comparing the shape of the plasmid molecules to such obtained on bare mica [23] [24], a significant condensation still can be seen.

Upon addition of chloroquine, a relaxing of the condensed structures is observed, though not as pronounced as in the previous section. The relaxation seems to progress more slowly on this surface, with complete relaxation reached an hour after the addition of the DNA binder chloroquine. Because individual strands can be seen before chloroquine addition as well, the best indicator of the relaxing phenomenon is the disappearance of the small but highly condensed structures marked by arrows in Fig. 7. When relaxation is completed, star-shaped structures can be seen on the surface indicating the position of former clusters (Fig. 8), though not as many as on gas-phase produced 3-aminopropyl-modified mica. However, the final conformation (i.e. after chloroquine addition and incubation) of plasmid DNA is similar on both types of mica. Also, no recoiling (positive supercoiling) was observed on mica surface, even after addition of a 10 mg/ml aqueous chloroquine solution (final concentration 0.6 mM).

4. Conclusion

Our results on both, gas- and liquid-phase prepared 3-aminopropyl-modified mica, clearly show a relaxation of condensed plasmid structures upon addition of chloroquine. The siloxane itself is mainly involved in the condensation process of supercoiled plasmid DNA. When mica is silanized in gas-phase, the siloxane is bound less stable to the mica surface and thus the siloxane surface concentration is lower. Higher concentration of mobile surface-adsorbed siloxanes and/or siloxanes in solution cause the circular DNA to condense very tightly. Lower surface concentration in turn leads to lower binding capacities.

Siloxanes on 3-aminopropyl-modified mica obtained by solution-silanization were more stable bound to the surface. Bound plasmid molecules were condensed, however, less tightly than in the previous case. The so-produced plasmids condensed into rod-like structures show many structural details.

By adding chloroquine, the condensation was fully reversed until individual double-strands of DNA bound to the mica surface became visible. During relaxation AFM images were monitored in solution, thus a time-resolved chloroquine-caused plasmid relaxation with approximately one frame in two to five minutes was recorded. Full relaxation was observed after 30 minutes with gas-phase produced 3-aminopropyl-modified mica, and 60 minutes with ones produced in solution. However, changes in the extent of condensation were seen after 5 minutes.

We think that our findings may play a role in DNA nanotechnology, especially when using specifically designed nucleotide sequences being able to form any desired structure. These sequences could be hidden in DNA nanoparticles until a deconvolution, e.g. induced by an intercalator, takes place. Another interesting field of use of DNA is as a conducting wire in biochips [25] [26], where with our technique a conducting network may be generated upon relaxation.

These experiments also show the suitability of AFM imaging in solution on DNA condensation studies and suggest a new method for investigating DNA binders on nanoscopic scale.

5. Acknowledgement

We gratefully acknowledge Boehringer-Ingelheim RCV (Vienna, Austria) for financial support of this work and for providing plasmid samples. We also thank Andreas Reininger (JKU Linz, Austria) for AFM measurements and Andreas Ebner (JKU Linz, Austria) for helpful discussions.

6. Figures

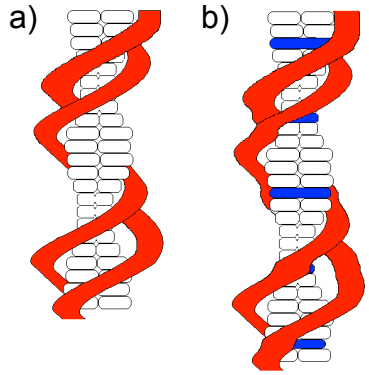

Figure 25: A sketch of double stranded DNA without (a) and with (b) an intercalator (shown in blue). Note the deforming of the backbone (shown in red) which changes the twist of the double helix.

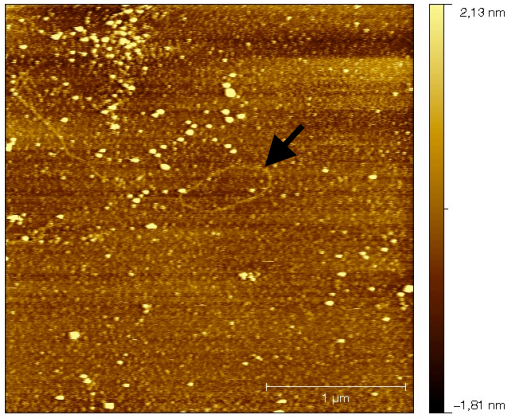

Figure 26: Plasmid DNA sample bound to gas-phase produced 3-aminopropyl-modified mica, 2.9 x 2.9µm

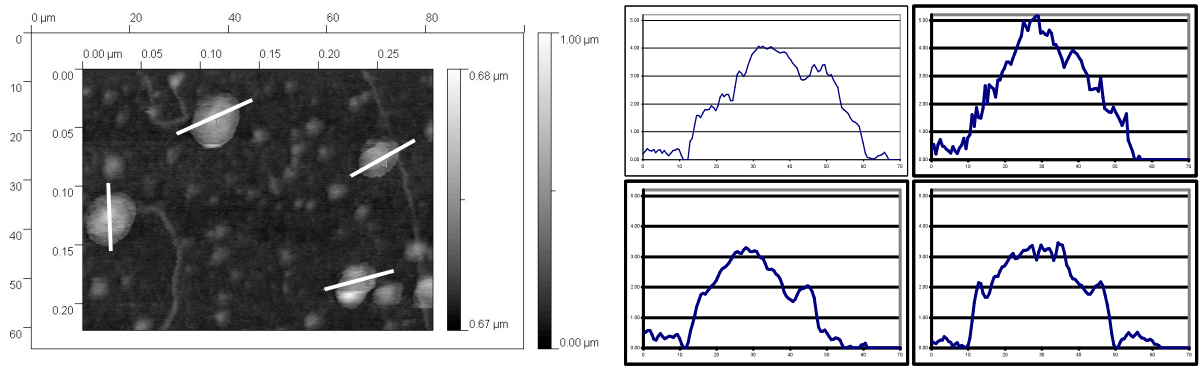

Figure 27: cross sections of different condensed plasmid clusters from Fig. 2A, x-axis: width (70 nm), y-axis: height (5.2 nm)

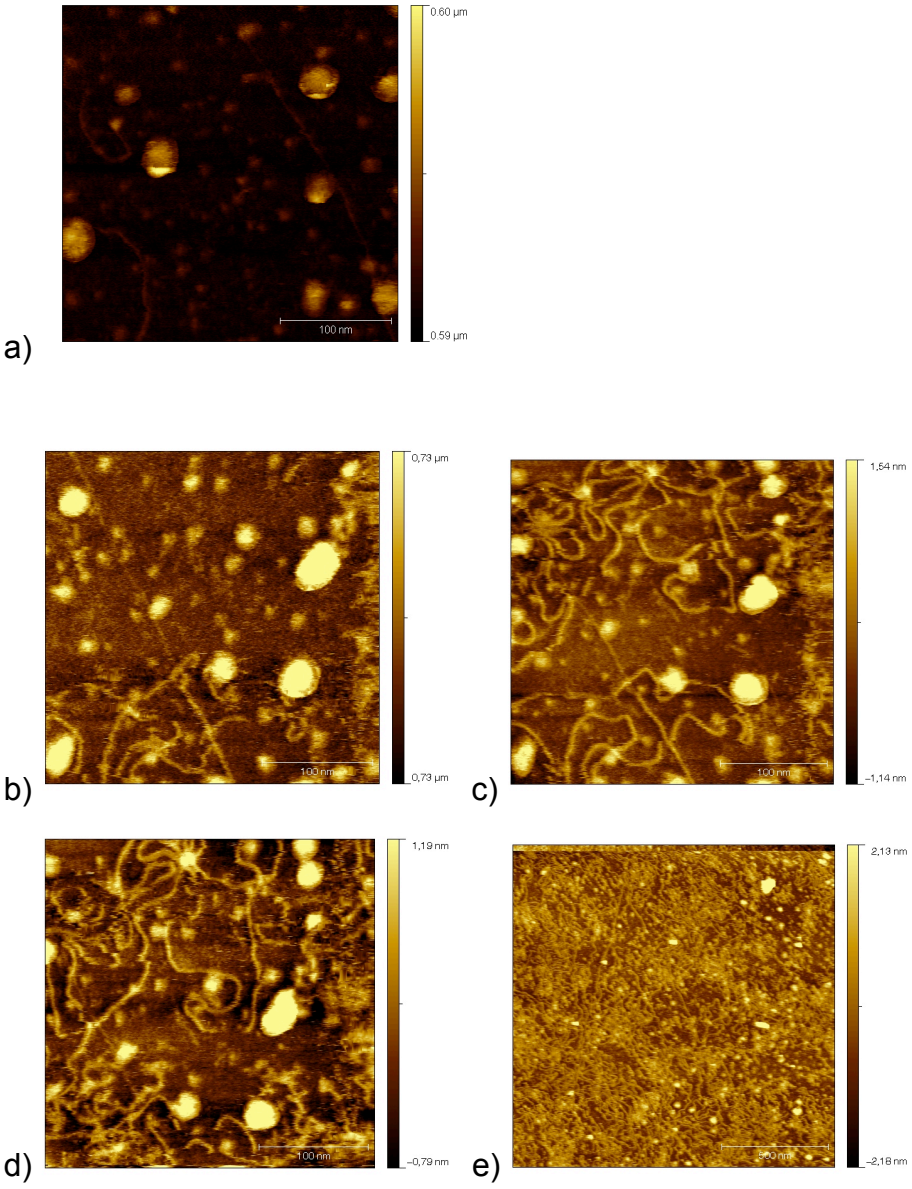

Figure 28: sequentially recorded AFM images of condensed plasmid DNA before (a) and after chloroquine addition (5 minutes (b), 10 minutes (c) and 15 minutes (d)) without changing position. Image (e) was recorded 30 minutes after chloroquine addition with a bigger scan size; 299 x 299 nm (a) - (d), 1.49 x 1.49 µm (e)

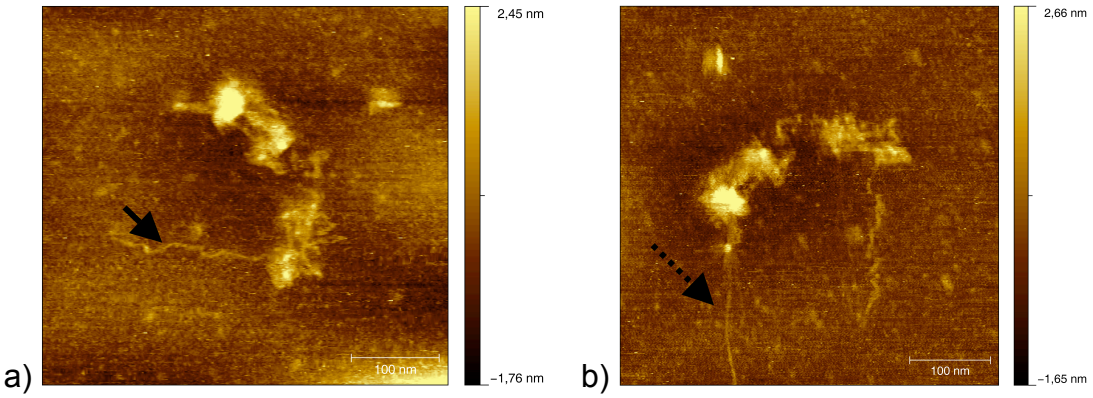

Figure 29: Two sequentially recorded AFM images of a DNA cluster. Between their recording the scanning orientation has been changed by 90 degrees; 0.46 x 0.46 µm

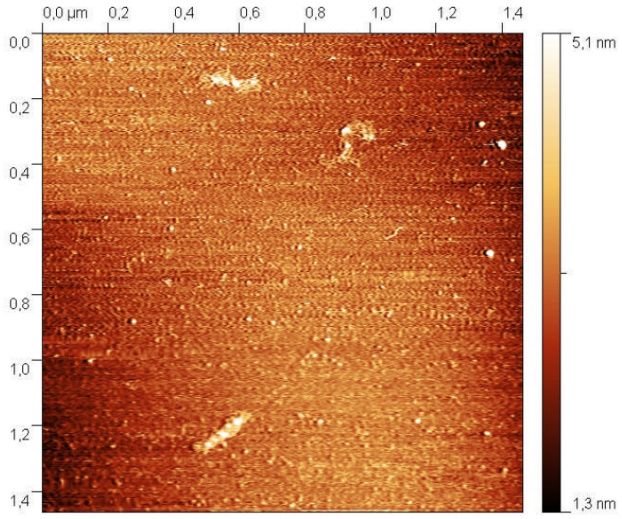

Figure 30: Plasmid DNA sample bound to liquid-phase produced 3-aminopropyl-modified mica, 1.44 x 1.44µm

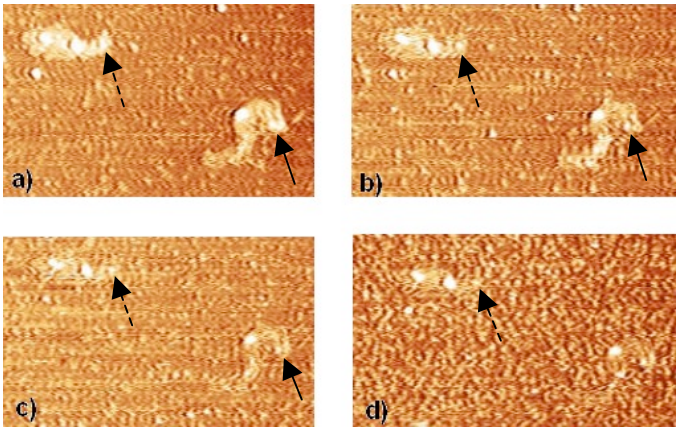

Figure 31: sequentially recorded AFM images of condensed plasmid DNA after chloroquine addition (5 minutes (a), 10 minutes (b), 15 minutes (c) and 30 minutes (d)) without changing position. All images have same dimensions.

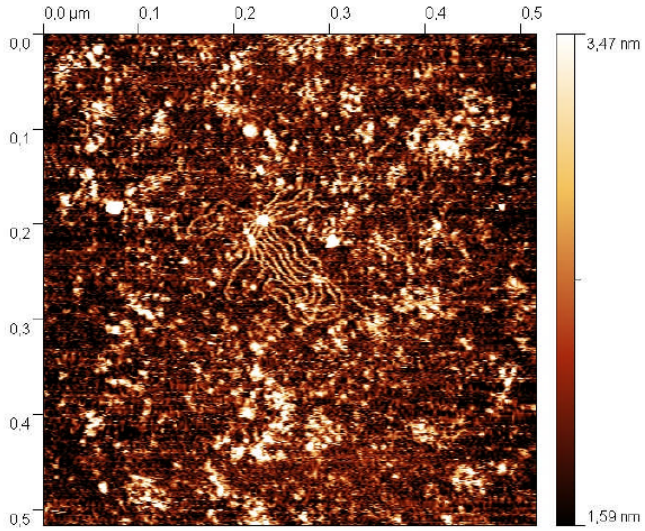

Figure 32: star-shaped relaxed plasmid DNA cluster (60 min after addition of chloroquine)

7. References

[1] Vologodskii AV (2000) Cyclic Polym. (2nd Ed.) 47-83

[2] Bates AD, Maxwell A (2006) In: (ed) DNA Supercoiling, 2nd Oxford University Press, New York

[3] Wheate NJ, Brodie CR, Collins JG, Kemp S, Aldrich-Wright JR (2007) Mini-Reviews in Medicinal Chemistry 7:627-648

[4] Utsuno K, Tsuboi M, Katsumata S, Iwamoto T (2001) Chem. Pharm. Bull. 49:413-417

[5] de Carmejane O, Schwinefus JJ, Morris MD (1999) Proceedings of SPIE-The International Society for Optical Engineering 3602:346-354

[6] Reyes-Dominguez Y, Contreras-Ferrat G, Ramirez-Santos J, Membrillo-Hernandez J, Gomez-Eichelmann MC (2003) Journal of Bacteriology 185:1097-1100

[7] Kienberger F, Costa LT, Zhu R, Kada G, Reithmayer M, Chtcheglova L, Rankl C, Pacheco ABF, Thalhammer S, Pastushenko V, Heckl WM, Blaas D, Hinterdorfer P (2007) Biomaterials 28:2403-2411

[8] Lyubchenko YL, Gall AA, Shlyakhtenko LS, Harrington RE, Jacobs BL, Oden PI, Lindsay SM (1992) J. Biomol. Struct. Dyn. 10:589-606

[9] Uji-i H, Foubert P, De Schryver FC, De Feyter S, Gicquel E, Etoc A, Moucheron C, Kirsch-De Mesmaeker A (2006) Chem.--Eur. J. 12:758-762

[10] Ebner A, Hinterdorfer P, Gruber HJ (2007) Ultramicroscopy 107:922-927

[11] Ziady A-G, Ferkol T, Dawson DV, Perlmutter DH, Davis PB (1999) J. Biol. Chem. 274:4908-4916
[12] Mann A, Khan MA, Shukla V, Ganguli M (2007) Biophys. Chem. 129:126-136
[13] Hartmann L, Haefele S, Peschka-Suess R, Antonietti M, Boerner HG (2008) Chem.--Eur. J. 14:2025-2033
[14] Sun B, Guan J-X, Xu L, Yu B-L, Jiang L, Kou J-F, Wang L, Ding X-D, Chao H, Ji L-N (2009) Inorg. Chem. (Washington, DC, U. S.) 48:4637-4639
[15] Liu Z, Li Z, Zhou H, Wei G, Song Y, Wang L (2005) J. Microsc. (Oxford, U. K.) 218:233-239
[16] Fang Y, Hoh JH (1998) Nucleic Acids Res. 26:588-593
[17] Bloomfield VA (1991) Biopolymers 31:1471-1481
[18] Mayan-Santos M-D, Martinez-Robles M-L, Hernandez P, Krimer D, Schvartzman JB (2007) Electrophoresis 28:3845-3853
[19] Viglasky V, Valle F, Adamcik J, Joab I, Podhradsky D, Dietler G (2003) Electrophoresis 24:1703-1711
[20] Tseng Yolanda D, Ge H, Wang X, Edwardson JM, Waring Michael J, Fitzgerald William J, Henderson Robert M (2005) J Mol Biol 345:745-758
[21] Pope LH, Davies MC, Laughton CA, Roberts CJ, Tendler SJB, Williams PM (2000) J. Microsc. (Oxford) 199:68-78
[22] Pope LH, Davies MC, Laughton CA, Roberts CJ, Tendler SJB, Williams PM (1999) Anal. Chim. Acta 400:27-32
[23] Bezanilla M, Manne S, Laney DE, Lyubchenko YL, Hansma HG (1995) Langmuir 11:655-659
[24] Yu J, Zhang Z, Cao K, Huang X (2008) Biochem. Biophys. Res. Commun. 374:415-418
[25] Unge M, Stafstroem S (2003) Nano Lett. 3:1417-1420
[26] Bjoerk P, Herland A, Scheblykin IG, Inganaes O (2005) Nano Lett. 5:1948-1953

Europass-Lebenslauf

Angaben zur Person

Nachname(n) / Vorname(n)	**MAHUT, Marek**
Adresse(n)	Huttengasse 13/2/20, A-1140 Wien
Telefon	Mobil: +43-676-5649539
E-mail	marek.mahut@univie.ac.at
Staatsangehörigkeit	Slowakische Republik
Geburtsdatum	27.10.1983
Geschlecht	männlich

Schul- und Berufsbildung

Zeitraum	ab Oktober 2007 (voraussichtliche Promotion im Juli 2010)
Bezeichnung der erworbenen Qualifikation	Doktorat der Naturwissenschaften (Chemie)
Hauptfächer/berufliche Fähigkeiten	Analytische Chemie, Trennungen von Biomolekülen, Entwicklung und Herstellung von neuen Trennmaterialien
Name und Art der Bildungs- oder Ausbildungseinrichtung	Universität Wien, Währinger Straße 38, A-1090 Wien Betreuer: Professor Michael Lämmerhofer
Stufe der nationalen oder internationalen Klassifikation	Dr. / PhD.
Zeitraum	Oktober 2002 – Juli 2007
Bezeichnung der erworbenen Qualifikation	Magister der Naturwissenschaften
Hauptfächer/berufliche Fähigkeiten	Analytische Chemie, Organische Chemie
Name und Art der Bildungs- oder Ausbildungseinrichtung	Universität Wien, Währinger Straße 38, A-1090 Wien Betreuer der Diplomarbeit: Professor Wolfgang Lindner
Stufe der nationalen oder internationalen Klassifikation	Mag. / MSc.
Zeitraum	September 1998 – Juni 2002

Bezeichnung der erworbenen Qualifikation	Matura
Hauptfächer/berufliche Fähigkeiten	Biochemie, Biotechnologie und Gentechnologie
Name und Art der Bildungs- oder Ausbildungseinrichtung	HBLVA XVII (HTL), Rosensteingasse 79, A-1170 Wien aufgestiegen von der 1. in die 3. Klasse, 2. Klasse übersprungen Betreuerin der Diplomfacharbeit: Dr. Bibiana Meixner

Gewünschte Beschäftigung / Gewünschtes Berufsfeld

Biochemie, Biotechnologie

Berufserfahrung

Zeitraum	Oktober 2007 – April 2010
Beruf oder Funktion	Wissenschaftlicher Mitarbeiter am Institut für Analytische Chemie
Wichtigste Tätigkeiten und Zuständigkeiten	Synthese von chromatographischen Liganden, chirale HPLC, präparative LC, HPLC von Plasmid DNA, Elektrophorese von DNA, Analyse von Fermentationsproben, atomkraftmikroskopische Messungen, Arbeiten mit Zellkulturen, Kooperation mit Boehringer Ingelheim RCV
Name und Adresse des Arbeitgebers	Institut für Analytische Chemie, Universität Wien, Währinger Straße 38, A-1090 Wien
Tätigkeitsbereich oder Branche	Forschung
Zeitraum	März 2006 – Juli 2006
Beruf oder Funktion	Wissenschaftlicher Mitarbeiter (ERASMUS Programm)
Wichtigste Tätigkeiten und Zuständigkeiten	Herstellung und Applikation einer doppelten nano-Elektrospray Ionenquelle für Massenspektrometrie zur Untersuchung der Vancomycin-Peptid (Lys-Ala-Ala) Wechselwirkung, Messungen am FT-ICR Massenspektrometer; Betreuer: Professor Peter J. Derrick
Name und Adresse des Arbeitgebers	Department of Chemistry, University of Warwick, CV4 8UW Coventry, Vereinigtes Königreich
Tätigkeitsbereich oder Branche	Forschung
Zeitraum	Jänner 2004 - September 2005
Beruf oder Funktion	Wissenschaftlicher Mitarbeiter am Institut für Organische Chemie
Wichtigste Tätigkeiten und Zuständigkeiten	Totalsynthese von Antibiotika-Antagonisten, Synthese von Spürsubstanzen (Tracer) für PET-Tomographie auf Zuckerbasis mit vollständiger spektroskopischer Charakterisierung der Produkte Betreuer: Professor Friedrich Hammerschmidt
Name und Adresse des Arbeitgebers	Institut für Organische Chemie, Universität Wien, Währinger Straße 38, A-1090 Wien
Tätigkeitsbereich oder Branche	Forschung
Zeitraum	August 2001
Beruf oder Funktion	Praktikum
Wichtigste Tätigkeiten und Zuständigkeiten	Analyse von OP-Mustern, Halbfertigprodukten und Hilfsstoffen nach festgelegten Methoden (ÖAB, Ph.Eur.); Durchführung von Kalibrierungen
Name und Adresse des Arbeitgebers	Gerot Pharmazeutika GmbH, Arnethgasse 3, A-1160 Wien, Abteilung: Qualitätssicherung (seit 2009: G.L.Pharma GmbH)
Tätigkeitsbereich oder Branche	Pharmazeutische Industrie
Zeitraum	Juni 2001 – Juli 2001
Beruf oder Funktion	Wissenschaftlicher Mitarbeit in molekularer Biologie
Wichtigste Tätigkeiten und Zuständigkeiten	Arbeiten an der Diplomfacharbeit ("Untersuchung von Endophyten des Stammes Pseudomonas spp. in Kartoffelpflanzen auf genetischem Wege"), Gelelektrophoretische Techniken (AGE, TGGE, DGGE), DNA-Sequenzierung, PCR, Klonierungen; Betreuerin: Dr. Angela Sessitsch
Name und Adresse des Arbeitgebers	Austrian research centers, A-2444 Seibersdorf, Austria (heute: Austrian Institute of Technology)
Tätigkeitsbereich oder Branche	Forschung
Zeitraum	Juli 2000 – September 2000

Beruf oder Funktion	Laborassistent, Institut f. Biochemie der Pflanzen
Wichtigste Tätigkeiten und Zuständigkeiten	Isolierung und Präparation von Mikrosomen aus Pflanzen; Dünnschichtchromatographie von Pflanzenfarbstoffen Betreuer: Professor Karl Stich
Name und Adresse des Arbeitgebers	Technische Universität Wien, Getreidemarkt 9, A-1060 Wien
Tätigkeitsbereich oder Branche	Forschung

Persönliche Fähigkeiten und Kompetenzen

Muttersprache(n) **Slowakisch**

Sonstige Sprache(n)

Selbstbeurteilung	Verstehen				Sprechen				Schreiben	
Europäische Kompetenzstufe (*) (*) *Referenzniveau des gemeinsamen europäischen Referenzrahmens*	Hören		Lesen		An Gesprächen teilnehmen		Zusammen-hängendes Sprechen			
Deutsch	C2	Kompetente Sprach-verwendung	C2	Kompetente Sprach-verwendung	C2	Kompetente Sprach-verwendung	C2	Kompetente Sprach-verwendung	C2	Kompetente Sprach-verwendung
Englisch	C1	Kompetente Sprach-verwendung	C1	Kompetente Sprach-verwendung	C1	Kompetente Sprach-verwendung	C1	Kompetente Sprach-verwendung	C1	Kompetente Sprach-verwendung
Tschechisch	C2	Kompetente Sprach-verwendung	C2	Kompetente Sprach-verwendung	C2	Kompetente Sprach-verwendung	C2	Kompetente Sprach-verwendung	C1	Kompetente Sprach-verwendung
Ungarisch	A1	Elementare Sprach-verwendung	A1	Elementare Sprach-verwendung	A1	Elementare Sprach-verwendung	A1	Elementare Sprach-verwendung	A2	Elementare Sprach-verwendung

Soziale Fähigkeiten und Kompetenzen	- gute Fähigkeit zur Einstellung auf multikulturelles Umfeld, erworben durch meine Forschungsaktivitäten in multinationalen Arbeitskreisen in Österreich und im Ausland - gute Kommunikationsfähigkeit, erworben durch zahlreiche Teilnahmen an Konferenzen in Europa und in den USA
Organisatorische Fähigkeiten und Kompetenzen	- gewisse Erfahrung in Personalführung durch reguläre Betreuung von Studenten während ihrer Diplomarbeiten und diversen Praktika
Technische Fähigkeiten und Kompetenzen	- Reparatur und Wartung von chromatographischen und elektrophoretischen Systemen, erworben während meiner Diplomarbeit und Dissertation - Batch-Produktion von stationären Phasen für die Chromatographie bis zum Kilogrammmaßstab gemäß GMP und GLP, erworben während meiner Dissertation
IKT-Kenntnisse und Kompetenzen	- exzellentes Umgehen mit Microsoft Office (Word, Excel, PowerPoint, Outlook) und Internet-Browsing-Progammen (Internet Explorer, Firefox, Safari) - Basiskenntnisse im Umgang mit graphischer Software (Adobe Photoshop) - Betriebssysteme: Microsoft Windows und Apple MacOS
Sonstige Fähigkeiten und Kompetenzen	- Bergwandern, Fußball und Squash - Amateurphotographie
Führerschein(e)	Klasse B

Zusätzliche Angaben

Posterpräsentationen:
1. “Limitations of indirect chromatographic determination of absolute configuration on chiral stationary phases”, HPLC 2009, 28.06. bis 02.07.2009 in Dresden
2. “Multi-modal peptide separations (RP, AEX, Ion-exclusion, HIC, HILIC modes) with a single column containing a mixed-mode reversed-phase/weak-anion exchange material”, Euroanalysis 2009, 06. bis 10.09.2009, Innsbruck
3. Eine aktualisierte Version von Poster 2 wurde später an der ISPPP 2009, vom 25. bis 28.10.2009 in Delray Beach, Florida, USA, präsentiert.

Publikationsliste:
Bis jetzt konnten keine Publikation von meiner Dissertation erscheinen, da zurzeit eine Patentanmeldung zusammen mit Boehringer Ingelheim erfolgt. Daher kann zur Zeit nur eine Liste der zu publizierenden Artikel angegeben werden:

1. “ Chromatographic separation of plasmid DNA isoforms with quinine-based ligands ”
2. “ Chromatographic separation of plasmid DNA topoisomers of different linking numbers “
3. “ Molecular recognition principles and stationary phase characteristics for chromatographic separation of circular plasmid DNA topoisomers “
4. “ Time-resolved chloroquine-induced relaxation of supercoiled plasmid DNA bionanoparticles“